

**WL-TR-96-3119**

**ENHANCEMENT OF THE  
AEROSERVOELASTIC CAPABILITY  
IN ASTROS**



**P. C. CHEN  
D. D. LIU  
D. SARHADDI  
ZONA Technology, Inc.  
2651 W. Guadalupe Rd, Ste B-228  
Mesa AZ 85202**

**A. G. STRIZ  
The University of Oklahoma**

**D. J. NEILL  
Universal Analytics, Inc.**

**M. KARPEL  
Technion - I. I. T.**

*100% QUANTITY INSPECTED &*

**SEPTEMBER 1996**

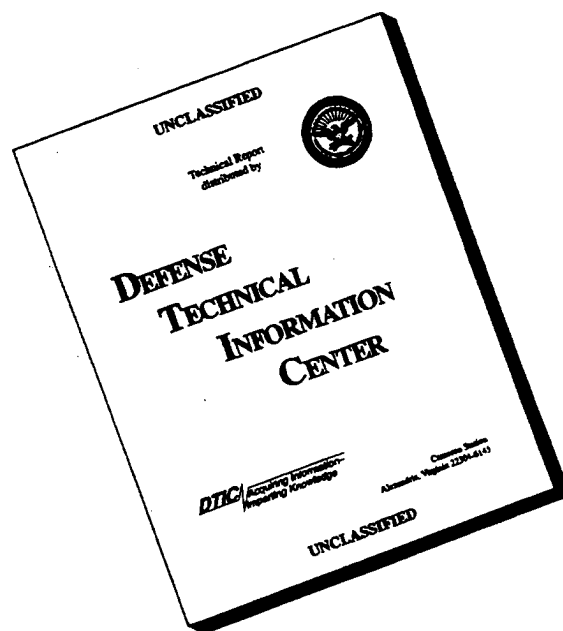
**PHASE I FINAL REPORT FOR THE PERIOD SEPTEMBER 1995  
- MAY 1996**

**Approved for public release; distribution unlimited**

**FLIGHT DYNAMICS DIRECTORATE  
WRIGHT LABORATORY  
AIR FORCE MATERIEL COMMAND  
WRIGHT-PATTERSON AIR FORCE BASE OH 45433-7562**

**19961015 027**

# DISCLAIMER NOTICE



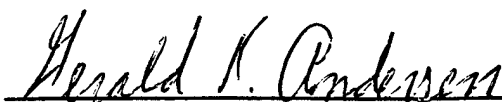
**THIS DOCUMENT IS BEST QUALITY AVAILABLE. THE COPY FURNISHED TO DTIC CONTAINED A SIGNIFICANT NUMBER OF PAGES WHICH DO NOT REPRODUCE LEGIBLY.**


# NOTICE

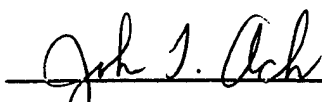
WHEN GOVERNMENT DRAWINGS, SPECIFICATIONS, OR OTHER DATA ARE USED FOR ANY PURPOSE OTHER THAN IN CONNECTION WITH A DEFINITELY GOVERNMENT-RELATED PROCUREMENT, THE UNITED STATES GOVERNMENT INCURS NO RESPONSIBILITY OR ANY OBLIGATION WHATSOEVER. THE FACT THAT THE GOVERNMENT MAY HAVE FORMULATED OR IN ANY WAY SUPPLIED THE SAID DRAWINGS, SPECIFICATIONS, OR OTHER DATA, IS NOT TO BE REGARDED BY IMPLICATION, OR OTHERWISE IN ANY MANNER CONSTRUED, AS LICENSING THE HOLDER, OR ANY OTHER PERSON OR CORPORATION; OR AS CONVEYING ANY RIGHTS OR PERMISSION TO MANUFACTURE, USE, OR SELL ANY PATENTED INVENTION THAT MAY IN ANY WAY BE RELATED THERETO.

THIS REPORT IS RELEASABLE TO THE NATIONAL TECHNICAL INFORMATION SERVICE (NTIS). AT NTIS, IT WILL BE AVAILABLE TO THE GENERAL PUBLIC, INCLUDING FOREIGN NATIONS.

THE TECHNICAL REPORT HAS BEEN REVIEWED AND IS APPROVED FOR PUBLICATION.

  
GERALD R. ANDERSEN, 1LT, USAF  
Project Engineer  
Design Methods Development Section

  
GEORGE R. HOLDERBY, Chief  
DESIGN DEVELOPMENT BRANCH  
STRUCTURES DIVISION

  
JOHN T. ACH  
Asst for Research & Technology  
Structures Division

IF YOUR ADDRESS HAS CHANGED, IF YOU WISH TO BE REMOVED FROM OUR MAILING LIST, OR IF THE ADDRESSEE IS NO LONGER EMPLOYED BY YOUR ORGANIZATION PLEASE NOTIFY WL/FIBAD, WPAFB OH 45433-7542 HELP MAINTAIN A CURRENT MAILING LIST.

COPIES OF THIS REPORT SHOULD NOT BE RETURNED UNLESS RETURN IS REQUIRED BY SECURITY CONSIDERATIONS, CONTRACTUAL OBLIGATIONS, OR NOTICE ON A SPECIFIC DOCUMENT.

REPORT DOCUMENTATION PAGE			Form Approved OMB No. 0704-0188	
Public reporting burden for this collection of information is estimated to average 1 hour per response, including the time for reviewing instructions, searching existing data sources, gathering and maintaining the data needed, and completing and reviewing the collection of information. Send comments regarding this burden estimate or any other aspect of this collection of information, including suggestions for reducing this burden, to Washington Headquarters Services, Directorate for Information Operations and Reports, 1215 Jefferson Davis Highway, Suite 1204, Arlington, VA 22202-4302, and to the Office of Management and Budget, Paperwork Reduction Project (0704-0188), Washington, DC 20503.				
1. AGENCY USE ONLY (Leave blank)		2. REPORT DATE 01 MAY 1996		3. REPORT TYPE AND DATES COVERED FINAL 01 SEP 1995 - 01 MAY 1996
4. TITLE AND SUBTITLE ENHANCEMENT OF THE AEROSERVOELASTIC CAPABILITY IN ASTROS PHASE I, FINAL REPORT			5. FUNDING NUMBERS C F33615-95C-3219 PE 65502F PR 3005 TA 30 WU 27	
6. AUTHOR(S) P. C. Chen, D. D. Liu, and D. Sarhaddi, ZONA; A. G. Striz, University of Oklahoma; D. J. Niell, UAI; M. Karpel, Technion - I. I. T.				
7. PERFORMING ORGANIZATION NAME(S) AND ADDRESS(ES) ZONA Technology, Inc. 2651 W. Guadalupe Rd., Ste. B-228 Mesa, AZ 85202			8. PERFORMING ORGANIZATION REPORT NUMBER  ZONA 96-13	
9. SPONSORING/MONITORING AGENCY NAME(S) AND ADDRESS(ES) Flight Dynamics Directorate Wright Laboratory Air Force Material Command WPAFB OH 45433-7542 POC: Lt Gerald R. Andersen, WL/FIBAD, 937-255-6992			10. SPONSORING/MONITORING AGENCY REPORT NUMBER  WL-TR-96-3119	
11. SUPPLEMENTARY NOTES				
12a. DISTRIBUTION AVAILABILITY STATEMENT  APPROVED FOR PUBLIC RELEASE; DISTRIBUTION IS UNLIMITED			12b. DISTRIBUTION CODE	
13. ABSTRACT (Maximum 200 words)  This report documents the results of an STTR Phase I feasibility study to investigate potential aerodynamic and aeroservoelastic enhancements to the "Automated Structural Optimization System (ASTROS)." This study included the development of the Unified S-Domain Aerodynamics package which provides capability for aerodynamic modeling of arbitrary and complex aircraft geometries, including stores, throughout the entire flight regime, including transonic and hypersonic flight. The aerodynamics module utilizes four existing aerodynamic codes to accomplish this airload prediction capability. Additionally, a new aerodynamic geometry module was created to simplify the aerodynamic modeling of an aircraft regardless of the particular analysis code being employed. This research effort also included the development of a software design blueprint for an aeroservoelastic analysis and design module. Through a state-space formulation of the problem, this module allows the inclusion of control system design variables such as gain and phase margins, vibration frequencies, and damping ratios in the design and optimization of flexible aircraft structures.				
14. SUBJECT TERMS ASTROS, Aeroservoelasticity, Unsteady Transonics/Hypersonics, Minimum-State Approach, Unified S-Domain Aerodynamics, Multidisciplinary Optimization, Preliminary Design			15. NUMBER OF PAGES 108	
			16. PRICE CODE	
17. SECURITY CLASSIFICATION OF REPORT UNCLASSIFIED	18. SECURITY CLASSIFICATION OF THIS PAGE UNCLASSIFIED	19. SECURITY CLASSIFICATION OF ABSTRACT UNCLASSIFIED	20. LIMITATION OF ABSTRACT SAR	

## REPORT DOCUMENTATION PAGE - ABSTRACT CONTINUED

### ANTICIPATED BENEFITS/POTENTIAL, COMMERCIAL, APPLICATIONS OF THE RESEARCH DEVELOPMENT:

There are many potential areas of application for the ASTROS/ASE. It will provide the aerospace industry an excellent design/analysis tool for aircraft such as the High Speed Civil Transport (HSCT) or the Active Aeroelastic Wing (AAW), among other ongoing and future projects. Other gross potentials of the ASTROS/ASE include its integration with Probabilistic Design Methods, its Designing of Smart Structures and its further inclusion of emerging robust control technology.

### TECHNICAL ABSTRACT (SUMMARY REPORT)

The objective of the Phase I STTR contract is to sufficiently develop the Aeroservoelastic (ASE) discipline and to the grounds for its eventual integration into ASTROS (Automated Structural Optimization System). The ZONA Team attempts to achieve two major technical goals in order to accomplish this objective.

First, a Unified S-Domain Aerodynamics (USDA) package, as derived from the UAIC (the Unified Aerodynamic Influence Coefficient) approach of four major ZONA aerodynamic software (called the ZAERO Module) covering the complete flight Mach number regime, have been developed. A feasibility study has been conducted for three wing planforms, namely, i) the NASP Demonstrator Model, ii) the AGARD Standard 445.6 Wing (solid and weakened planforms) and iii) the Modeled F-16 Wing. Emphasis was placed on the feasibility of employing the developed USDA, via Karpel's Minimum State Technique (MIST), for transonic and hypersonic flutter investigation of these wing planforms. The feasibility study was concluded successfully assuring the USDA's capability for ASE applications.

Second, a Software Design Blueprint for the ASE Module architecture and plans for its integration into ASTROS are provided. Thus, with the approved Software Design Blueprint for ASE as a basis, the subsequent integration of ASTROS/ASE can be implemented. Technically or commercially, the resulting integrated ASTROS code will acquire a competitive edge over all existing MDO software.

In parallel to the above effort, additional tasks were conducted to further substantiate the present technical goals; these are:

- i) Transonic unsteady pressure results of the Lessing Wing and the LANN Wing: For further validation of the ZTAIC code (see Appendix A).
- ii) Development planning of an Aerodynamic Geometry Module (AGM) that will provide ASTROS with a universal set of geometric definitions for the ZAERO module.

The findings of the Phase I studies can be summarized as follows:

#### On The ZAERO Module:

- i) The unified AIC formulation is ideal for a MDO environment such as the one provided by ASTROS.
- ii) The unified feature of ZAERO for all Mach numbers will surpass existing aerodynamic modules including those presently within ASTROS.
- iii) The success of the USDA results ensure the feasibility of ASTROS/ASE applications.

#### On The ASE Blueprint:

The approach and the overall capability of the ASE in preparation for future integration with ASTROS has been defined (see Section 4.0). Four specific scenarios pertinent to the ASTROS/ASE applications clearly elucidate its future capability.

## TABLE OF CONTENTS

<u>Section</u>	<u>Page</u>
1 Introduction .....	1
2 The ZAERO Module .....	2
2.1 Overview of the ZAERO Module .....	2
2.2 Feasibility Study of the ZAERO/USDA Methodology .....	12
3 The Aerodynamic Geometry Module (AGM) .....	21
3.1 The Aerodynamic Geometry Module of ZAERO .....	21
3.2 Generation of Aerodynamic Influence Coefficient (AIC) Matrices .....	27
4 Software Design Blueprint of ASTROS/ASE Module .....	35
4.1 Scenarios for the ASTROS/ASE Applications .....	35
4.2 Overview of the ASE Module .....	37
4.3 Description of the ASE Block .....	39
4.4 Generalized Matrices .....	39
4.5 Control Model .....	41
4.6 Rational Aerodynamic Approximation .....	43
4.7 Control Margins .....	46
4.8 State-Space ASE Model .....	48
4.9 Flutter .....	52
4.10 Gust Model .....	53
4.11 Gust Response .....	54
5 Modification of ASTROS for ZAERO and ASE Integration .....	56
5.1 Integration Overview .....	56
5.2 ASE Design Overview .....	58
5.3 Solution Control .....	58
5.4 MAPOL Modifications .....	59
6 Future Research and Development .....	61
6.1 Anticipated Successful Results of Phase II .....	61
6.2 Plans for Phase III .....	61
6.3 Significance and Impact of Phase II on Phase III .....	62
7 Potential Applications .....	63
7.1 Potential Technical Applications .....	63
7.2 Potential Commercial Application .....	63
7.3 Potential Use by the Federal Government .....	64
References .....	65
Appendix A .....	67

## LIST OF FIGURES / TABLES

<u>Figure</u>		<u>Page</u>
2.1.1	ZONA Aerodynamic Module.	2
2.1.2	Damp-in-pitch Derivatives of a Rectangular Wing with Diamond Airfoil Section ( $h/c=0.5$ ) (a) $C_{M_b}$ vs. Semi-Wedge Angle at $M=2.0$ (b) $C_{M_b}$ vs. Semi-Wedge Angle at $M=10.0$ and (c) $C_{M_b}$ vs. Mach Number at Semi-Wedge Angle of $15^\circ$ .	4
2.1.3	Flutter Boundary of a $70^\circ$ Delta Wing with 6% Biconvex Airfoil Section.	4
2.1.4	Stability Derivatives of a NACA Wing-Body Combination $AR=2.0$ Computed by ZONA7 (a) Sketch of a Wing-Body Combination: Delta Wing with Centered Body of Revolution (b) Damping-in-Pitch Moment Coefficients with Pitching Axis at $0.35c$ (c) Moment-Curve Slopes with Pitching Axis at $0.35c$ .	6
2.1.5	Unsteady Spanwise Normal Force and Pitching Moment for the Clean F-5 Wing and the Underwing Store Configuration at $M=1.35$ and Reduced Frequency $k=0.1$ .	6
2.1.6	Out-of-Phase Pressures on Two Spanwise Stations: $70^\circ$ Delta Wing ( $M=0.8$ , $k=0.5$ , $x_0=0.5c$ ).	7
2.1.7	Unsteady Pressure Distributions Along the Store of NLR Wing-Tiptank-Pylon Store Configuration at (a) $\theta=157.5$ deg and (b) $\theta=292.5$ deg $M=0.45$ , $\alpha=0$ deg., $k=0.305$ and $x_0=0.15C_R$ .	7
2.1.8	The Lessing Wing (a) Configuration (b) Magnitude of the First Bending (c) Phase Angle (in degrees) of the First Bending, $M=0.9$ , $k=0.13$ .	9
2.1.9	Lann Wing Comparison of In-Phase and Out-of-Phase Pressures at Two Spanwise Locations: Pitching Oscillation About 62% Root-Chord at $M=0.82$ , $k=0.205$ .	10
2.1.10	Northrop F-5 Wing with Oscillating Flap: Comparison of In-Phase and Out-of-Phase Pressures with Hinge Line at 82% Chord at Sections 1 and 3, $M=0.9$ , $k=0.274$ .	11
2.2.1	Aerodynamic Model of NASP Demonstrator Wing.	14
2.2.2	Minimum-State (MIST) Fit of Generalized Aerodynamic Forces (GAF), NASP Demonstrator Model (a) $M=5.0$ , (b) $M=10.0$ , (c) $M=15.0$ .	14
2.2.3	Root-Locus Plots of NASP Demonstrator Model at $M=5.0$ , $10.0$ and $15.0$ .	15

## LIST OF FIGURES / TABLES (continued)

<u>Figure</u>		<u>Page</u>
2.2.4	Comparison of Flutter Speed and Frequency of 445.6 Weakened Wing at $M=0.678$ , $0.90$ and $0.95$ .	17
2.2.5	Comparison of Flutter Speed and Frequency of 445.6 Solid Wing at $M=0.90$ and $0.95$ .	17
2.2.6	Minimum-State Approximation of Generalized Aerodynamic Forces of 445.6 Weakened Wing at $M=0.95$ Computed by ZTAIC.	18
2.2.7	Root-Locus Plots of 445.6 weakened Wing at $M=0.95$ Using S-Domain Aerodynamics Computed by ZTAIC and ZONA6.	18
2.2.8	Flutter Speeds and Frequencies of Modeled F-16 Wing Computed by ZTAIC, CAPTSD and XTRAN3.	20
2.2.9	Minimum-State Approximations of Generalized Aerodynamic Forces of Modeled F-16 Wing at $M=0.95$ Computed by ZTAIC and ZONA6.	20
3.1.1	New Bulk Data Entries for Aerodynamic Modeling of an Arbitrary Wing-Body-Tail Configuration.	22
3.2.1	Flow Chart of ZONA6/ZONA7 Computation Procedure.	31
4.1.1	Active Flexible Wing (AFW) Roll Performance with Flutter Constraints.	35
4.1.2	Trade-Off Study of Gust Load alleviation by Passive and Active Means.	35
4.1.3	Store-Flutter Suppression of a Generic Advanced Fighter (GAF) with Structural Uncertainties.	36
4.2.1	General Flow Chart of the ASE Module.	38
4.7.1	Block Diagram of the MIMO ASE System.	47
5.4.1	Basic Structure of the ASTROS MAPOL Sequence.	59
 <u>Table</u>		 <u>Page</u>
2.2.1	Comparison of Flutter Dynamic Pressures and Frequencies of NASP Demonstrator Model at $M=5.0$ , $10.0$ and $15.0$ .	15





## FOREWORD

This report was prepared by ZONA Technology, Inc., the prime contractor, and its Team members (The University of Oklahoma (OU), Universal Analytics, Inc. (UAI), and Dr. Mordechay Karpel) for FIBAD, Wright Laboratory, WPAFB, Ohio. It describes the work performed under the Phase I contract of AF/STTR No. F33615-95-C-3219 in response to the Topic No. AF95T009 entitled "Enhancement of the Aeroservoelastic Capabilities in ASTROS." The contractual period was from September 01, 1995 through May 01, 1996. Lt. Gerald Anderson of WL/FIBAD was the technical monitor.

The contributors of this report are: Mr. P.C. Chen (principal investigator), Dr. D.D. Liu and Mr. D. Sarhaddi of ZONA Technology; Dr. A.G. Striz of the University of Oklahoma was the research institute counterpart; Mr. D.J. Neill of UAI and Dr. M. Karpel of Technion served as consultants to the present contract.

During the course of the present phase of the development in ASTROS, the technical advice and assistance that the ZONA Team received from Mr. Ray Kolonay, Dr. V.B. Venkayya, Mr. Ed Pendleton and Mr. Larry Huttshell of Wright Laboratory are gratefully acknowledged.

## SECTION 1

### INTRODUCTION

Current performance of advanced fighters and bombers requires high maneuverability, agility and stealth under a wide range of flight conditions. Their design goal tends to achieve at more flexible and less inherently stable aircraft throughout the complete (subsonic/transonic/supersonic) flight regime.

One such advanced conceptual design is the Active Aeroelastic Wing (AAW, Refs 1, 2), currently being pursued by the Air Force and Rockwell/North American. A recent design concept of the high Speed Civil Transport (HSCT) also places particular emphasis on the fly-by-wire control of the aircraft flexibility and its relaxed stability. Clearly, a system that could handle such interactions between structures, unsteady aerodynamics and active control is warranted. Such a system, known as Aeroservoelasticity (ASE), is a Multidisciplinary Technology and has been in rapid progress over the last two decades (Refs 3-9).

Active Aeroelastic Wing (AAW) technology is a multi-disciplinary synergistic technology in which the proper handling of the interaction between aerodynamics, control and structures would allow a thin, high aspect ratio wing planform to be aeroelastically-deformed in achieving optimum performance. Software support for the AAW design, such as ASTROS with an ASE capability, would therefore be most desirable.

There exist two major developments in aeroelastic codes that can handle ASE to a certain extent, namely, the ISAC code developed by NASA/Langley (Ref 3) and MSC/NASTRAN Version 68 (Ref 10). However, neither one can handle the design/analysis ASE problem adequately in that the ISAC code lacks the capability in optimization and design and MSC/NASTRAN's ASE capability is not yet fully developed. In the last decade, ASTROS has made rapid progress (Refs 11-19) and has demonstrated its outstanding capability in many areas of MDO technology except ASE. Thus, the proposed Phase I work in the development and integration of the ASE into ASTROS, once accomplished, will become a cutting-edge software technology.

In Phase I of STTR (AF95T009), ZONA Technology, Inc. and its team members, Oklahoma University, Universal Analytics, Inc. and Dr. Mordechai Karpel (the ZONA Team) have been committed to the ASE development in ASTROS and have worked out the ASE Software Design Blueprint for the ASE module architecture and its integration into ASTROS. In parallel to this effort, a prototypical ZONA Aerodynamic (ZAERO) module (Refs 19, 20), which would readily generate the Unified Aerodynamics (UAIC) for all Mach numbers and Unified S-Domain Aerodynamics (USDA) for ASE applications, has been developed and properly interfaced with ASTROS. A feasibility study, which included the testing of USDA as a tool for the flutter on three wing planforms extending to the Transonic and Hypersonic flow regimes, was conducted successfully. From these studies, it was demonstrated that the ZAERO module is by far a more general tool than the current Aero Module in ASTROS. Also, it has become apparent that the ZAERO-generated USDA is an excellent tool for ASE application, valid throughout the complete flight regimes (Ref 20).

## SECTION 2

### THE ZAERO MODULE

#### 2.1 Overview of the ZAERO Module

The ZAERO module consists of four major unsteady aerodynamic codes that jointly cover the complete domain of all Mach number ranges, namely ZONA51U, ZONA6, ZONA7 and ZTAIC. As can be seen in Figure 2.1.1, the AERO modules currently integrated within MSC/NASTRAN and ASTROS only possess purely subsonic and supersonic capabilities.

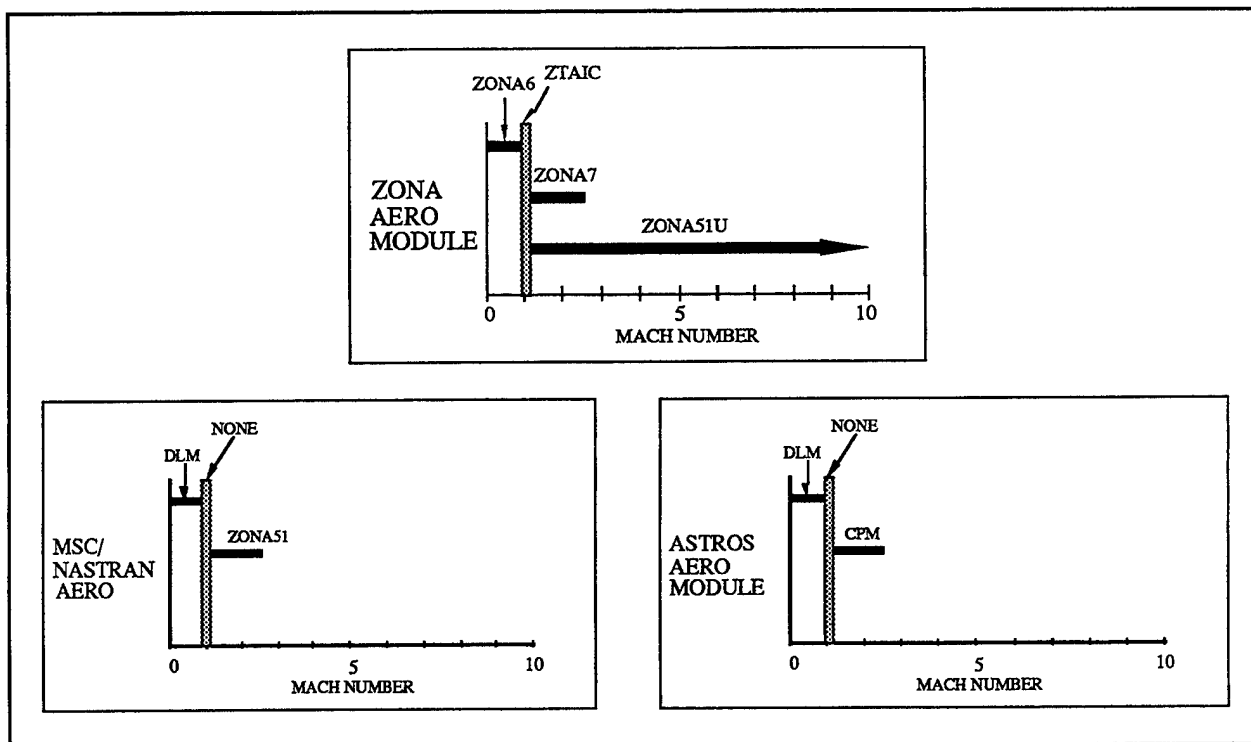


Figure 2.1.1 ZONA Aerodynamic Module.

By contrast, the ZAERO module serves as a unified aerodynamic tool which provides computed data from unsteady pressures to GAF's throughout all Mach numbers by means of the unified AIC approach. In fact, it is the UAIC of the ZAERO Module that has efficiently provided the k-domain solution, and, hence, the s-domain solution for subsequent ASE application.

The development of codes in the ZAERO module have been the major endeavor of ZONA Technology in the last decade. The following is a brief account of the capabilities of these four computer codes; namely

- ZONA51U
- ZONA7/ZONA6
- ZTAIC

- *ZONA51U: Generates Unified Unsteady Hypersonic/Supersonic Aerodynamics for Lifting Surface Systems (Refs 21, 22).*

A Unified Supersonic/Hypersonic Lifting Surface Method has been developed by ZONA recently (Refs 21, 22). This method combines the Supersonic Lifting Surface Theory (such as ZONA51, Ref 23) with a nonlinear correction matrix  $\bar{E}_{ij}$  based on Donovan & Linnell's uniformly valid-higher-order Hypersonic/Supersonic scheme. This correction matrix takes the flow nonlinearity as well as the flow rotationality due to oscillatory shock waves into account, which covers both the Mach wave and Newtonian limits. For aeroelastic applications, ZONA51U has been applied to various wing planforms with thickness distributions (e.g. Rectangular Wings with Diamond/Wedge profiles and a 70° Delta Wing, see Figs 2.1.2 and 2.1.3, Refs 21, 22). Computed results are found to agree well with those computed by Euler methods; flutter results are validated with measured data. It is found that ZONA51U improves substantially over the linear theory results in terms of pressures and stability derivatives, and provides more conservative flutter boundaries due to the thickness effect. Furthermore, the input format of ZONA51U is nearly the same as that of ZONA51 with only an additional input card on the Wing Profile Slope. The CPU time for ZONA51U is also comparable to that of ZONA51.

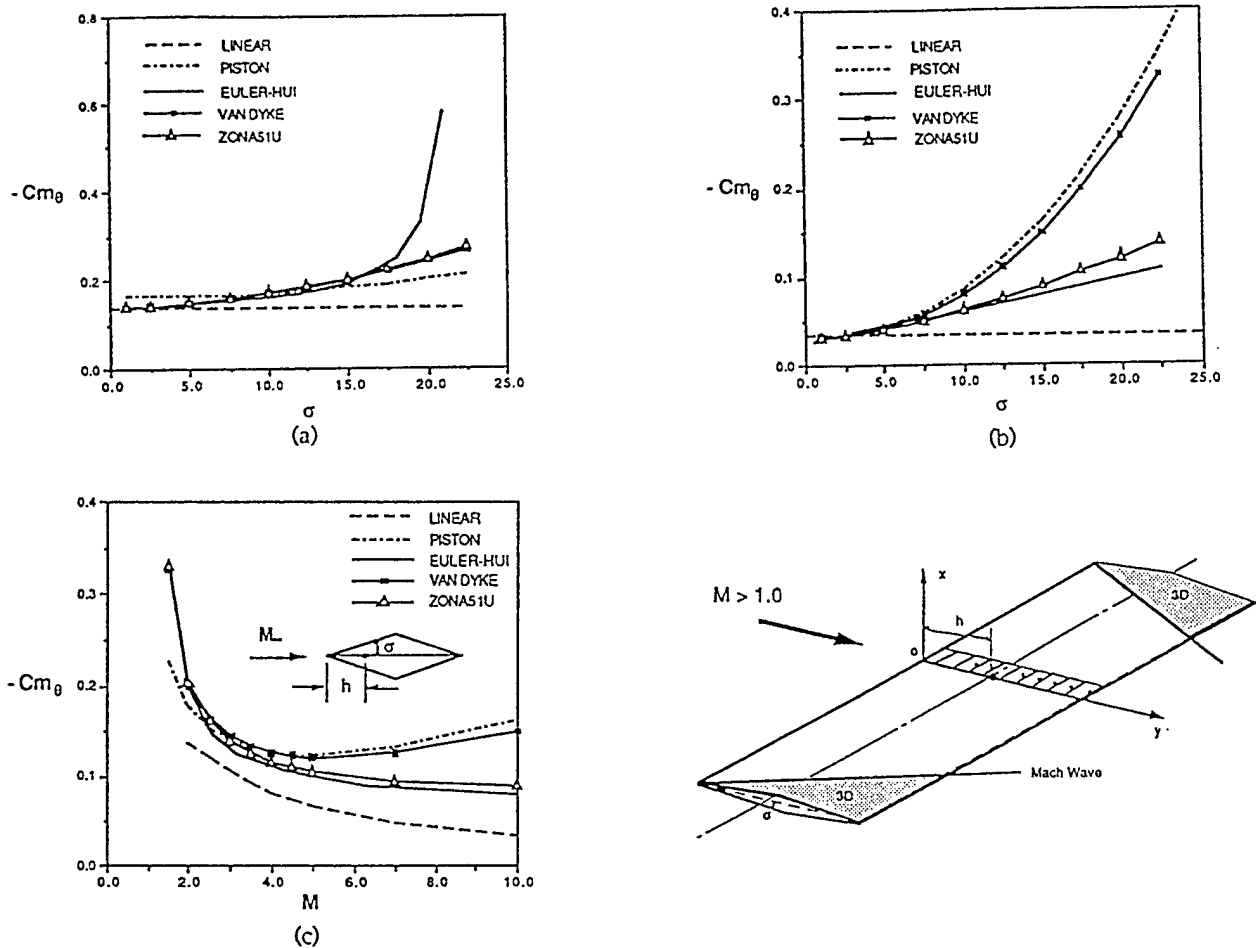


Figure 2.1.2 Damp-in-pitch Derivatives of a Rectangular Wing with Diamond Airfoil Section ( $h/c=0.5$ ) (a)  $C_{M\theta}$  vs. Semi-Wedge Angle at  $M=2.0$  (b)  $C_{M\theta}$  vs. Semi-Wedge Angle at  $M=10.0$  and (c)  $C_{M\theta}$  vs. Mach Number at Semi-Wedge Angle of  $15^\circ$ .

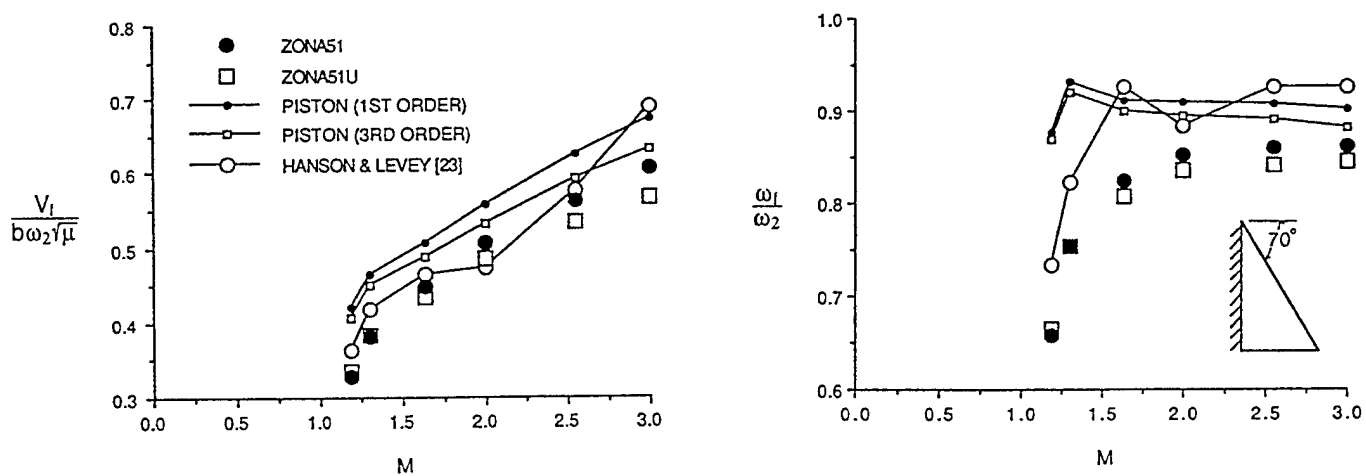


Figure 2.1.3 Flutter Boundary of a  $70^\circ$  Delta Wing with 6% Biconvex Airfoil Section.

- *ZONA7/ZONA6: Generates Unsteady Supersonic/Subsonic Aerodynamics for Aircraft Configurations with External Stores (Refs 26, 27, 28, 29).*

Prior to 1990, all unsteady aerodynamic methods for aeroelastic computations were based on lifting-surface models (e.g. DLM, Ref 30). The aerodynamic effects due to the presence of bodies and due to the wing-body interference are largely ignored. However, coupled external-store wing flutter, a problem that is of frequent concern to the Air Force, cannot be resolved by the lifting surface modeling alone. To demonstrate this effect, Fig 2.1.4 shows the stability derivatives of a NACA wing-body combination based on wing-only and wing-body analysis using ZONA7. Fig 2.1.5 presents the spanwise unsteady forces and moments of a NLR wing (F-5 wing) with underwing fin-missile and pylon. It is seen that, in both cases, the discrepancies between the wing-only results and the wing-body results are substantial.

ZONA6 is the subsonic counterpart of ZONA7 except that it includes the important body-wake effect for fuselage and stores. It should also be noted that ZONA6's lifting surface option (referred to as ZONA61) has the same order in paneling scheme as that of ZONA51 and therefore is more robust scheme than that of DLM (Ref 22).

Fig 2.1.6 presents the out-of-phase pressures on two spanwise stations on a 70° Delta Wing. It is seen that, using typical panel cuts, DLM breaks down at  $M = 0.8$  and  $k = 0.5$ .

Fig 2.1.7 presents the unsteady pressure along the underwing store of a NLR Wing-Tiptank-Pylon-Store configuration. It is clearly seen that large discrepancies exists between the body-only and the wing-body results.

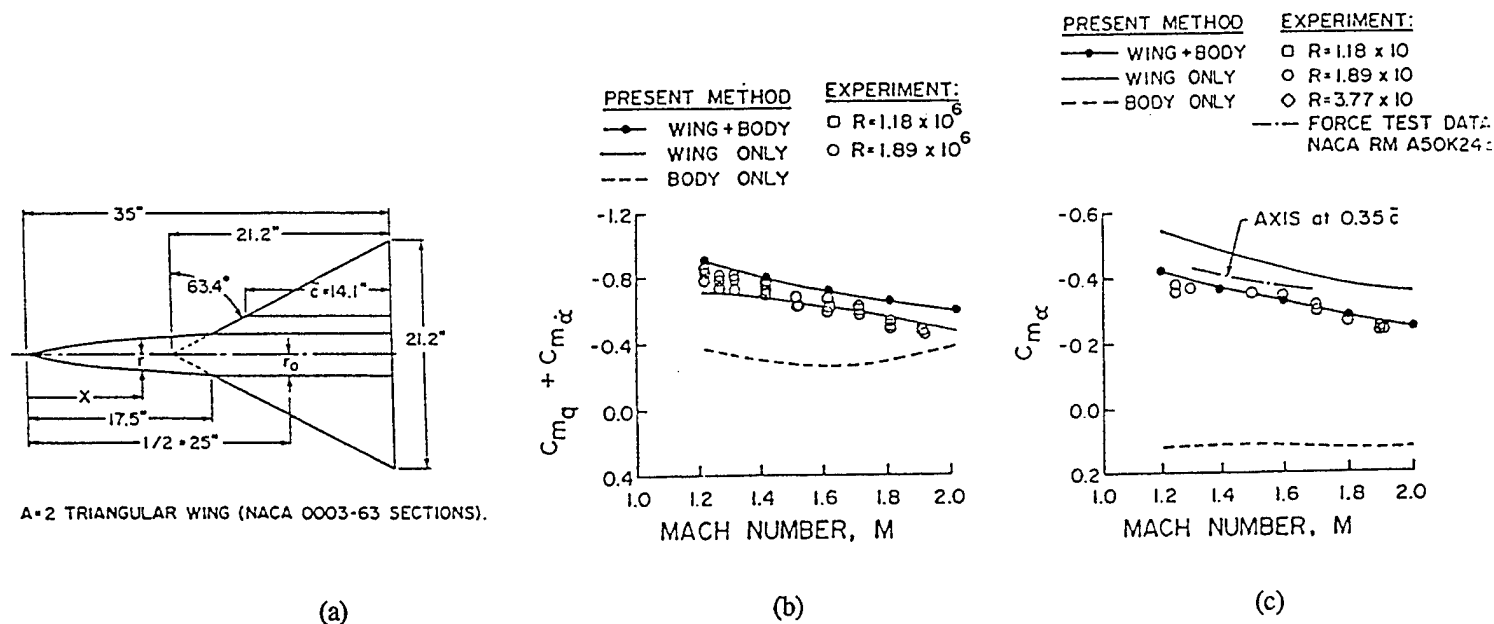


Figure 2.1.4 Stability Derivatives of a NACA Wing-Body Combination AR=2.0 Computed by ZONA7 (a) Sketch of a Wing-Body Combination: Delta Wing with Centered Body of Revolution (b) Damping-in-Pitch Moment Coefficients with Pitching Axis at 0.35c (c) Moment-Curve Slopes with Pitching Axis at 0.35c.

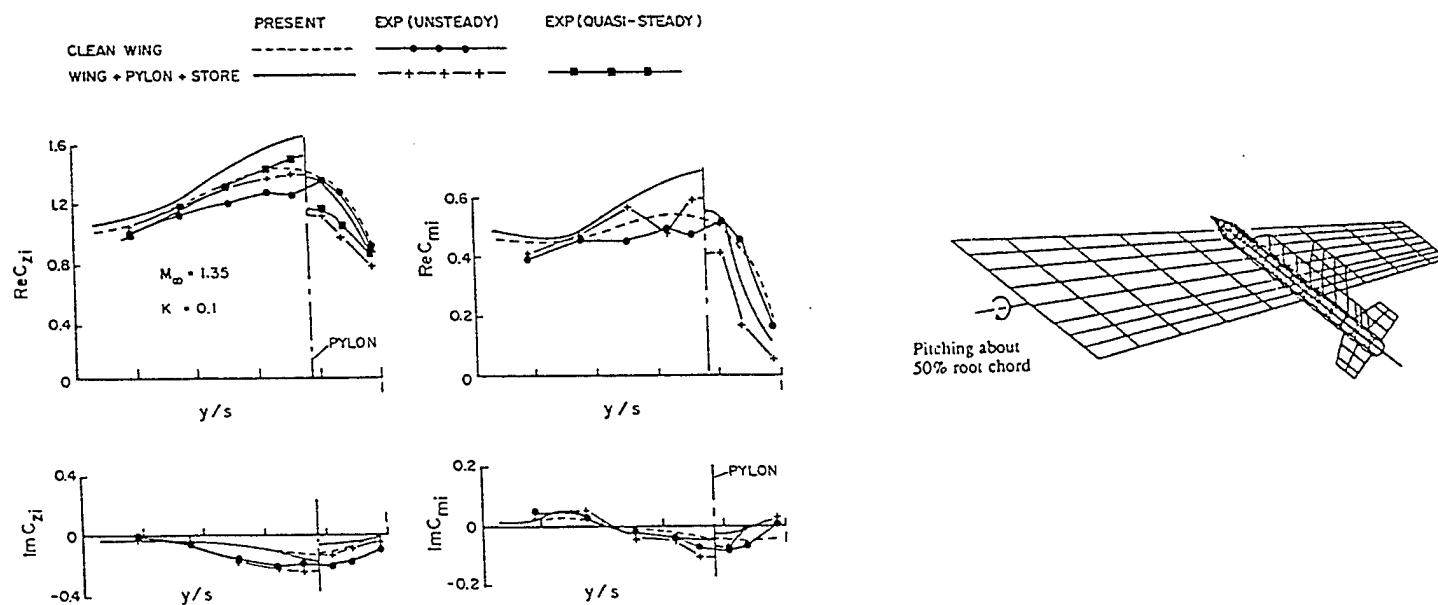


Figure 2.1.5 Unsteady Spanwise Normal Force and Pitching Moment for the Clean F-5 Wing and the Underwing Store Configuration at  $M=1.35$  and Reduced Frequency  $k=0.1$ .



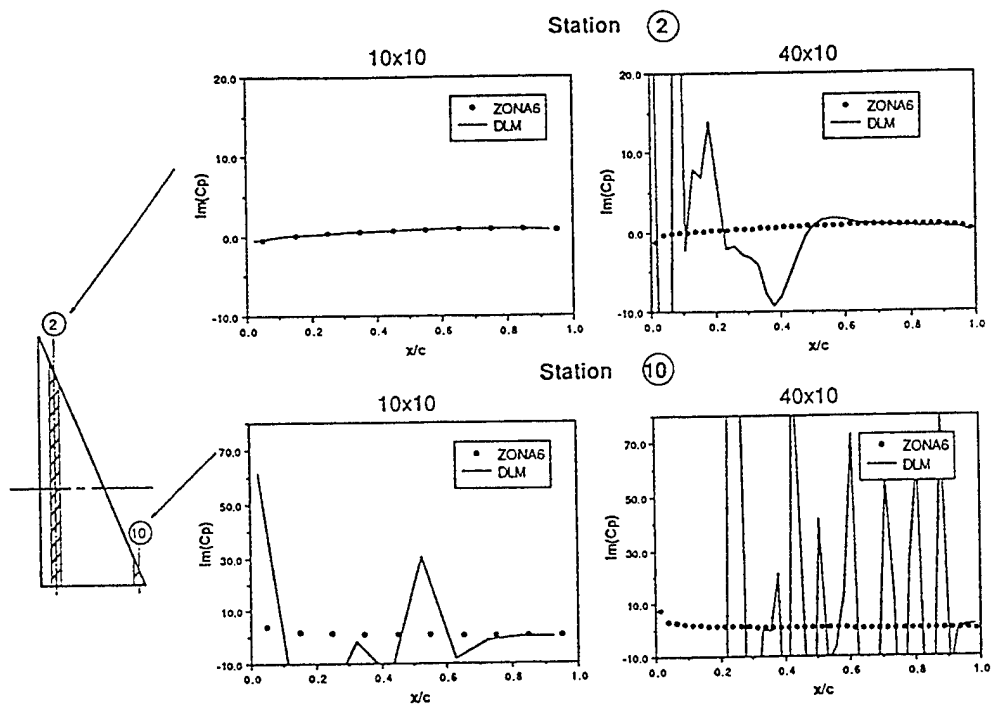


Figure 2.1.6 Out-of-Phase Pressures on Two Spanwise Stations: 70° Delta Wing ( $M=0.8$ ,  $k=0.5$ ,  $x_0=0.5c$ ).

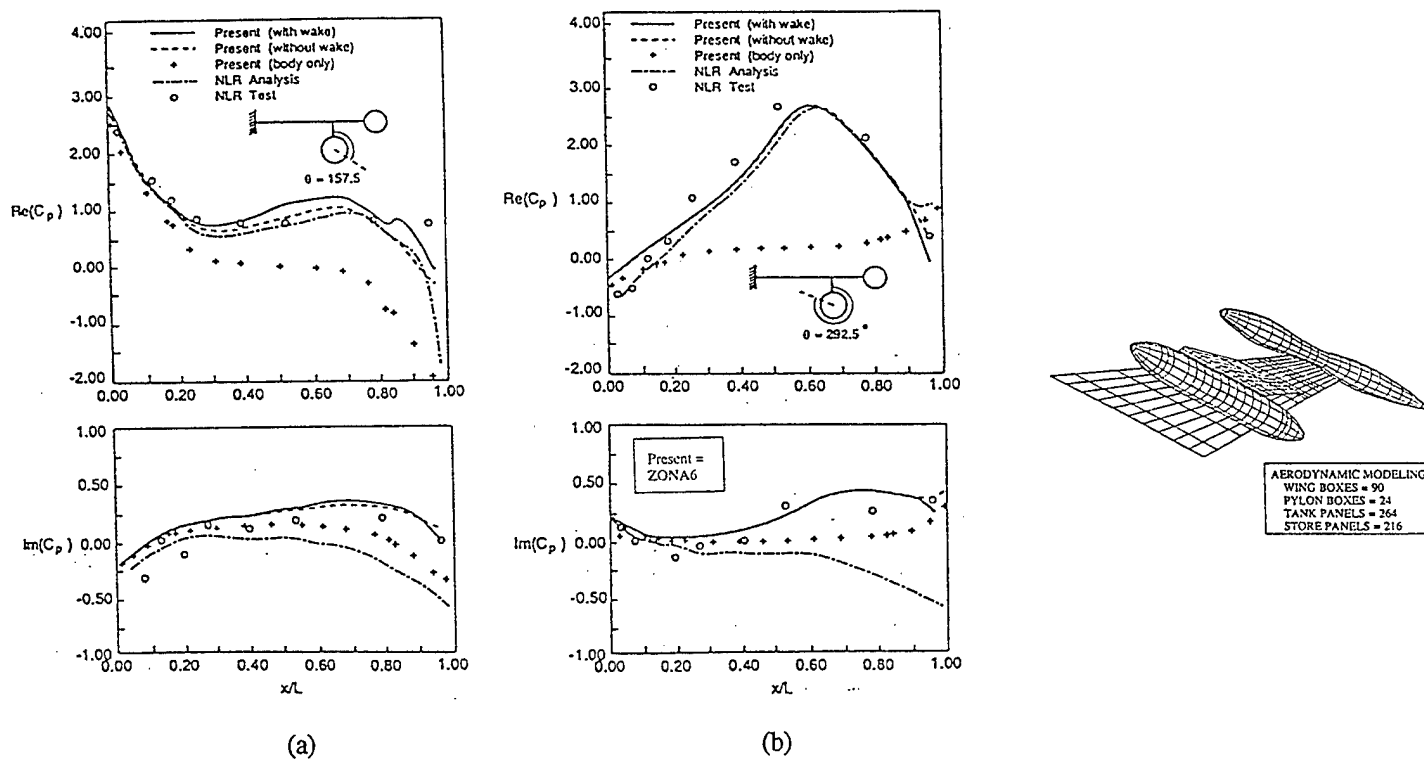
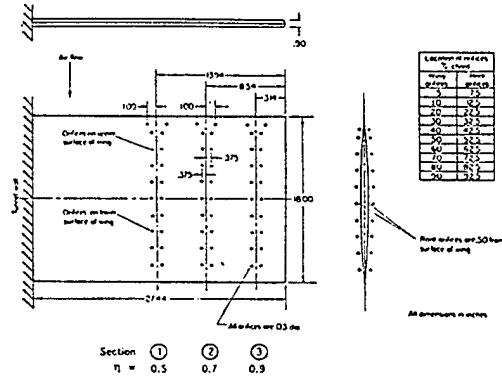


Figure 2.1.7 Unsteady Pressure Distributions Along the Store of NLR Wing-Tiptank-Pylon Store Configuration at (a)  $\theta=157.5^\circ$  and (b)  $\theta=292.5^\circ$   $M=0.45$ ,  $\alpha=0^\circ$ ,  $k=0.305$  and  $x_0=0.15C_R$ .

- **ZTAIC:** *Generates Unsteady Transonic Aerodynamics for Lifting Surface Systems (Refs 32, 33).*

Since 1985, ZONA has been following up on the development of the Transonic Strip (TES) Method originally supported by NAVAIR/ONR (Refs 31, 32) for unsteady flow computations of arbitrary wing planforms. The TES method consists of two consecutive steps added to a given nonlinear Transonic Small Disturbance Code such as ZTRAN (Ref 34), namely the chordwise mean flow correction and the spanwise phase correction. Based on the TES concept, ZONA's Transonic Aerodynamic Influence Coefficient (ZTAIC) method is developed to fully automate the computation procedure resulting in a AIC matrix (Ref 33). The computation procedure requires direct pressure input from other computed or measured data. Otherwise, it does not require airfoil shape or grid generation for a given planform. Meanwhile, all the mean-flow shock jumps are properly included in the resulting unsteady aerodynamics through the AIC formulation. Results computed by ZTAIC have been validated with existing results for a number of wing planforms with various aspect ratios. These include (shown here): the Lessing Wing at  $M=0.9$  (Ref 35, Fig 2.1.8); the LANN Wing at  $M=0.82$  (Ref 36, Fig 2.1.9); and the Norhtrop F-5 Wing with control surface (Ref 37, Fig 2.1.10). More validated cases as a part of the cases studied in Phase I will be shown in following sections. ZONA's essential improvement lies in the ZTAIC code development, which not only can provide compatible transonic AIC's in accord with ASTROS' format but also achieves considerable savings in computer time and reasonable accuracy. Furthermore, ZTAIC has a user oriented input format which is fully compatible with that of DLM.

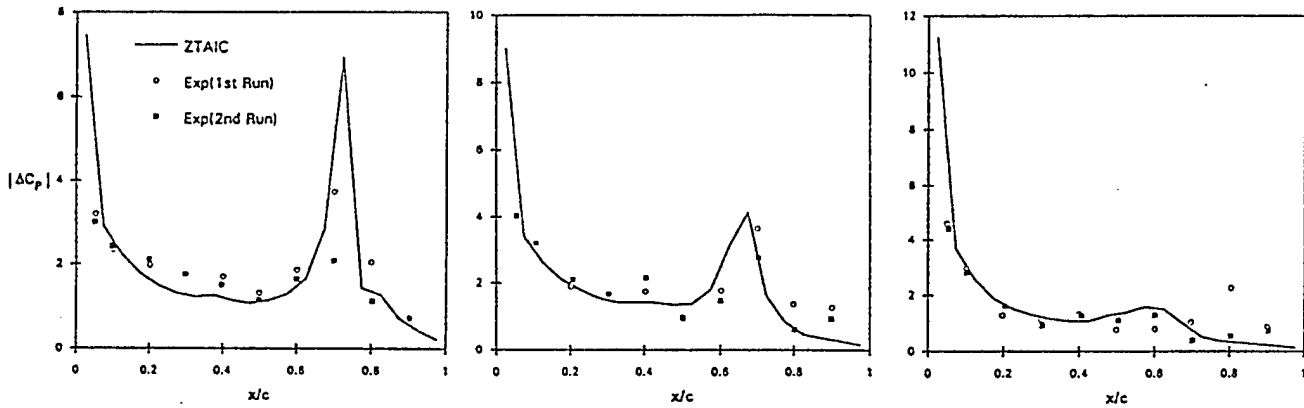


(a)

Section 1  
 $\eta = 0.5$

Section 2  
 $\eta = 0.7$

Section 3  
 $\eta = 0.9$

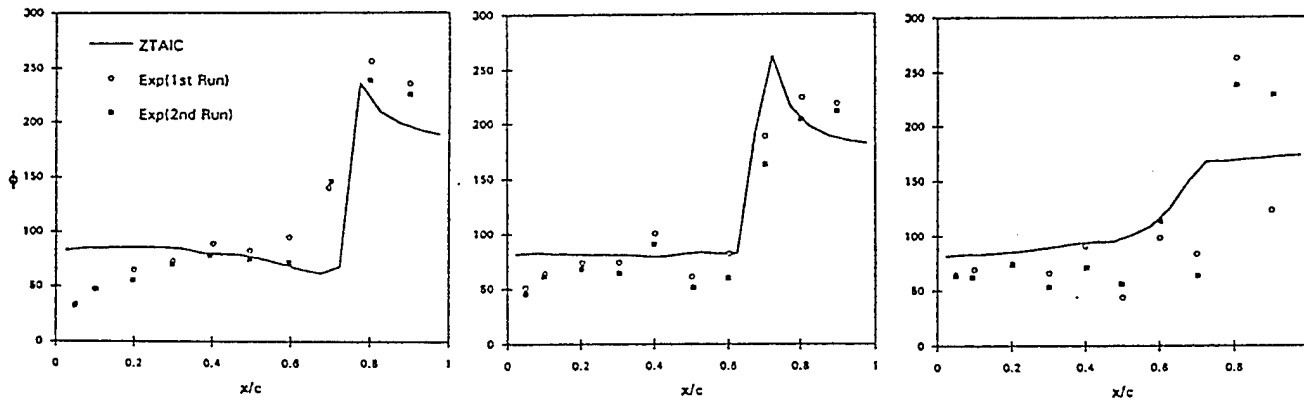


(b)

Section 1  
 $\eta = 0.5$

Section 2  
 $\eta = 0.7$

Section 3  
 $\eta = 0.9$



(c)

Figure 2.1.8 The Lessing Wing (a) Configuration (b) Magnitude of the First Bending (c) Phase Angle (in degrees) of the First Bending,  $M=0.9$ ,  $k=0.13$ .

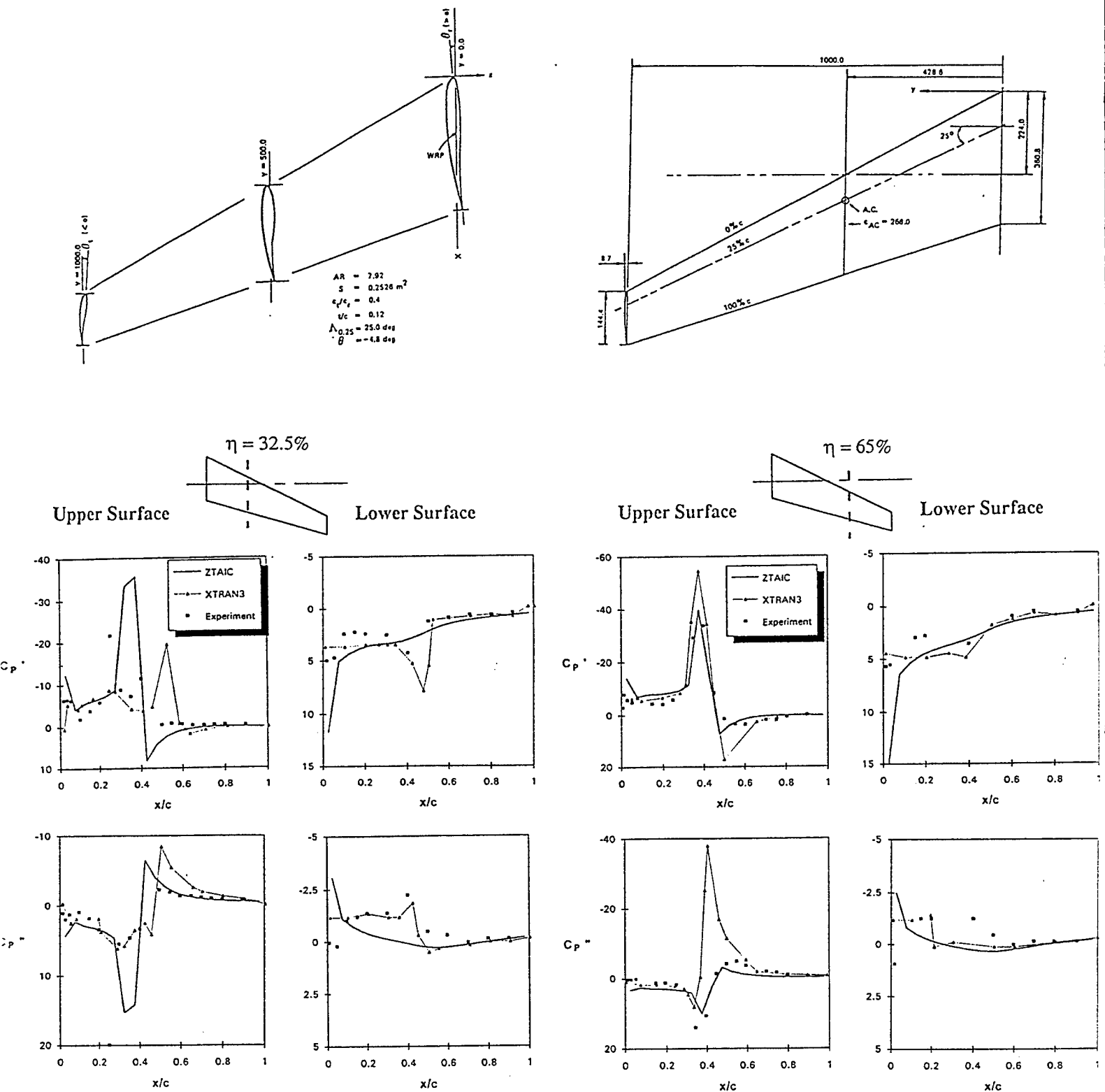
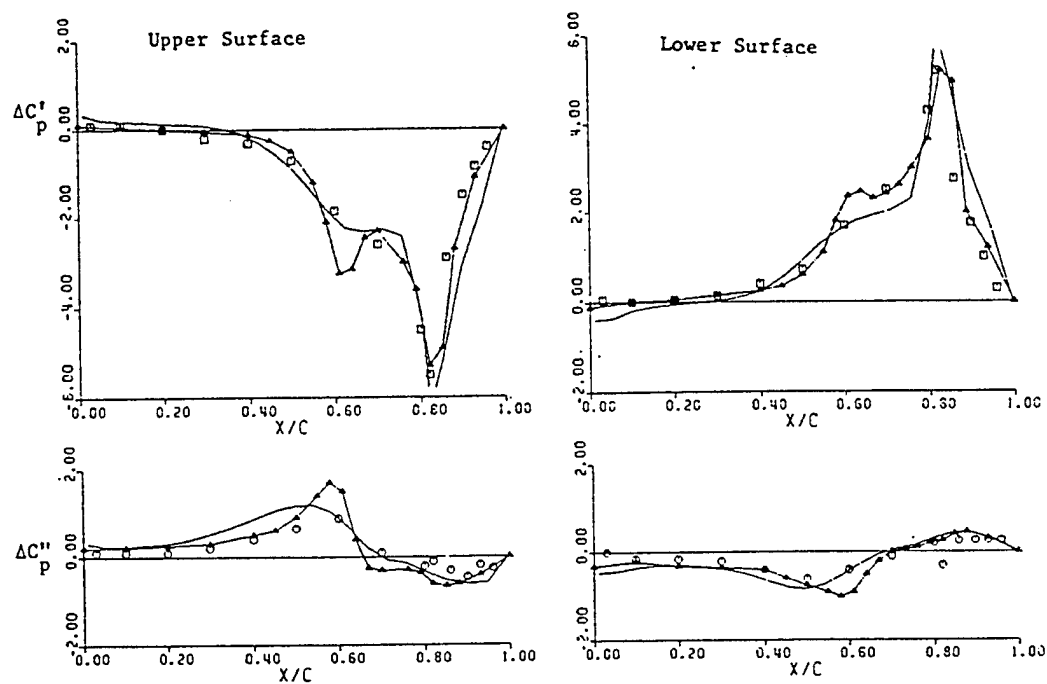
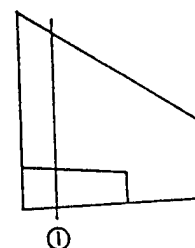


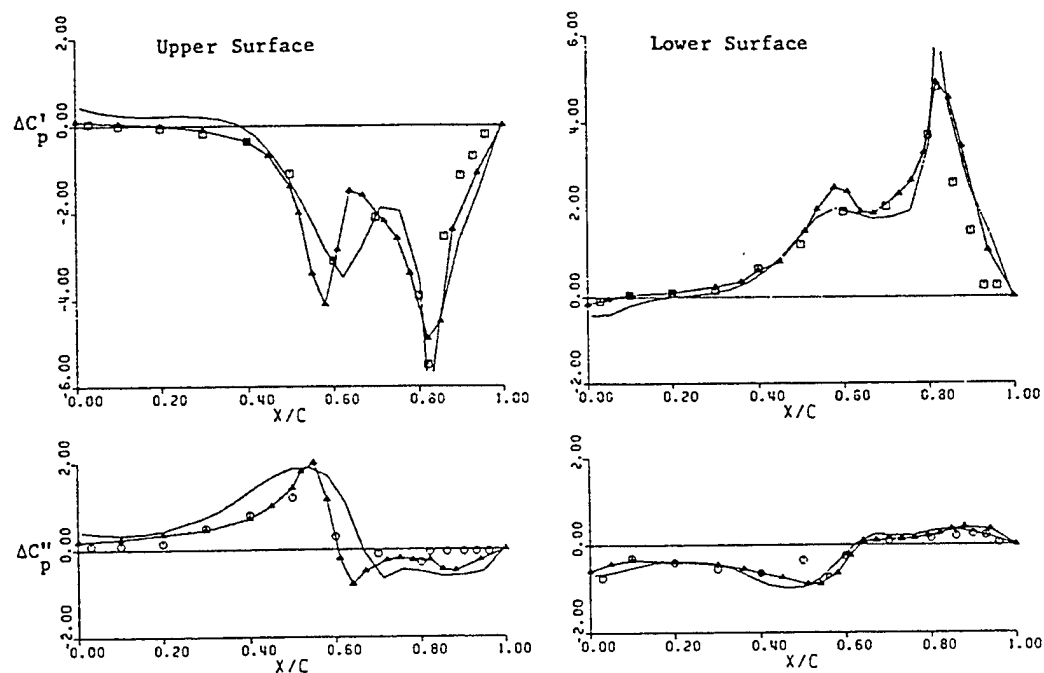
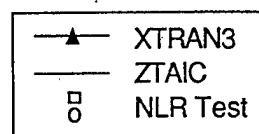
Figure 2.1.9 Lann Wing Comparison of In-Phase and Out-of-Phase Pressures at Two Spanwise Locations: Pitching Oscillation About 62% Root-Chord at  $M=0.82$ ,  $k=0.205$ .



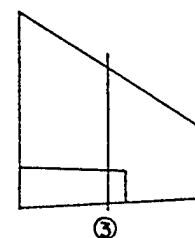
18% Spanwise Location



$M_\infty = 0.90$   
 $k_c = 0.274$   
 $\alpha_0 = 0^\circ$   
 $x_0 = 0.82 C$   
 $\delta = 0.5^\circ$



51% Spanwise Location



$M_\infty = 0.90$   
 $k_c = 0.274$   
 $\alpha_0 = 0^\circ$   
 $x_0 = 0.82 C$   
 $\delta = 0.5^\circ$

Figure 2.1.10 Northrop F-5 Wing with Oscillating Flap: Comparison of In-Phase and Out-of-Phase Pressures with Hinge Line at 82% Chord at Sections 1 and 3,  $M=0.9$ ,  $k=0.274$ .

## 2.2 Feasibility Study of ZAERO/USDA Methodology

In Phase I, the proven feasibility study of the USDA focused mainly on the unified hypersonic/supersonic and transonic flow regimes for proper verification with the existing measured data and CFD results. Three major wing planforms were considered:

- *the NASP Demonstrator Model (Ref 38)*
- *the AGARD Standard 445.6 Wing (Solid and Weakened Planforms) (Ref 39)*
- *the Modeled F-16 Wing (Ref 40)*

In all of the figures, the ZONA51U and ZTAIC codes were used to generate the k-domain aerodynamics, first by means of ZONA's UAIC formulation. The USDA for each case is then obtained through Karpel's expedient s-domain fit, called MIST (the Minimum State Technique, see Eq (4.6.2), Refs 41, 42), on the GAF's of the k-domain aerodynamics. Finally, the s-domain flutter results are presented in Root-Locus plots and were compared with those generated by the V-g method.

## • NASP Demonstrator Wing

Fig 2.2.1 shows the physical dimensions and the aerodynamic modeling of this planform. Notice that the wing cross-section is a hexagon profile.

Fig 2.2.2 presents the results of the Generalized Aerodynamic Forces (GAF's) for modes 3 and 4 in the s-domain at three hypersonic Mach numbers, namely  $M_\infty = 5.0, 10.0$  and  $15.0$ .

In obtaining these results, MIST requires only five aerodynamic approximated roots covering a range of reduced frequency from  $k = 0$  to  $k = 0.75$ . It is seen that the correlation between the k-domain results and that of the USDA are excellent.

Fig 2.2.3 presents the Root-Locus plot at these three Mach numbers for 8 modes. For cases at  $M_\infty = 5.0, 10.0$  and  $15.0$ , mode 4 is found to flutter at dynamic pressures  $q_f$  at 130, 184 and 213 psi, respectively.

Extensive comparison of various computed results has been carried out in the present NASP wing case. In Table 2.2.1, the flutter results of ZONA51U using the V-g method (k-domain) and using USDA (s-domain) are compared with those of Piston theory and the NASA CFD codes (QSCFD2d and 3d, Ref 43). Several observations can be made with respect to the collected data:

- Good agreement is found between the flutter  $q$ 's of the V-g method and the s-domain method based on ZONA51U. Flutter frequencies are also found to agree well.
- Piston theory results follow the general trend predicted by ZONA51U, except that the former results tend to become overestimated at high Mach numbers.
- Substantial discrepancies are found between the NASA/CFD results and the ZONA51U results: ZONA51U predicts more conservative flutter speeds at higher altitudes, whereas the NASA/CFD codes predict less conservative speeds at lower altitudes. In fact, ZONA51U gives the most conservative answers for all cases in this study. Our confidence on these flutter results stems from our thorough verification/validation of the ZONA51U code (Refs 21, 22). However, further validation with test data is warranted for this particular study.

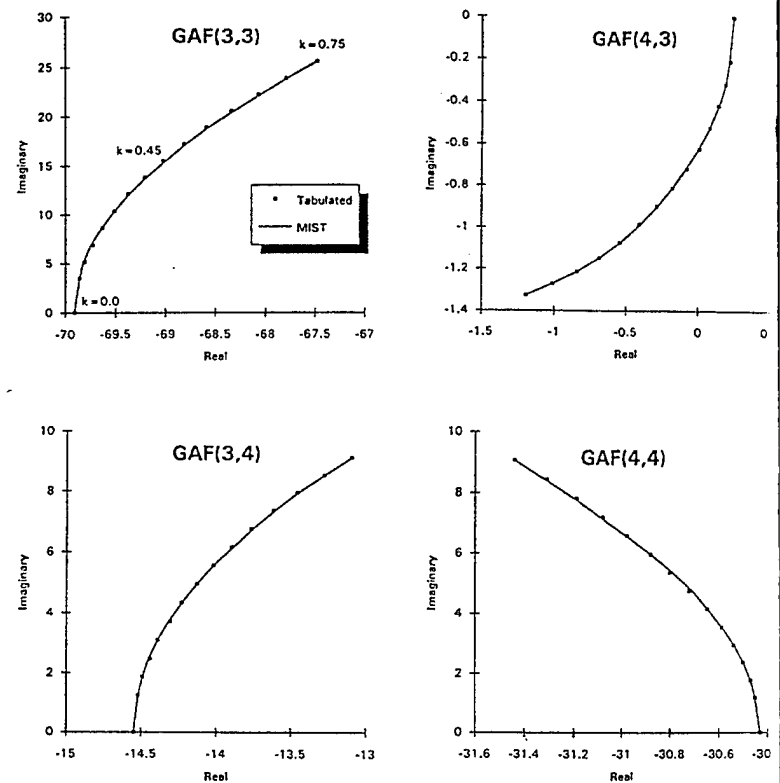
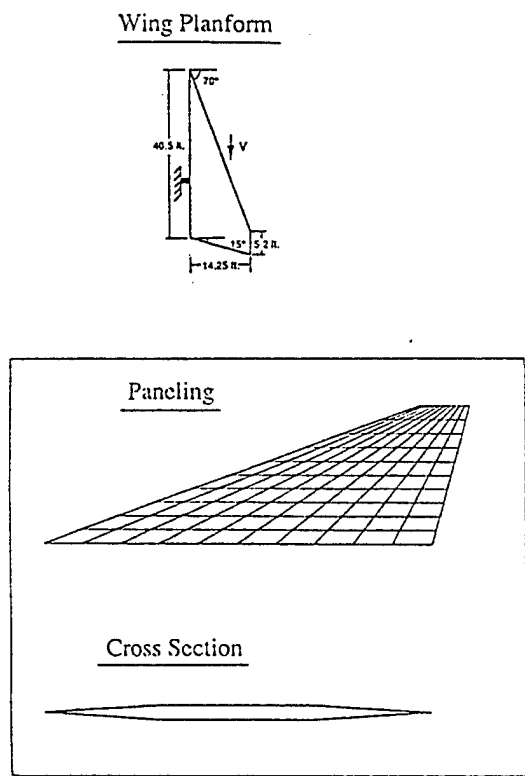
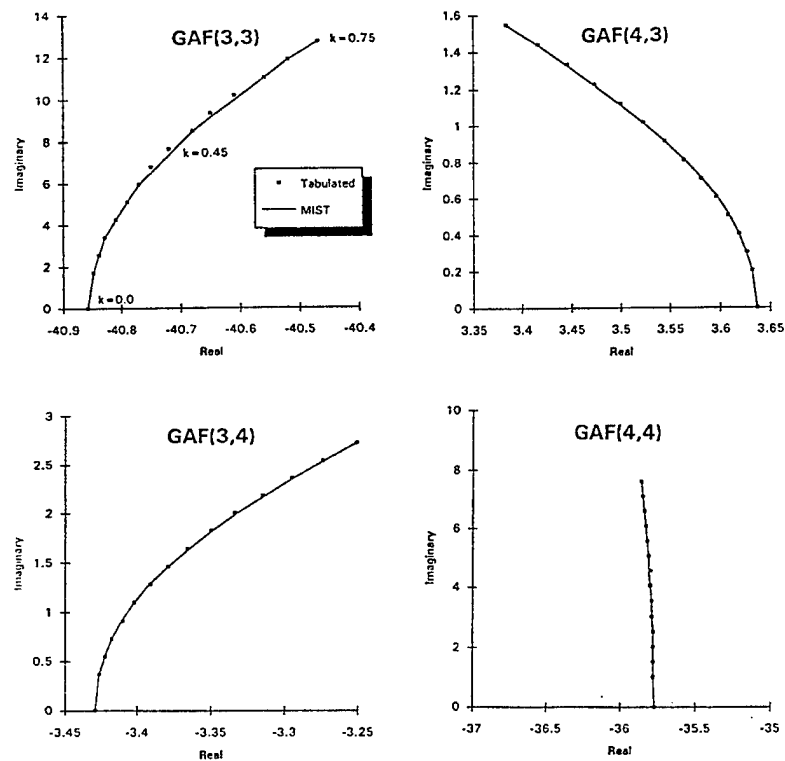
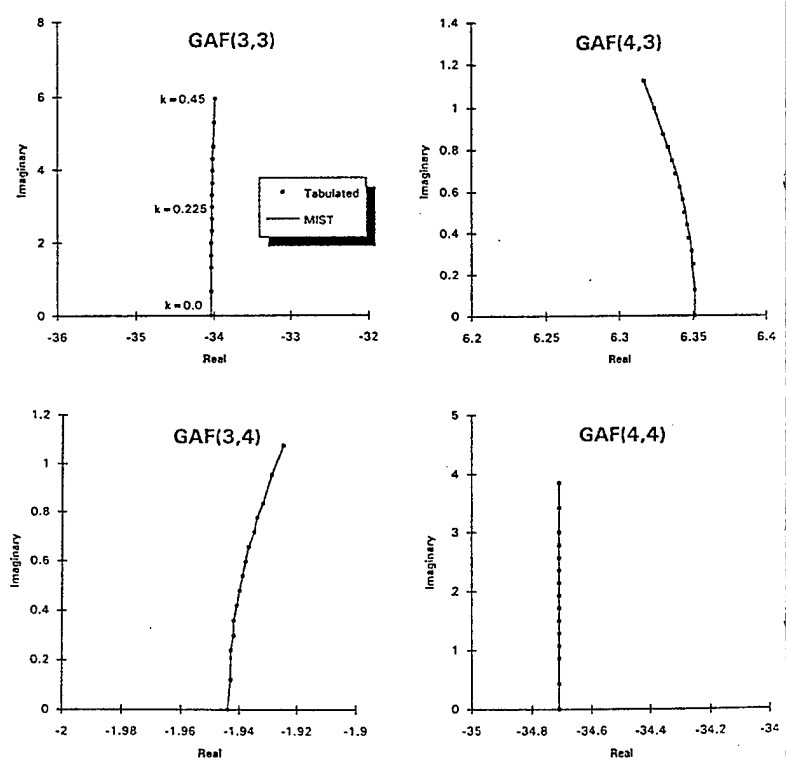


Figure 2.2.1 Aerodynamic Model of NASP Demonstrator Wing.



(b)



(c)

Figure 2.2.2 Minimum-State (MIST) Fit of Generalized Aerodynamic Forces (GAF), NASP Demonstrator Model  
(a)  $M=5.0$ , (b)  $M=10.0$ , (c)  $M=15.0$



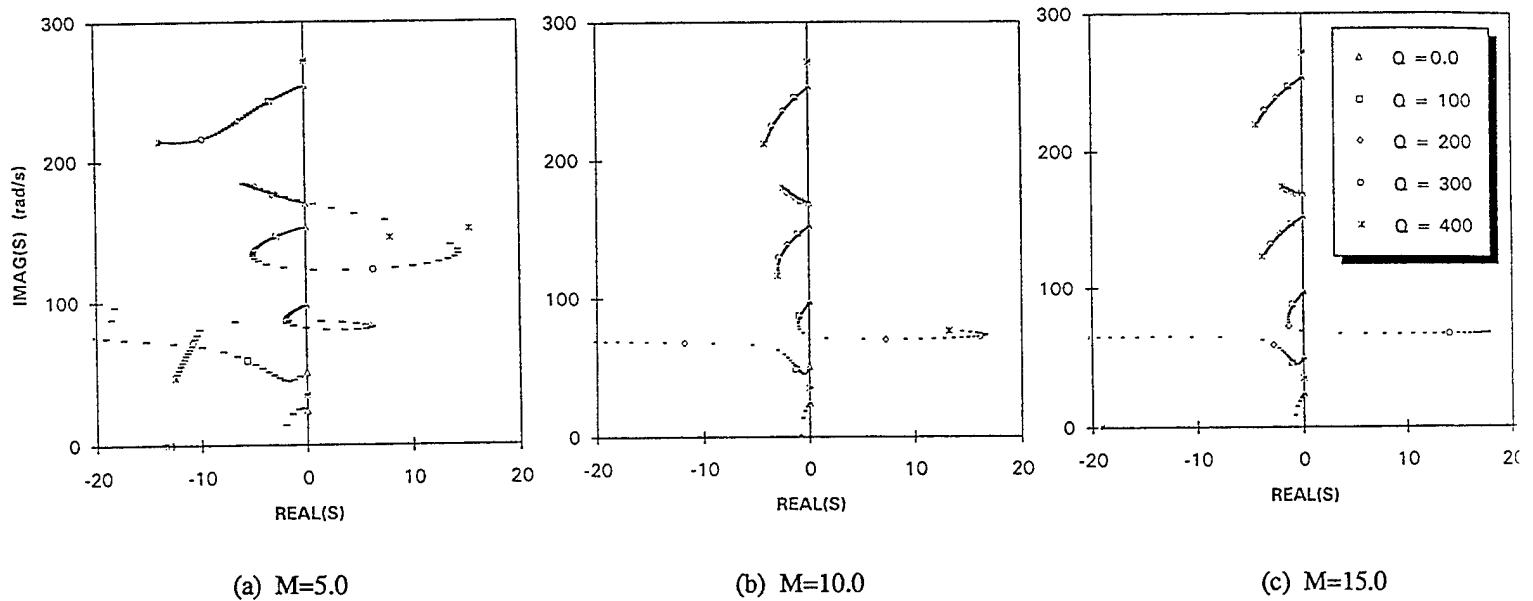


Figure 2.2.3 Root-Locus Plots of NASP Demonstrator Model at M=5.0, 10.0 and 15.0.  
 (a) 8 Modes,  $Q_f = 130$  psi,  $\omega_f = 82$  r/s on Mode 4  
 (b) 8 Modes,  $Q_f = 184$  psi,  $\omega_f = 71$  r/s on Mode 4  
 (c) 8 Modes,  $Q_f = 213$  psi,  $\omega_f = 68$  r/s on Mode 4

Aerodynamic Method	Mach Number								
	5			10			15		
	$q_f$ psi	$\omega_f$ r/s	$h$ (Kft)	$q_f$ psi	$\omega_f$ r/s	$h$ (Kft)	$q_f$ psi	$\omega_f$ r/s	$h$ (Kft)
Piston Theory	129	78	18	184	78	42	250	72	51
QSCFD 2d	169	80	11	331	81	28	982	224	22
QSCFD 3d	----	----	----	330	82	28	981	224	22
ZONA51U - V-g Method	129	82	18	175	73	42	206	70	55
- S-Domain	130	82	18	184	71	41	213	68	54

$h$  = Approximate matchpoint altitude.

Table 2.2.1 Comparison of Flutter Dynamic Pressures and Frequencies of NASP Demonstrator Model at M=5.0, 10.0 and 15.0.

### • *The AGARD Standard 445.6 Wing*

The AGARD Standard 445.6 wing planform has two structural models: the solid wing and the weakened wing. This is an ideal case for testing ZTAIC's AIC capability, since the aerodynamic shapes of the two structural models are identical and, therefore, the AIC matrix remains the same.

Fig 2.2.4 presents the flutter results of the weakened wing. At a subsonic Mach number, say  $M_\infty = 0.678$ , the ZTAIC result is in perfect agreement with that of ZONA6, as expected. At other supercritical transonic Mach numbers, say  $M_\infty = 0.95$ , ZTAIC predicts a pronounced transonic dip which is comparable to results predicted by the CAP-TSD code (Ref 44).

Fig 2.2.5 presents the flutter results for the solid wing. Since the mean planform remained unaltered for the aerodynamics, the AIC's used here would be the same as those used for its weakened counterpart. Thus, only a re-start of the code (using the previously generated AIC matrix) was required for all remaining cases. This amounted to only one minute of CPU time per case, a great savings. Again, the ZTAIC results for these cases agree well with the CAP-TSD result and measured data. This demonstrates that ZTAIC is ideally suited for aeroelastic optimization, particularly in the ASTROS MDO environment. Fig 2.2.6 presents the MIST fit of the GAF's for the 445.6 weakened wing at  $M_\infty = 0.95$ . Unlike the previous cases, some slight discrepancy is found in the GAF (1,2), which might be caused the stringent feature of the supercritical mean flow at this Mach number.

Fig 2.2.7 presents the root-locus plot of the same case using the MIST fit results of the above. The flutter speed predicted here ( $V_f = 1015$  fps) is in reasonable agreement with the one predicted by the V-g method ( $V_f = 944$  fps, see Table of Fig 2.2.4). The discrepancy is caused by slight discrepancies in the MIST-fit in the transonic range (e.g. see  $Q_{12}$  of Fig 2.2.6).

Test Cases		Wind Tunnel Data		ZONA6 --- (Linear)		ZTAIC $\Delta$ (Nonlinear)		CAPTSD $\diamond$ (Nonlinear)	
M	$\rho$ (slug/ft <sup>3</sup> )	$\omega_f$ (Hz)	$V_f$ (ft/sec)	$\omega_f$ (Hz)	$V_f$ (ft/sec)	$\omega_f$ (Hz)	$V_f$ (ft/sec)	$\omega_f$ (Hz)	$V_f$ (ft/sec)
0.678	0.000404	17.98	759.1	19.81	766.0	19.30	761.0	19.2	768
0.900	0.000193	16.09	973.4	16.31	984.0	16.38	965.2	15.8	952
0.950	0.000123	14.50	1008.4	16.18	1192.0	13.46	944.0	12.8	956

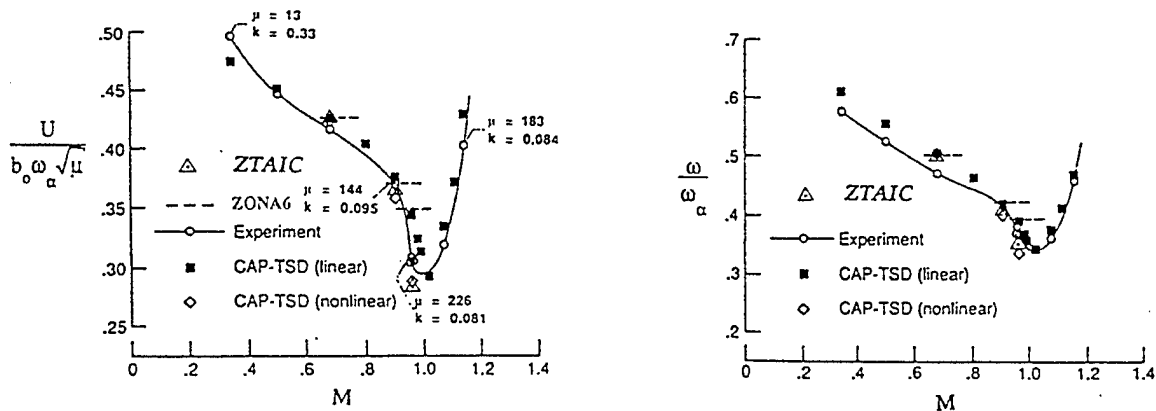


Figure 2.2.4 Comparison of Flutter Speed and Frequency of 445.6 Weakened Wing at M=0.678, 0.90 and 0.95.

Test Cases		Wind Tunnel Data*		ZONA6 (Linear)		ZTAIC** (Nonlinear)		CAPTSD* (Nonlinear)	
M	$\rho$ (slug/ft <sup>3</sup> )	$\omega_f$ (Hz)	$V_f$ (ft/sec)	$\omega_f$ (Hz)	$V_f$ (ft/sec)	$\omega_f$ (Hz)	$V_f$ (ft/sec)	$\omega_f$ (Hz)	$V_f$ (ft/sec)
0.90	0.00357	27.00	452.0	26.75	439.0	25.71	418.0	25.8	435.0
0.95	0.00320	26.91	479.0	26.89	462.0	25.46	450.0	26.2	472.1

\* Interpolated between Mach 0.87, 0.92 and 0.96.

\*\* Restart Run Using AIC's of Weakened Wing (1 min cpu/case).

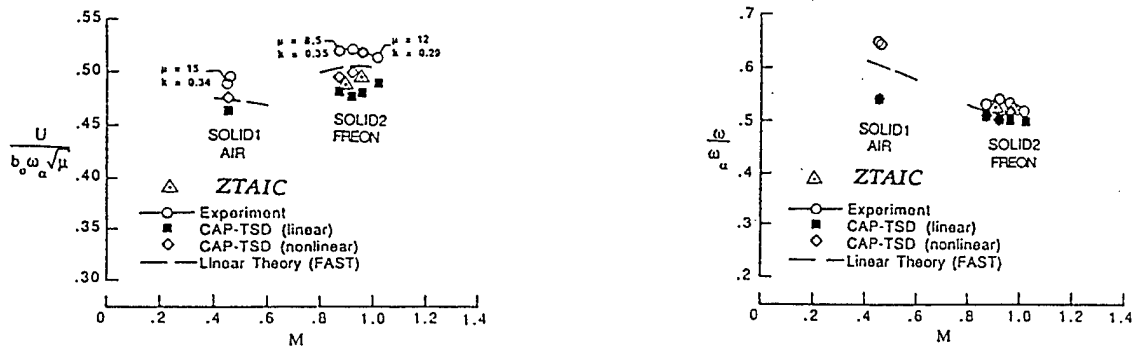


Figure 2.2.5 Comparison of Flutter Speed and Frequency of 445.6 Solid Wing at M=0.90 and 0.95.

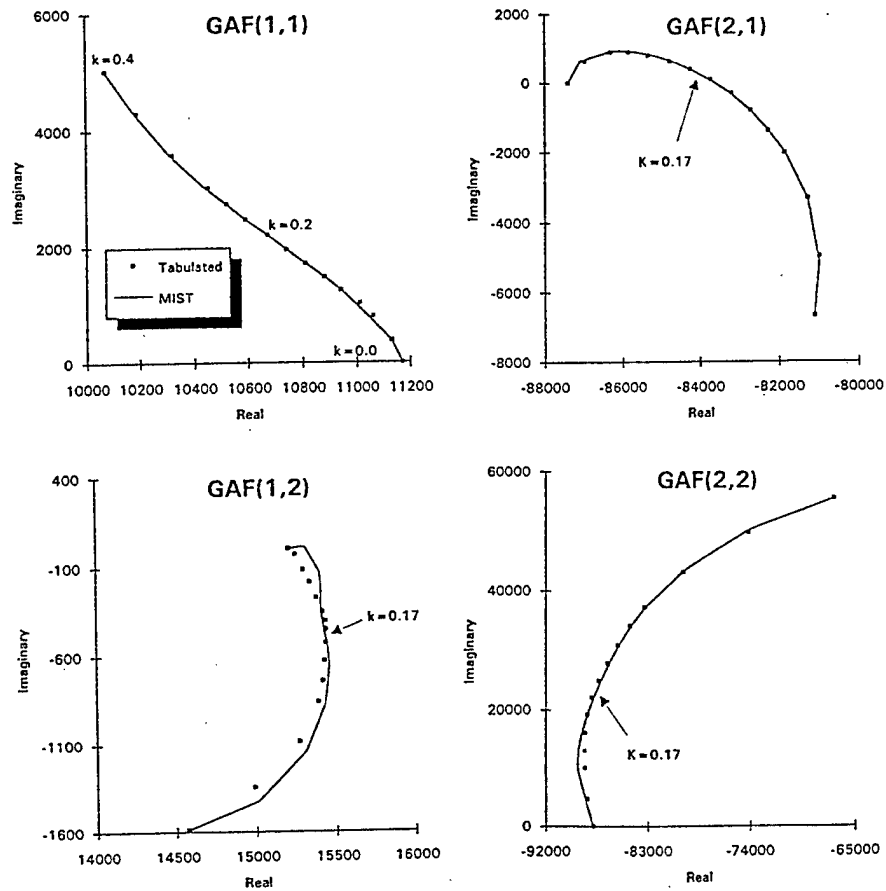


Figure 2.2.6 Minimum-State Approximation of Generalized Aerodynamic Forces of 445.6 Weakened Wing at  $M=0.95$  Computed by ZTAIC.

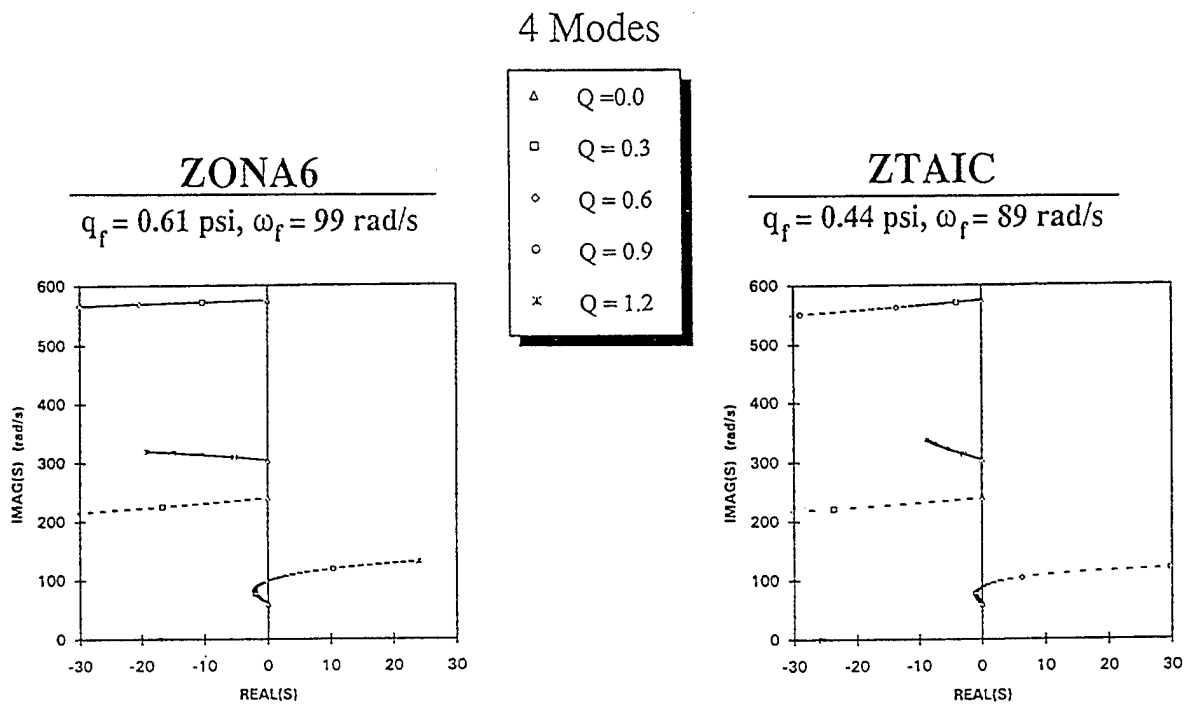


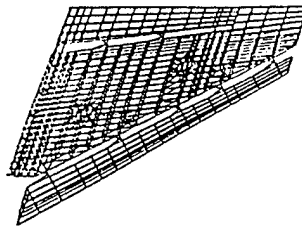
Figure 2.2.7 Root-Locus Plots of 445.6 Weakened Wing at  $M=0.95$  Using S-Domain Aerodynamics Computed by ZTAIC and ZONA6.

- *Modeled F-16 Wing*

Fig 2.2.8 presents the structural model and the flutter boundary of a modeled F-16 wing. It is seen that the flutter results of ZTAIC are in good agreement with those of XTRAN3 and CAPTSD, particularly at  $M_\infty = 0.95$ . It should be noted that the flutter mechanism changes from  $M_\infty = 0.9$  to  $M_\infty = 0.95$ , as indicated by the jump in the flutter frequency (from 6.8 Hz to 19 Hz). ZTAIC concurs with the other two codes in the prediction of this mechanism.

Fig 2.2.9 presents the MIST-fit of the s-domain results for four GAF's. For this case, MIST achieves a better fit than for the case of the 445.6 wing. Notice that the dotted lines in the background is the fitted subsonic GAF's using ZONA6. Substantial differences can be seen between the results of ZTAIC and ZONA6, showing strong transonic characteristics for this wing at  $M_\infty = 0.95$ .

# Flutter Speed and Frequency vs. Mach Number 4% Parabolic Arc Airfoil Section



Structural Model

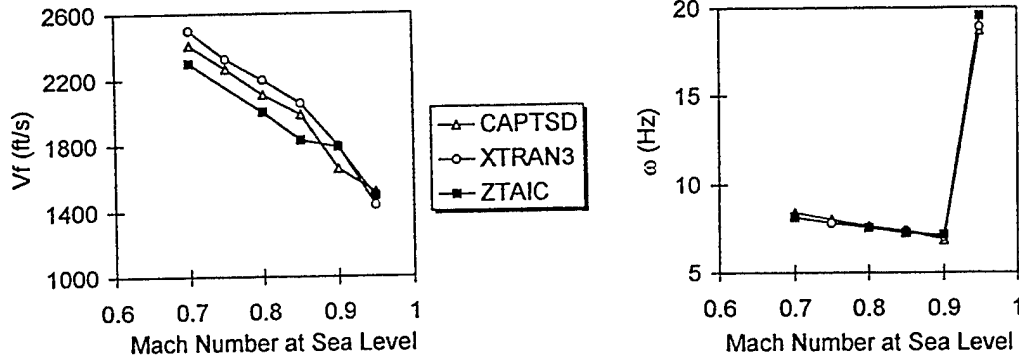


Figure 2.2.8 Flutter Speeds and Frequencies of Modeled F-16 Wing Computed by ZTAIC, CAPTSD and XTRAN3.

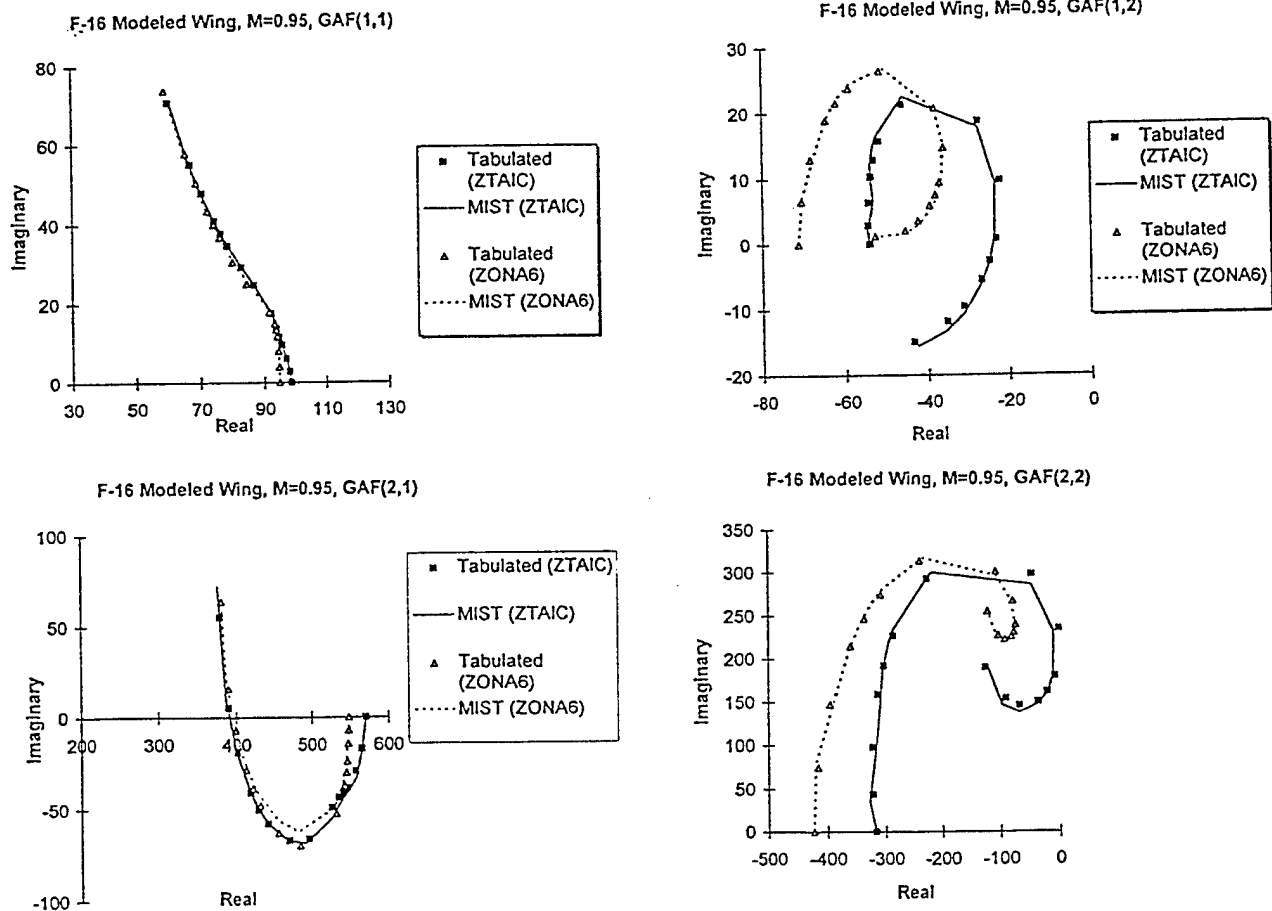


Figure 2.2.9 Minimum-State Approximations of Generalized Aerodynamic Forces of Modeled F-16 Wing at  $M=0.95$  Computed by ZTAIC and ZONA6.

## SECTION 3

### AERODYNAMIC GEOMETRY MODULE (AGM)

#### 3.1 The Aerodynamic Geometry Module of ZAERO

The development of the Aerodynamic Geometry Module (AGM) is motivated by the lack of a unified input format for various aerodynamic methods which would compute the steady and/or unsteady aerodynamics in their valid Mach number ranges. Specifically different flight conditions require different computational methods and, consequently, require different geometric parameters of the aerodynamic configuration. The proposed AGM will provide ASTROS' AERO module with a universal set of geometric definitions for the ZONA6, ZONA7, ZONA51U and ZTAIC codes in ZAERO Module. With the understanding that the USSAERO code, currently imbedded in ASTROS' AERO Module, will be replaced by other higher-order panel methods, the AGM will also have the capability of interfacing with other higher-order panel methods such as QUADPAN, PANAIR and ZONAIR (Refs 24, 25).

With respect to the geometric definitions, there are generally three types of panel methods (for both steady and unsteady codes):

- (i) *Lifting Surface Methods:* The singularity is placed on the mean-surface of the lifting surface such as the Doublet Lattice Method (DLM), Constant Pressure Method (CPM), ZTAIC, ZONA51U, and the Carmichael flat plate method.
- (ii) *High -Order Surface Panel Methods:* The singularity is placed on the exact surface of the configuration. There is no discrimination between body-like components and wing-like components. These methods include QUADPAN, PANAIR and ZONAIR.
- (iii) *Hybrid Methods:* The singularity is placed on the mean surface of the wing-like components and on the exact surface of the body-like components. These methods include ZONA6 and ZONA7.

Based on the aforementioned, two types of input will be incorporated into AGM: the "surface-panel" input for higher-order panel methods and the "thin-wing" input for the lifting surface methods. For hybrid methods, no additional type of input is needed, since the connectivity between the "thin-wing" and the "surface-panel" can be suitably defined.

#### *Surface Panel Input*

The most convenient way to define surface panels for modeling an arbitrary configuration is the NASTRAN type of input. Five new bulk data entries will be employed: AGRID, AQUAD, ATRIA, AQDMEM and ABAR.

AGRID defines a location of an aerodynamic grid. AQUAD and ATRIA define a quadrilateral and triangular surface panels, respectively. AQDMEM is used to model an arbitrary wake panel. ABAR defines a flat wake sheet extending from the wing trailing edge or the end of a truncated body to infinity. Fig (3.1.1) demonstrates the use of these new bulk data entries in modeling an arbitrary wing-body-tail configuration.

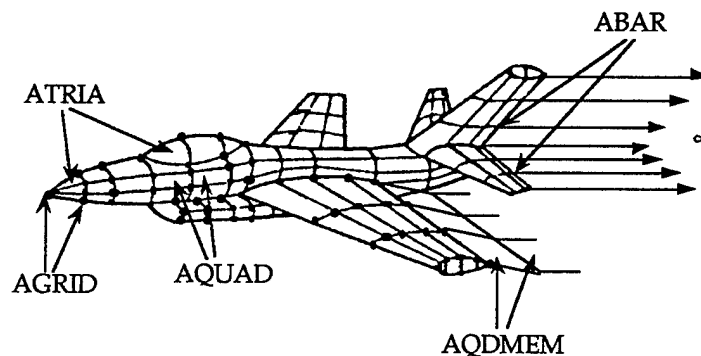


Figure 3.1.1 New Bulk Data Entries for Aerodynamic Modeling of an Arbitrary Wing-Body-Tail Configuration.

The boundary condition of a solid body in inviscid flow is satisfied by imposing the zero-normal-flow condition (no flow can penetrate into the body) on the body surface. However, this is not true for an inlet face where the flow is allowed to penetrate into the body. To define this kind of boundary condition, all AQUAD and ATRIA cards are referred to as a set of "property cards" defined by the PAERO bulk data entry. The PAERO card allows the user to specify the percentage of the mass flow ratio that is allowed to penetrate into the body. The value of this percentage can be found based on the engine operating condition (e.g., for zero mass flow ratio, the zero-normal-flow condition is imposed).

The user may often be interested in computing aerodynamic loads on a group of components (e.g. the loads on an external store). A new bulk data entry "ACORD" is defined which specifies the identification number of a local coordinate system and the identification number of a group of components.

In what follows, detailed definitions for each of the above new bulk data entries are given.

- **Input Data Entry: AGRID**

Description: Defines the location of a geometric grid point of the aerodynamic model.

Format and Example

1	2	3	4	5	6	7	8	9	10
AGRID	ID	CORD	X	Y	Z				
AGRID	2	3	1.0	2.0	1.0				

Field:

ID Aerodynamic grid identification number (integer > 0)  
CORD Identification number of ACORD bulk data entry (integer > 0)  
X, Y, Z Location of the grid point in the local coordinate system defined in the ACORD bulk data entry

- **Input Data Entry: AQUAD**

Description: Defines an aerodynamic surface panel that has four corner points (quadrilateral panel).

Format and Example

1	2	3	4	5	6	7	8	9	10
AQUAD	ID	IP	ID1	ID2	ID3	ID4			
AQUAD	3	1	2	3	6	7			

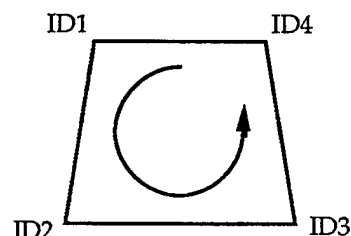


**Field:**

ID Identification number of the surface panel (integer > 0)  
 IP Identification number of PAERO bulk data entry for defining the aerodynamic boundary condition on the panel (integer > 0)  
 ID1, ID2, ID3, ID4 Four AGRID ID's specifying the corner points of the panel

**Remarks:**

The sequence of the four grid ID's defines the out-normal of the AQUAD panel. For an observer standing on the wet surface (the surface on which the flow is passing) of the panel, the sequence of these four grids must follow the right-hand-rule as shown in the figure to the right.



- Input Data Entry: ATRIA**

Description: Defines a aerodynamic surface panel that has three corner points (triangular panel).

**Format and Example**

1	2	3	4	5	6	7	8	9	10
ATRIA	ID	IP	ID1	ID2	ID3				
ATRIA	4	1	3	4	7				

**Field:**

ID Identification number of the surface panel (integer > 0)  
 IP Identification number of PAERO bulk data entry for defining the aerodynamic boundary condition on the panel (integer > 0)  
 ID1, ID2, ID3 Three AGRID ID's specifying the corner points of the panel

**Remarks:**

The sequence of the three grid ID's defines the out-normal of the ATRIA panel. For an observer standing on the wet surface (the surface on which the flow is passing) of the panel, the sequence of these three grids must follow the right-hand-rule.

- Input Data Entry: AQDMEM**

Description: Defines a wake panel on an arbitrary wake surface that is shed from the trailing edge of a wing or the end section of a truncated body.

**Format and Example**

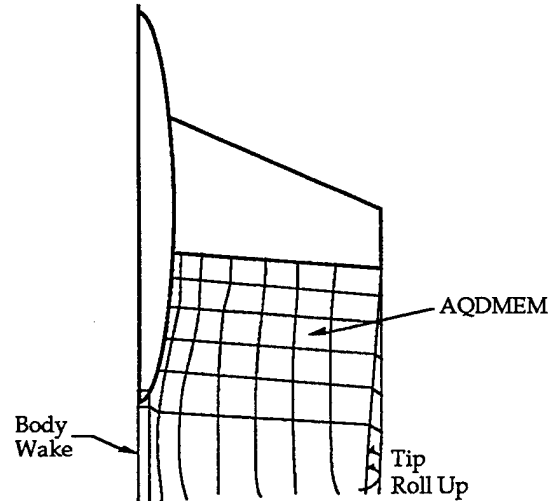
1	2	3	4	5	6	7	8	9	10
AQDMEM	ID	IP	ID1	ID2	ID3	ID4			
AQDMEM	7	---	3	4	6	8			

**Field:**

ID Identification number of AQDMEM (integer > 0)  
 IP Not Used  
 ID1, ID2, ID3, ID4 Four AGRID ID's specifying the corner points of the panel

Remarks:

1. The figure to the right shows an arbitrary wake surface shed from the trailing edge of the wing and end section of the body. AQDMEM cards are employed to model this wake surface.
2. The AQDMEM immediately behind the trailing edge must be attached to the wing/body trailing edge (i.e. the grid ID of the leading edge of AQDMEM must be identical to the grid ID of the trailing edge of the wing/body).
3. On the wake surface, the boundary condition  $\frac{\partial \phi}{\partial x} = 0$  is imposed.



• **Input Data Entry: ABAR**

Description: Defines a line segment from which the wake is shed downstream to infinity.

Format and Example

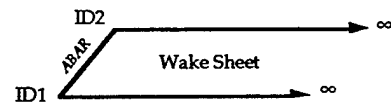
1	2	3	4	5	6	7	8	9	10
ABAR	ID	IP	ID1	ID2					
ABAR	3	---	2	4					

Field:

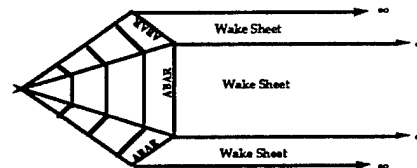
ID Identification number of the ABAR bulk data entry  
 IP Not Used  
 ID1, ID2, ID3 Two AGRID ID's defining the line segment

Remarks:

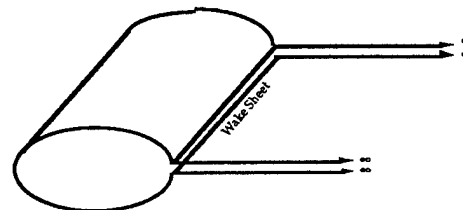
1. If the wake surface is assumed to be a flat sheet extending from the trailing edge of the wing/body, one ABAR is sufficient to define one strip of the wake sheet.
2. ABAR must be attached to one, but no more than one, AQUAD or ATRIA, (i.e. the line segment must be one of the sides of a AQUAD or ATRIA panel).
3. The wake sheet shed downstream from the line segment is demonstrated in the figure to the right. The edge of the wake sheet starts from the grid point and stretches to infinity, parallel to the X-axis.



4. For a truncated end body, the ABAR's must be attached to the trailing edge of all panels at the end of the body.



5. In modeling a thick wing type of body, two grid points with the same X, Y and Z locations must be specified at the trailing edge of the body. Two ABAR's are attached to the upper and lower side of the trailing edge. In this way, the potential jump of the wake effect can be represented by the potential difference between these two wake sheets.



- **Input Data Entry: PAERO**

Description: Defines the aerodynamic boundary condition of a surface panel.

Format and Example

1	2	3	4	5	6	7	8	9	10
PAERO	ID	FLWRT							
PAERO	3	0.0							

Field:

ID Identification number of PAERO  
 FLWRT Amount of mass ratio (in percentage) which is allowed to penetrate into the panel  
 FLWRT=0.0 represents a solid surface (the zero-normal-velocity boundary condition is imposed)  
 FLWRT=100.0 represents an inlet face with no flow leakage

- **Input Data Entry: ACORD**

Description: Defines a group of aerodynamic components.

Format and Example

1	2	3	4	5	6	7	8	9	10
ACORD	ID	CP	DELTA	XMCNT	YMCNT	ZMCNT			
ACORD	3	7	0.0	1.0	2.3	4.0			

Field:

ID Identification number of the ACORD bulk data entry (All AGRID data entries must refer to ACORD)  
 CP Identification number of local coordinate system in which the location of AGRID is defined  
 DELTA Inclination angle of the body axis to the free stream defined in the local coordinate system, positive nose up, and measured in degrees. This parameter will not change the panel position. Its effect is introduced in the boundary condition. Therefore, DELTA must be a small value. Since most under-wing stores have a small inclination angle to the free stream, this input would facilitate the user with a simpler definition of inclined bodies  
 XMCNT, YMCNT, ZMCNT Pitch and yaw moment center defined in the local coordinate system and used only for calculating the pitch and yaw moment of each subsystem

### *Lifting Surface Input*

In defining an aerodynamic panel element (a lifting surface), the CAERO1 data entry of ASTROS is modified to cope with the thickness distribution for ZONA51U and steady pressure distribution for ZTAIC. The connectivity of the lifting surface to a surface panel model can also be specified. This is done by defining a new bulk data entry "CAERO7" as follows:

- **Input Data Entry: CAERO7**

Description: Defines a lifting surface (panel) for the ZONA6, ZONA7, ZONA51U and ZTAIC methods.

Format and Example

1	2	3	4	5	6	7	8	9	10
CAERO7	EID	IP	NSPAN	NCHORD	LSPAN	ISCP			+ABC
CAERO7	1	1	10	10	3	2			

1	2	3	4	5	6	7	8	9	10
CAERO7	XRL	YRL	ZRL	RCH	LRCHD	RFOIL			+AB
+ABC	0.0	0.0	0.0	1.0	3	1			

1	2	3	4	5	6	7	8	9	10
CAERO7	XTL	YTL	ZTL	TCH	LTCHD	TFOIL			
+AB	0.0	1.0	0.0	0.5	10	1			

**Field:**

EID Identification number of CAERO7  
IP Identification number of ACORD entry specifying the group of the CAERO7  
NSPAN Number of spanwise boxes  
LSPAN Number of chordwise boxes  
ISCP Identification number of ITAIC entry for specifying the steady pressure input of each strip (Used only for the ZTAIC method)  
XRL, YRL, ZRL Location of the leading edge at root in the local coordinates and defined in the ACORD entry  
RCH Root chord length  
LRCHD If LRCHD>0, LRCHD is the identification number of an AEFAC data entry containing a list of division points for chordwise boxes along the root chord  
If LRCHD<0, -LRCHD is the identification number of an AEFAC data entry containing a list of AGRID ID's. Thus the root is attached to a surface panel model. This provides the "connectivity" information of the lifting surface model with the surface panel model.  
RFOIL Identification of a PAFOIL entry specifying the thickness and camber of the airfoil at the root (Only used for the ZONA51U method)  
XTL, YTL, ZTL Same as XRL, YRL, ZRL, but for the tip  
TCH Tip chord length  
LTCHD Same as LRCHD, but for the tip  
TFOIL Same as RFOIL, but for the tip

• **Input Data Entry: ITAIC**

Description: Defines a set of AEFAC entries for steady pressure input for each strip.

**Format and Example**

1	2	3	4	5	6	7	8	9	10
ITAIC	ISCP	NX1	IAX1	IACPU1	IACPL1	NX2	IAX2	IACPU2	+ABC
ITAIC	4	20	1	3	3	20	1	4	

1	2	3	4	5	6	7	8	9	10
ITAIC	IACPL2	---	---	---	NXN	IAXN	IACPUN	IACPLN	+ABC
+ABC	3	---	---	---	21	10	1	2	

**Field:**

ISCP Identification number of ITAIC indexed by the CAERO7 entry if the ZTAIC method is used  
NXi The number of steady pressure points to be input along the i-th strip  
IAXi ID of AEFAC entry that defines NXi number of X locations of the steady pressure ( $0.0 \leq X \leq 1.0$ ) of the i-th strip  
IACPUi ID of AEFAC entry that defines NXi number of pressure coefficients on the upper surface of the i-th strip  
IACPLi ID of AEFAC entry that defines NXi number of pressure coefficients on the lower surface of the i-th strip

**Remarks:**

The total number of NXi, IAXi, IACPUi and IACPLi must be NSPAN, where NSPAN is defined in the CAERO7 entry.

- **Input Data Entry: PAFOIL**

Description: Defines the airfoil thickness and camber for the ZONA51U method.

Format and Example

1	2	3	4	5	6	7	8	9	10
PAFOIL	PID	NX	IAFX	IATU	IATL	ICAM	RADIUS		
PAFOIL	PID	21	3	4	7	5	0.10		

Field:

PID Identification number of PAFOIL indexed by the CAERO7 entry  
 NX Number of X locations in percent chord to define the thickness and camber ( $0.0 \leq X \leq 100.0$ )  
 IAFX Identification number of AEFAC entries containing NX numbers of X locations. The first and last values must be 0.0 and 100.0, respectively.  
 IATU Identification number of AEFAC entries containing NX numbers of upper surface ordinates in percent chord  
 IATL Same as IATU, but for the lower surface  
 ICAM Identification number of AEFAC entries containing NX numbers of camber ordinates in percent chord  
 RADIUS Radius of leading edge in percent chord

It is sufficient that all geometric data needed by the ZONA6, ZONA7, ZONA51U and ZTAIC codes can be provided by the new bulk data entries. We believe that the proposed AGM is also capable of coping with other higher-order panel codes if they are incorporated into ASTROS.

### 3.2 Generation Of Aerodynamic Influence Coefficient (AIC) Matrices

The primary function of the ZAERO module is to generate Unified Aerodynamic Influence Coefficient (UAIC) matrices for the entire Mach range. Since, by definition, the AIC matrix is independent of the structural deformations (i.e. the modes), the ZAERO module will be incorporated outside of the ASTROS optimization loop. All AIC matrices are computed only once and saved in the CADDB database.

Once all of the AIC matrices are generated by ZAERO, the Generalized Aerodynamic Forces (GAF's) for each optimization step have to be computed. Since the UAIC's GAF's share the same definition as those generated by the Doublet Lattice Method (DLM) and Constant Pressure Method (CPM), the GAF's can be adopted directly by ASTROS' p-k method for flutter analysis/design.

In what follows, the AIC matrices of the ZAERO module (including ZONA6, ZONA7, ZTAIC and ZONA51U) are formulated. In the absence of a surface panel model these AIC matrices are equivalent the "QKK" matrices of ASTROS generated by the DLM or CPM lifting surface methods. However, for surface panel methods, these AIC formulations are generalized for wing-body configurations and are discussed as follows:

#### *Influence Coefficient Matrices For Wing-Body Configurations*

As discussed in the Aerodynamic Geometry Module (AGM), ZONA6 and ZONA7 are the hybrid methods in which the aircraft configuration is broadly divided into two categories: the body-like components modeled by surface panel methods and the wing-like components by lifting surface methods. A constant unsteady source singularity ( $\sigma$ ) is applied on each body panel, while, a constant unsteady pressure singularity ( $\Delta C_p$ ) is distributed on each wing panel. Five influence coefficient matrices, namely  $[PIC]$ ,  $[UIC]$ ,  $[VIC]$ ,  $[WIC]$  and  $[NIC]$  for the potential axial velocity, lateral velocity, vertical velocity and normal velocity influence coefficient matrices,

respectively, are constructed to relate the unknown singularities ( $\sigma$  and  $\Delta C_p$ ) to the perturbation potential  $\{\phi\}$  and velocities  $\{u\}$ ,  $\{v\}$  and  $\{w\}$  at all panels, i.e.

$$\{\phi\} = [PIC] \begin{Bmatrix} \sigma \\ \Delta C_p \end{Bmatrix} = \begin{bmatrix} PIC_{BB} & PIC_{WB} \\ PIC_{BW} & PIC_{WW} \end{bmatrix} \begin{Bmatrix} \sigma \\ \Delta C_p \end{Bmatrix} \quad (3.2.1)$$

$$\{u\} = [UIC] \begin{Bmatrix} \sigma \\ \Delta C_p \end{Bmatrix} = \begin{bmatrix} UIC_{BB} & UIC_{WB} \\ UIC_{BW} & UIC_{WW} \end{bmatrix} \begin{Bmatrix} \sigma \\ \Delta C_p \end{Bmatrix} \quad (3.2.2)$$

$$\{v\} = [VIC] \begin{Bmatrix} \sigma \\ \Delta C_p \end{Bmatrix} = \begin{bmatrix} VIC_{BB} & VIC_{WB} \\ VIC_{BW} & VIC_{WW} \end{bmatrix} \begin{Bmatrix} \sigma \\ \Delta C_p \end{Bmatrix} \quad (3.2.3)$$

$$\{w\} = [WIC] \begin{Bmatrix} \sigma \\ \Delta C_p \end{Bmatrix} = \begin{bmatrix} WIC_{BB} & WIC_{WB} \\ WIC_{BW} & WIC_{WW} \end{bmatrix} \begin{Bmatrix} \sigma \\ \Delta C_p \end{Bmatrix} \quad (3.2.4)$$

$$\{(u, v, w) \cdot \vec{n}\} = [NIC] \begin{Bmatrix} \sigma \\ \Delta C_p \end{Bmatrix} = \begin{bmatrix} NIC_{BB} & NIC_{WB} \\ NIC_{BW} & NIC_{WW} \end{bmatrix} \begin{Bmatrix} \sigma \\ \Delta C_p \end{Bmatrix} \quad (3.2.5)$$

where  $\vec{n} = n_x \mathbf{i} + n_y \mathbf{j} + n_z \mathbf{k}$  is the out-normal vector of each panel and the subscripts denote:

*BB* = the influence at the body control points due to the body panels  
*BW* = the influence at the wing control points due to the body panels  
*WB* = the influence at the body control points due to the wing panels  
*WW* = the influence at the wing control points due to the wing panels

Notice that unlike the lifting surface methods, such as the Doublet Lattice Method (DLM) and Constant Pressure Method (CPM) in which only one influence matrix is required, namely, the partition matrix  $NIC_{WW}$  in Eq (3.2.5), the wing-body configurations require five matrices for the unsteady force computations. The unknown singularities  $\sigma$  and  $\Delta C_p$  are solved by relating the right hand side of Eq (3.2.5) to the wing-body boundary conditions which will be discussed next.

#### *Unsteady Wing-Body Boundary Condition*

The boundary condition of the wing-like component (lifting surface method) is the well known expression:

$$(u, v, w) \cdot \vec{n} = F_w \quad (3.2.6)$$

where  $F_w = \frac{\partial h}{\partial x} + ikh$

$h$  is the normal displacement (or the mode shape)

$\frac{\partial h}{\partial x}$  is the slope of  $h$

Eq (3.2.6) is the standard boundary condition employed for the lifting surface methods such as DLM, CPM, ZONA51U and the ZTAIC codes. For an arbitrary body-like component experiencing oscillatory motion, the body fixed boundary condition on the body surface reads:

$$(\vec{V} - \vec{V}_B) \cdot \vec{n} = 0 \quad \text{at } S_o = 0 \quad (3.2.7)$$

where

$$\begin{aligned} S_o &= S_o(x, y, z), \text{ the mean body surface function} \\ \vec{V} &= \text{total flow velocity on the body surface } S_o = 0 \\ \vec{V}_B &= \text{the velocity due to the body surface motion} \end{aligned}$$

The elastic body modes can be generalized to contain two sets of components, namely, the one defined in the pitch plane  $h_z$ , and the one defined in the yaw plane  $h_y$ . Perturbing Eq (3.2.7) with respect to the small elastic body modes  $h_z$  and  $h_y$  results in a generalized unsteady boundary condition in the body-fixed system:

$$(u, v, w) \cdot \vec{n} = F_B \quad (3.2.8)$$

where

$$\begin{aligned} F_B &= -z_B n_x (h_z'' u_o + ik h_z') - n_z (h_z' + ik h_z) \\ &\quad - y_B n_x (h_y'' u_o + ik h_y') - n_y (h_y' + ik h_y) \end{aligned} \quad (3.2.9)$$

$$\begin{aligned} z_B, y_B &= \text{the } z \text{ and } y \text{ coordinate of the control point} \\ u_o &= \text{the steady perturbation velocity in the } x\text{-direction} \\ h_z, h_y &= \text{body mode shapes projected in the } x\text{-}z \text{ and } x\text{-}y \text{ plane respectively} \\ h_z', h_y' &= \text{the slopes of } h_z \text{ and } h_y \text{ respectively} \\ h_z'', h_y'' &= \text{the curvatures of } h_z \text{ and } h_y \text{ respectively} \\ ( )', ( )'' &= \frac{d}{dx} ( ), \frac{d^2}{dx^2} ( ), \text{ differential operator with respect to } x. \end{aligned}$$

Note that in the boundary condition for lifting surfaces, Eq (3.2.6), the downwash function  $F_w$  is only a function of the wing mode  $h$  and the reduced frequency  $k$ . By contrast, the downwash function  $F_B$  of Eq (3.2.9) for bodies is a function of normal vector  $\vec{n}$ , the steady velocity, the mode shapes  $h_y$  and  $h_z$  and their derivatives, and reduced frequency  $k$ . This implies that while the unsteady lifting surface solution is totally uncoupled from the steady mean flow influence, the unsteady body solution must include the steady mean flow influence which enters through the boundary condition, Eq (3.2.9).

In contrast to the  $F_w$  expression in Eq (3.2.6), the  $F_B$  expression in Eq (3.2.9) contains second order derivatives in  $h_z$  and  $h_y$ , which are related through a required transformation from the wing-fixed coordinate system to the present body-fixed coordinate system.

Combining Eqs (3.2.5), (3.2.6) and (3.2.8) yields the unknown singularity strength on the wing-like and body-like components, i.e.

$$\begin{Bmatrix} \sigma \\ \Delta C_p \end{Bmatrix} = [NIC]^{-1} \begin{Bmatrix} F_B \\ F_w \end{Bmatrix} \quad (3.2.10)$$

### Pressure Coefficients, Generalized Forces

Based on the work of Garcia-Fogeda and Liu (Ref 45), the unsteady pressure coefficient on the body-like component expressed in the body-fixed coordinates, reads

$$C_p = -2S_o \left\{ (1 + u_o) \left( u - z_B h_z'' u_o - y_B h_y'' u_o \right) + v_o v + w_o w \right. \\ \left. + h_z' w_o + h_y' v_o + ik \left( \phi + h_z w_o + h_y v_o - z_B h_z' u_o - y_B h_y' u_o \right) \right\} \quad (3.2.11)$$

where

$$S_o = \left[ 1 - \frac{\gamma-1}{2} M_\infty^2 (2u_o + u_o^2 + v_o^2 + w_o^2) \right]^{\frac{1}{\gamma-1}}$$

$u_o, v_o, w_o$  = the steady mean perturbation velocities on the body

$\phi, u, v, w$  = the unsteady perturbation potential and velocities on the body

According to Eq (3.2.11), the unsteady pressure on body involves the steady solution of  $u_o, v_o$  and  $w_o$ . In principle, Eq (3.2.11) is also applicable to lifting surfaces. When placed at zero degrees angle of attack, the steady velocities for lifting surfaces are  $u_o = v_o = w_o = 0$ . Eq (3.2.11) is then reduced to the well-known expression,

$$\Delta C_p = -2 \left( u + ik \phi \right) \quad (3.2.12)$$

It should be remarked that the unsteady pressure  $C_p$  for bodies, Eq (3.2.11), involves coupling terms with the perturbation velocities of the steady mean flow, which incorporates the body thickness effect. By contrast, the unsteady pressure  $\Delta C_p$  for lifting surface, Eq (3.2.12) is uncoupled from the steady mean flow term.

The generalized aerodynamic forces (GAF's), defined as the work done by the unsteady forces, can be expressed in terms of the mode shapes and the pressure coefficients, i.e.

$$Q_{IJ} = \sum_{i=1}^{NB} C_{p_i}^{(J)} A_{B_i} \left[ \left( n_{x_i} \frac{dh_{z_i}^{(I)}}{dx} - z_{B_i} + n_{x_i} \frac{dh_{y_i}^{(I)}}{dx} - y_{B_i} \right) - (n_{z_i} h_{z_i}^{(I)} + n_{y_i} h_{y_i}^{(I)}) \right] \\ + \sum_{i=1}^{NW} \Delta C_{p_i}^{(J)} A_{W_i} h_i^{(I)} \quad (3.2.13)$$

where

$C_{p_i}^{(J)}$  = the unsteady pressure coefficient of the  $i$ -th body panel due to the  $J$ -th mode

$\Delta C_{p_i}^{(J)}$  = the unsteady pressure jump of the  $i$ -th wing panel due to the  $J$ -th mode

$A_{B_i}$  = the area of the  $i$ -th body panel

$A_{W_i}$  = the area of the  $i$ -th wing panel

$h_{z_i}^{(I)}, h_{y_i}^{(I)}$  = the  $I$ -th mode shape of the pitch and yaw planes on the  $i$ -th body panel

$\frac{dh_{z_i}^{(I)}}{dx}, \frac{dh_{y_i}^{(I)}}{dx}$  = the slope of the  $I$ -th mode shape of the pitch and yaw planes on the  $i$ -th body panel

$h_i^{(I)}$  = the  $I$ -th mode shape on the  $i$ -th wing panel



$NB, NW$  are the number of body panels and wing panels, respectively

When the generalized forces for the body component (first summation terms of Eq (3.2.13) ) are compared with that for the wing component (the second summation term), it can be seen that the terms associated with the  $I$ -th mode in  $Q_{IJ}$  due to the body thickness effect are essentially

$$C_{p_i}^{(J)} A_B \left( n_{x_i} \frac{dh_{z_i}^{(I)}}{dx} z_{B_i} + n_{y_i} \frac{dh_{y_i}^{(I)}}{dx} y_{B_i} \right)$$

This term is not accounted for in the slender-body approach employed in the Doublet Lattice Method.

### *Solution Procedure For Computing Unsteady Pressure And Generalized Forces Of Wing-Body Configurations*

Fig (3.2.1) presents the solution procedure in obtaining the wing-body unsteady pressure and generalized forces, which develops as follows:

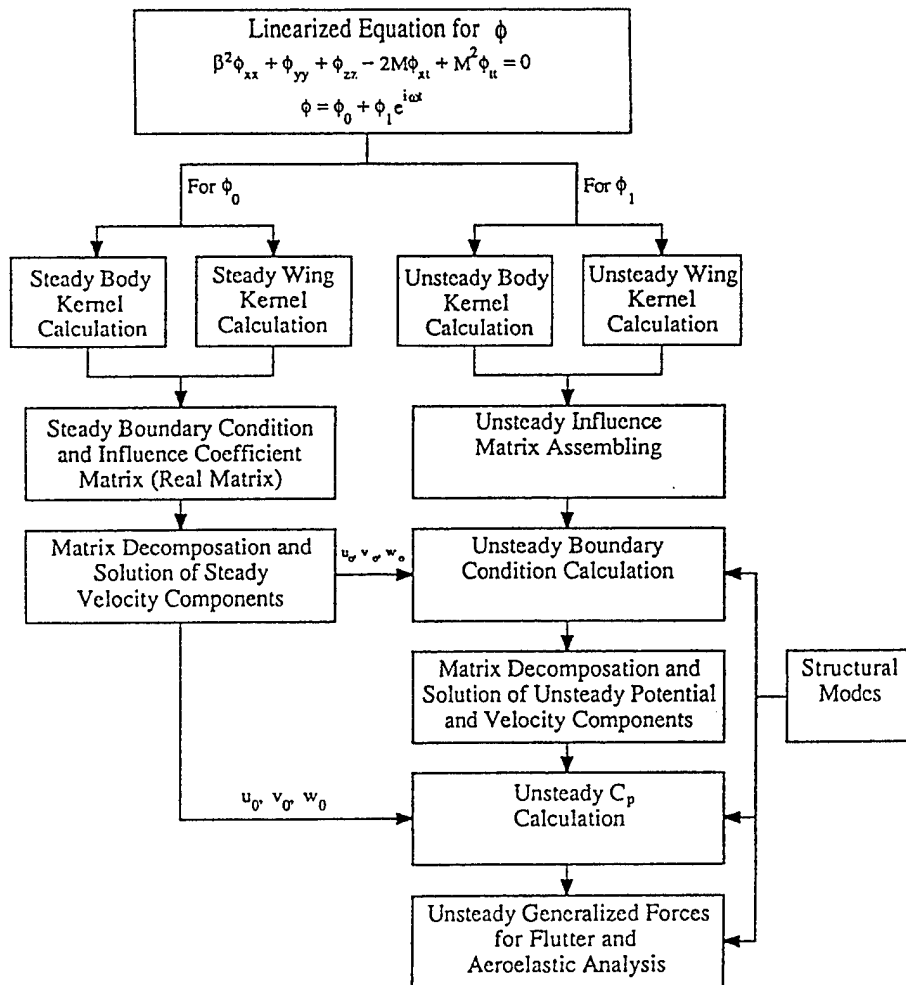


Figure 3.2.1 Flow Chart of ZONA6/ZONA7 Computation Procedure.

- a) Solve for steady perturbation velocities  $u_o$ ,  $v_o$  and  $w_o$ .
- b) Construct Influence Coefficient matrices  $[UIC]$ ,  $[VIC]$ ,  $[WIC]$ ,  $[PIC]$  and  $[NIC]$ .
- c) Construct Downwash functions  $F_B$  and  $F_W$  of Eqs (3.2.6) and (3.2.9); perform matrix decomposition on  $[NIC]$  and solve for  $\sigma$  and  $\Delta C_p$  from Eq (3.2.10).
- d) Compute unsteady velocities  $u$ ,  $v$  and  $w$  and unsteady potential  $\phi$  according to Eqs (3.2.1) through (3.2.4).
- e) Compute unsteady pressure  $C_p$  on body according to Eq (3.2.11).
- f) Compute generalized forces  $Q_{IJ}$  according to Eq. (3.2.13).

The above procedures require the structural modes in the computations of the downwash functions  $F_B$  and  $F_W$ , the unsteady pressure computation of  $C_p$  and generalized forces  $Q_{IJ}$ . This implies that these computations must be within the design loop of ASTROS which would be computationally inefficient. Therefore, reformulation of the above procedures to construct a set of AIC matrices which are independent of the structure is required for ASTROS design/optimization.

#### *Construction Of Unified Aerodynamic Influence Coefficient (UAIC) Matrices*

The definition of AIC is a square matrix which relates the downwash to the unsteady and lifting forces. To construct an AIC matrix for wing-like components is rather straightforward. It can be obtained according to the following derivation:

$$\{L_{wing}\} = \begin{bmatrix} [0] & [A_w] \end{bmatrix} [NIC]^{-1} \begin{Bmatrix} F_B \\ F_W \end{Bmatrix} \quad (3.2.14)$$

where

$\{L_{wing}\}$  = the normal forces on wing panels

$[A_w]$  = a diagonal matrix in which the element  $A_{wi}$  represents the area of the  $i$ -th wing panel

The procedure to obtain AIC for the body-like components is more complicated than that for wing-like components. Rewriting Eq (3.2.11) in matrix form and multiplying by the body panel area yields:

$$\{L_{body}\} = \begin{bmatrix} [B_{BB}] & [B_{WB}] \end{bmatrix} \begin{Bmatrix} F_B \\ F_W \end{Bmatrix} + \{d\} \quad (3.2.15)$$

where

$$\begin{aligned} [B_{BB}] & , [B_{WB}] = [A_B] [-2S_o] \left[ [1+u_o] \begin{bmatrix} [UIC_{BB}] & [UIC_{WB}] \end{bmatrix} \right. \\ & \left. + [v_o] \begin{bmatrix} [VIC_{BB}] & [VIC_{WB}] \end{bmatrix} \right] \end{aligned}$$

$$\begin{aligned}
& + [w_o] \left[ [WIC_{BB}] , [WIC_{WB}] \right] \\
& + [ik] \left[ [PIC_{BB}] , [PIC_{WB}] \right] [NIC]^{-1}
\end{aligned} \tag{3.2.16}$$

$\{L_{body}\}$  = the normal forces on body panels,

$$\begin{aligned}
d = & -2A S_o \left[ -(1+u_o) \left( z_B h_z'' u_o + y_B h_y'' u_o \right) \right. \\
& + h_z' w_o + h_y' v_o + ik \left( h_z w_o + h_y v_o - z_B h_z' u_o - y_B h_y' u_o \right) \left. \right]
\end{aligned} \tag{3.2.17}$$

$[A_B]$  = the element  $A_{Bi}$  represents the area of the  $i$ -th body panel

Combining Eqs (3.2.14) and (3.2.15) and separating the modes and the influence coefficients reveals that six matrices are required to relate the modes to the panel forces.

$$\begin{aligned}
\begin{Bmatrix} L_{body} \\ L_{wing} \end{Bmatrix} &= [AIC_Z] \begin{Bmatrix} h_z \\ h \end{Bmatrix} + [AIC_{ZX}] \begin{Bmatrix} \frac{dh_z}{dx} \\ \frac{\partial h}{\partial x} \end{Bmatrix} + [AIC_{ZXX}] \begin{Bmatrix} \frac{d^2 h_z}{dx^2} \\ 0 \end{Bmatrix} \\
&+ [AIC_Y] \begin{Bmatrix} h_y \\ 0 \end{Bmatrix} + [AIC_{YX}] \begin{Bmatrix} \frac{dh_y}{dx} \\ 0 \end{Bmatrix} + [AIC_{YXX}] \begin{Bmatrix} \frac{d^2 h_y}{dx^2} \\ 0 \end{Bmatrix}
\end{aligned} \tag{3.2.18}$$

where  $[AIC_Z]$ ,  $[AIC_{ZX}]$  and  $[AIC_{ZXX}]$  are the AIC matrices that relate the vertical displacements and their slopes and curvatures to the forces on the body and wing components respectively, whereas  $[AIC_Y]$ ,  $[AIC_{YX}]$  and  $[AIC_{YXX}]$  are for the lateral motion.

The construction of the six AIC matrices requires a major modification of the current ZONA51U, ZONA6, ZONA7, ZTAIC codes. The ASTROS matrix utility routines will be used for the matrix manipulations of Eqs (3.2.14) through (3.2.18).

### *Spline Matrix Of Wing-Body Configurations*

Eq (3.2.18) shows that in addition to the modes and slopes, the curvatures are also required in computing the wing-body unsteady aerodynamic forces. The surface spline technique in ASTROS can be adapted directly for the modal interpolations of lifting surface models (i.e. wing-like components). Similarly, the beam spline technique of ASTROS can be adapted directly for the interpolations of modes and slopes on surface panel models (i.e. body-like components). However, the interpolation technique of curvatures is lacking in the current version of ASTROS. A new beam spline technique will be developed that adopts the current ASTROS' beam spline technique as a basis and computes the curvature through analytical differentiation of the slopes.

Once the new beam spline technique is developed, spline matrices can be defined to relate the modal data at the structural grids to the modes, slopes and curvatures at the aerodynamic grids.

Consequently, the six AIC matrices defined in Eq (3.2.18) can be transformed into the structural grids by substituting these spline matrices into equation (3.2.18) and the generalized aerodynamic forces can be computed based on equation (3.2.13) accordingly.

### *ASTROS/ZAERO Integration*

Under the proposed effort, four new methods to generate the unsteady aerodynamic influence coefficients for use in ASTROS' ASE analyses will be implemented. The original Doublet Lattice Method (DLM) and Constant Pressure Method (CPM) will be modified to conform to the new aerodynamic matrix formats which will be required to support the archived import features that are proposed for all AIC generation methods.

For integration into ASTROS, two complexities have been introduced that require modifications to ASTROS. First, with the advent of numerous methods in each Mach range, the user must tell ASTROS which method to use. In the past, the Mach number essentially played that role. Secondly, ASTROS must identify the AIC's by more than the Mach number, reduced frequency and symmetry ( $M, k, sym$ ) triplet that is used for DLM and CPM. Now the method (ZONA51U, ZONA6, ZONA7 and ZTAIC) and splining strategy must be stored as well. In order to make the grouping more straightforward, and to allow the ARCHIVE/IMPORT features to support ASE response analyses, ASTROS will be modified to allow the user to name a collection of input describing a discretized aerodynamic configuration. That named model can then be ARCHIVED or IMPORTED as a single entity (i.e. a single collection of database entities).

To support the new methods in a more straightforward manner, the proposed AGM (Aerodynamic Geometry Module) will be implemented to create a single form (set of database entities) that is capable of describing all the various parts of any of the supported methods. Those geometrical descriptions that are common will be indistinguishable, with additions and modifications handled using rationalized database structures (relations and/or matrices).

The existing DLM and CPM in ASTROS will be modified to require their geometrical description in the same form as that of the AGM. This implies that the UNSTEADY module in ASTROS will be broken apart into a geometry engine and a computational engine. These improvements would become permanent features in standard ASTROS.

Another ramification of the ZAERO module is that the splining methodology will become method-dependent. Lifting surfaces in ASTROS are already treated differently than bodies - the surface spline is only available for lifting surfaces. While the basic spline technologies (beam spline and infinite surface spline) are adequate, their application will become method dependent. This implies that the ASTROS low level spline code will be used within an augmented SPLINE module that will handle the new requirements. First among the necessary changes is to make use of the AGM geometrical descriptions rather than the current ASTROS capabilities.

As a potential follow-on effort, the AGM geometry (which is very similar to an FE mesh) would be made available in forms compatible with graphical pre/post processors to display aerodynamic output quantities graphically. These features become readily available once the AGM and AIC data are archived to a CADDB database. External software could be developed by the end-user or third parties to support AIC model development in a very general way. This potential offers a chance to resolve one of the major limitations of ASE analysis in commercial FE codes in that the FE codes do not support "model checkout" and debug features for the unsteady aerodynamic model.

## SECTION 4

### SOFTWARE DESIGN BLUE-PRINT OF ASTROS/ASE MODULE

#### 4.1 Scenarios for ASTROS/ASE Applications

As discussed previously in section D, the proposed ASTROS/ASE module, once integrated with ASTROS, will bring to the ASTROS MDO environment a multidisciplinary synergistic technology that will provide a quick turnaround aeroelastic design/analysis capability throughout the complete flight regime. The following scenarios together with full-scale case studies of the AAW will elucidate the more versatile features of the ASTROS/ASE capability.

##### *Active Flexible Wing (AFW) Roll Performance with Flutter Constraints*

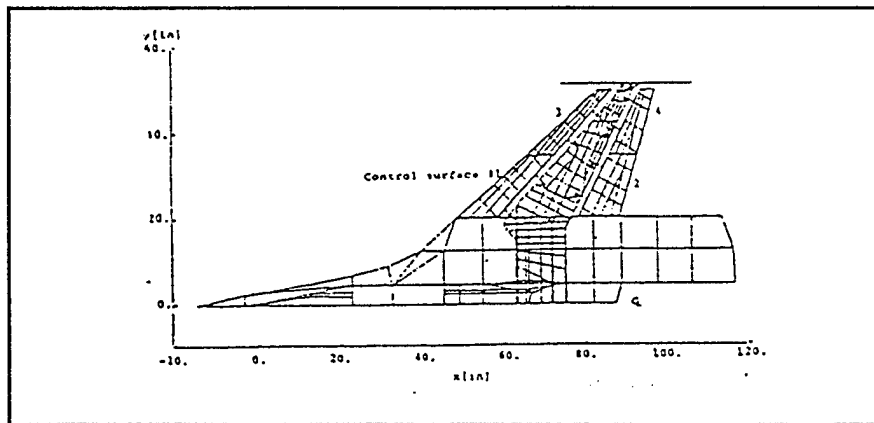


Figure 4.1.1

Figure 4.4.1 presents an AFW wind tunnel model which has two leading edge and two trailing edge control surfaces to meet the roll performance requirements. An initial control system design satisfies these constraints but introduces antisymmetric flutter. With the proposed ASTROS/ASE module, the control gains of the four control surfaces are added to the list of the design variables. The new ASE module and the static aeroelastic module are employed to optimize the control gains and the structural design variables for satisfying the flutter and roll performance constraints with a minimal weight penalty.

##### *Trade-Off Study of Gust Load Alleviation by Passive and Active Means*

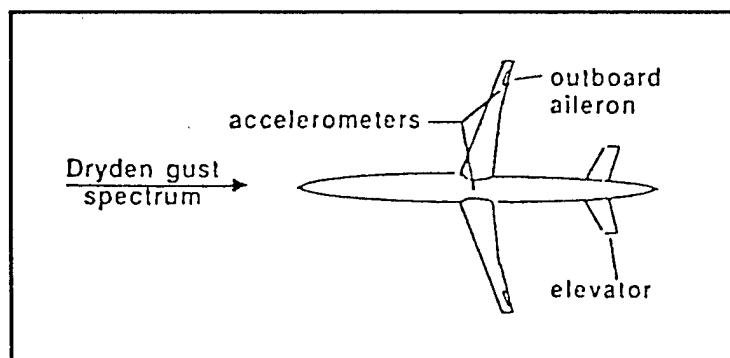


Figure 4.1.2

A drone aircraft such as the DAST (Drones for Aerodynamic and Structural Testing, Ref 46) shown in figure 4.1.2, is experiencing excessive wing root RMS bending moment in open-loop continuous gust analysis. With the new ASE module, the baseline structure is used as a starting point for two design studies:

- Passive Design - Add gust response constraints and repeat the structural design process.
- Active Design - Extract the plant state-space model for designing a load alleviation control system outside of ASTROS.
  - Due to the control system limitations, the control law helps but does not fully satisfy the gust response requirements.
  - Redesign the structure in the presence of the control system with gain-margin, phase margin and singular value constraints added to the list of constraints.

The results of both of the design are compared for trade-off studies of structural changes versus complexity of the control system.

#### ***Store-Flutter Suppression of a Generic Advanced Fighter (GAF) with Structural Uncertainties***

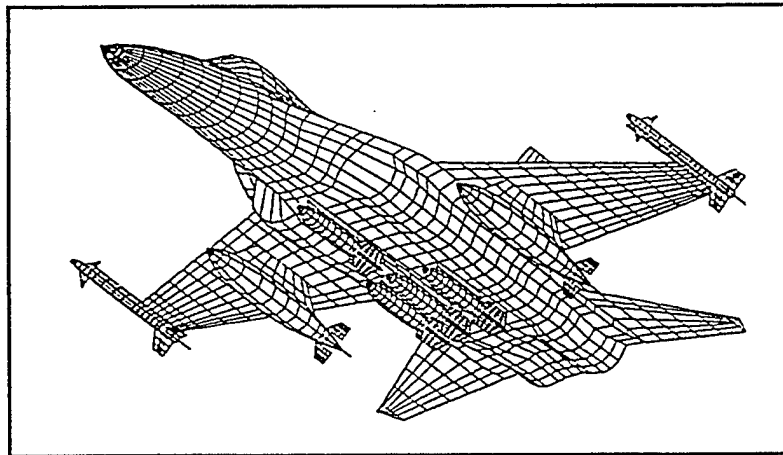


Figure 4.1.3

Figure 4.1.3 shows a generic advanced fighter (GAF) with various store carriers for the air-to-ground mission, requiring flutter clearance assurance. However, uncertainties of the stores/pylons structural properties may introduce an unexpected flutter problem which could be resolved by a robust control system for store flutter suppression. The state-space matrices of the aircraft with external stores and the derivatives of these matrices with respect to the structural properties of the stores/pylons will first be generated by the new ASE module. MATLAB's  $\mu$ -analysis tool box will then be used to design a control system which suppresses flutter over a range of parameter uncertainties. The designed control law will be introduced to ASTROS for the verification with various store models at different flight conditions.

#### ***Full-Scale Active Aeroelastic Wing (AAW) Studies***

The concepts of Active Aeroelastic Wing (AAW) Technology envision the use of wing aeroelastic flexibility as an advantage, with the wing control surfaces employed as tabs to

promote wing twist for aerodynamic control, whereas the current practice is to increase the wing stiffness in order to minimize flexibility. The AAW could offer a wing system that is significantly lighter in weight than current supersonic fighters while improving controllability and aerodynamic efficiency. AAW technology has been demonstrated through analysis and wind tunnel modeling (Refs 1, 2), and a full scale flight demonstration will be performed in the near future as evidenced by the recent PRDA from the Air Force. While keeping the wing sufficiently flexible, the Active Aeroelastic Wing may be subjected to a number of dynamic aeroelastic problems such as flutter, gust response, and/or store flutter. Apparently, flutter suppression and gust load alleviation by active means would be the feasible solution, which calls for a multidisciplinary design/analysis capability such as the proposed ASTROS/ASE software system. The ZONA team will, by utilizing the ASTROS/ASE module, perform a parallel study of the AAW full scale model design/analysis. The outcome of the full scale flight demonstration could also serve as a validation test case for the ASTROS/ASE module. ZONA Technology is currently working out with North American Rockwell/Seal Beach, CA, a MOU concerning the possible data exchange and collaboration on the proposed AAW project.

The following sections layout a software design blueprint of the proposed ASTROS/ASE module. A detailed flowchart of the ASE module that depicts all of its submodules and their interrelationships is represented. The functions of each submodule and its input and output in terms of matrix entities are discussed. Interrelationships between submodules are also identified in terms of ASTROS/MAPOL sequences and the CADDB database management system. New bulk data entries are defined as required.

#### **4.2 Overview of the ASE Module**

The planned ASE module will facilitate the inclusion of multi-input multi-output (MIMO) control system effects on the dynamic stability and response in the ASTROS multidisciplinary analysis and design optimization software package. Its overall capabilities will include:

- (i) Provide closed-loop robust stability analysis.
- (ii) Add continuous gust response capabilities.
- (iii) Allow the inclusion of stability and gust-response constraints in structural design optimization.
- (iv) Allow the inclusion of user-defined control parameters of a given control law in the multidisciplinary optimization process.
- (v) Export an efficient state-space representation of the aeroservoelastic system for subsequent analysis and control synthesis with commercially available tools such as MATLAB and MATRIX x.

The ASE module will be based on state-space formulations. The structure is represented by a set of baseline normal modes serving as generalized coordinates. The unsteady aerodynamic forces will be represented by minimum-state rational approximations of the ZAERO module generated transcendental frequency domain generalized force coefficient matrices. The control system will be represented by a state-space realization of user-defined series of polynomial transfer functions. A gust filter will be defined such that a white-noise input produces an approximation of either Dryden's or von Karman's power spectral density (PSD) of atmospheric continuous gusts.

The stability analysis and constraints will be based on root-loci, Nyquist curves and transfer-function singular values in the frequency domain. The gust response analysis and sensitivities will be based on the stochastic Lyapunov formulation.

A physical weighting algorithm will rate the aerodynamic data terms according to their aeroelastic importance. These rates will be used for:

- (i) Weighting the data terms in the rational approximation process.
- (ii) Rating the modes for application of size-reduction techniques.

There will be several options for the reduction of the order of the state-space equations. These options will allow a combination of modal truncation, static residualization, and dynamic residualization.

The new features will be applicable to open-loop as well as closed-loop systems.

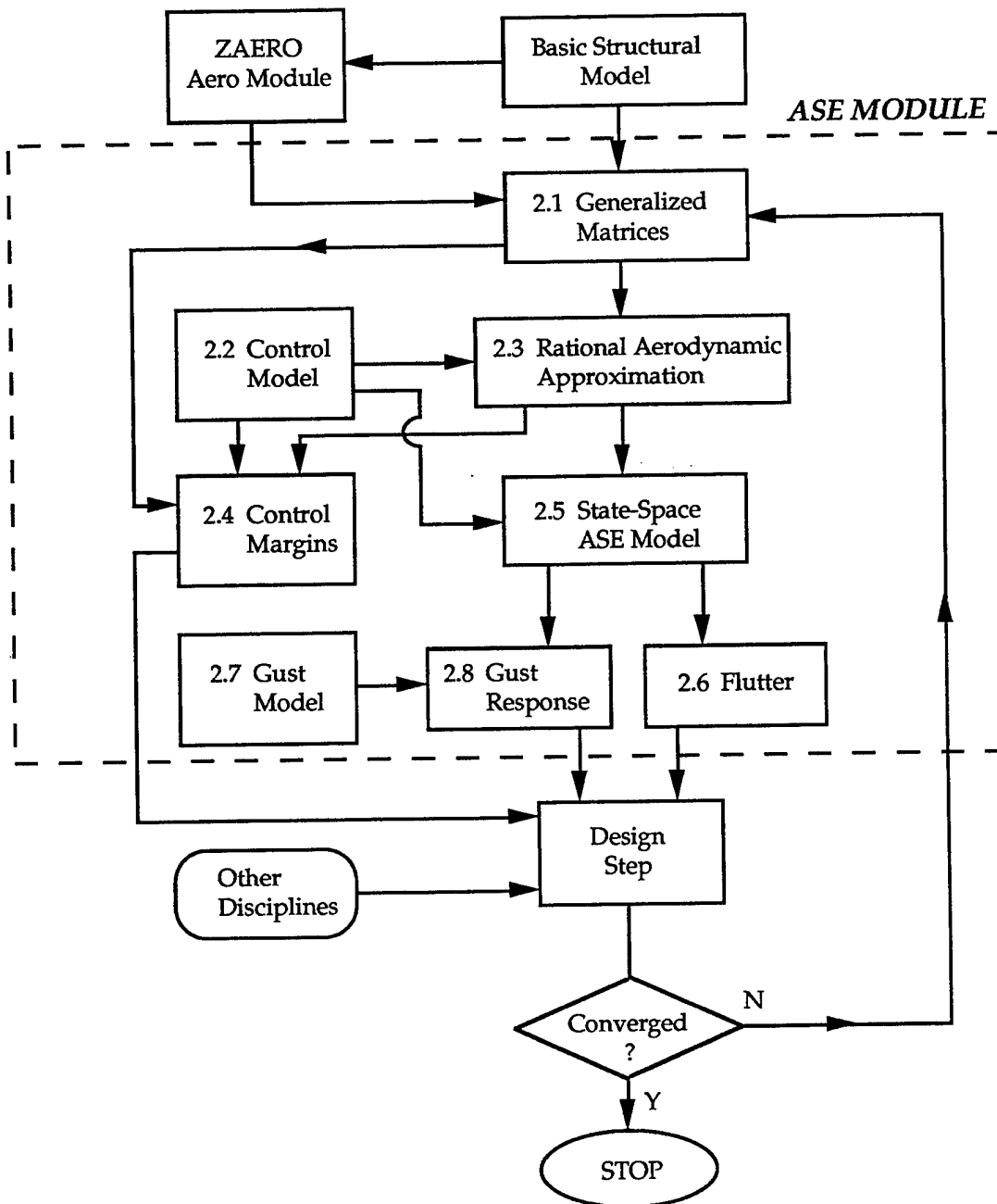


Figure 4.2.1 General Flow Chart of the ASE Module.



### 4.3 Description Of The ASE Blocks

A flow chart of the computation sequence associated with the planned ASE capabilities is shown in Figure 4.2.1. The flow chart is divided into three parts:

- (i) Preface structural and aerodynamic blocks which construct the  $g$ -set finite-element structural model and the  $k$ -set aerodynamic panel model, and the spline matrices that convert displacements and slopes between the two sets.
- (ii) The ASE module which performs the new features overviewed above and detailed below.
- (iii) The design optimization part which reads the ASE constraints and their sensitivities, combines them with those of the other ASTROS disciplines, and defines design changes, unless the process is converged. This part will remain identical to the current one, except for some possible minor changes.

The input, output and methods employed in the blocks of the ASE module and the new bulk data entries for each block are described below.

### 4.4 Generalized Matrices

Generate the structural and aerodynamic generalized matrices for ASE analysis.

#### Input:

- (i)  $g$ -set stiffness and mass sensitive matrices  $[DKVI]$  and  $[DMVI]$ , associated with the structural global design variables.
- (ii) The current values of the global design variables ( $v_i$ ).
- (iii) Aerodynamic AIC matrices, calculated by ZAERO module at user defined reduced-frequency values ( $k_i$ ).
- (iv) Kinematic modes generated by ZAERO in the aerodynamic grid:
  - Control modes  $[\phi_{kc}]$  of control surface unit rotations.
  - Gust complex modes  $[\phi_g(ik_i)]$  due to sinusoidal gusts.
  - Load modes  $[\phi_{kL}]$  for calculating section loads such as bending moments or torques.
  - Spline matrices between the aerodynamic and  $f$ -set structural coordinates.
  - Stress/strain coefficient matrices.

#### Output:

The coefficient matrices in the frequency-domain open-loop undamped aeroelastic equation of motion excited by control surface  $\{\delta_c\}$  and gust inputs  $\{W_g\}$

$$\begin{aligned} \left[ (i\omega)^2 [M_{hh}] + [K_{hh}] - q_\infty [Q_{hh}(ik)] \right] \{\xi\} = - \left( (i\omega)^2 [M_{hc}] - q_\infty [Q_{hc}(ik)] \right) \{\delta_c\} \\ + \frac{q_\infty}{V_\infty} [Q_{hg}(ik)] \{W_g\} \end{aligned} \quad (4.4.1)$$

and the aerodynamic and inertial load coefficient matrices

$$[Q_{Lh}(ik)], [Q_{Lc}(ik)], [Q_{Lg}(ik)], [M_{Lh}], \text{ and } [M_{Lc}]$$

This block expands the generalized matrices used in ASTROS Version 11 (Ref 12).

### Methods:

The ASE module will allow several design iterations with the same baseline modes. The operations in this block are divided into two cases:

(i) For the baseline structure:

- Calculate the normal modes  $[\phi_{ah}]$  in the  $a$ -set and recover to the  $f$ -set  $[\phi_{fh}]$ .
- Transform  $[\phi_{fh}]$  to the aerodynamic grids  $[\phi_{kh}]$ , as well as  $[\phi_{kc}]$  and  $[\phi_{kL}]$  to the structural  $f$ -set grids  $[\phi_{fc}]$  and  $[\phi_{fL}]$ .
- Use AIC's and  $k$ -set modes to calculate the generalized aerodynamic force matrices  $[Q_{hh}]$ ,  $[Q_{hc}]$ ,  $[Q_{hg}]$ ,  $[Q_{Lh}]$ ,  $[Q_{Lc}]$ , and  $[Q_{Lg}]$  for the tabulated  $k_i$  values.
- Recover the  $f$ -set  $[\phi_{fh}]$ ,  $[\phi_{fc}]$ , and  $[\phi_{fL}]$  to the  $g$ -set.
- Calculate sensor modal displacements  $[\phi_{sh}]$ .
- Use  $[DKVI]$ ,  $[DMVI]$ , and the  $g$ -set  $[\phi_{gh}]$ ,  $[\phi_{gc}]$ , and  $[\phi_{gL}]$  to calculate the generalized stiffness and mass sensitivity matrices associated with  $[K_{hh}]$ ,  $[M_{hh}]$ ,  $[M_{hc}]$ ,  $[M_{Lh}]$ , and  $[M_{Lc}]$ , (e.g.  $[DK_{hh}] = [\phi_{gh}]^T [DKVI] [\phi_{gh}]$ ).
- Extract the diagonal  $[M_{hh}]_b$  and  $[K_{hh}]_b$  and assemble the baseline  $[M_{hc}]_b$ ,  $[K_{hc}]_b$ , and  $[M_{Lc}]_b$  matrices, where subscript  $b$  represents the baseline model.

(ii) For a modified structure:

Modify the generalized stiffness and mass matrices according to the generalized sensitivity matrices and the current values of the design variables:

$$\text{e.g. } [K_{hh}]_M = [K_{hh}]_b + \sum (v_i - v_{ib}) [DK_{hh}]_i \quad (4.4.2)$$

where the subscript  $M$  denotes the modified structure.

Presently in ASTROS,  $[DKVI]$  and  $[DMVI]$  are not constant for nonlinear design variables; i.e. design variables that cannot be factored from the elemental stiffness and mass matrices  $K_{ee}$  and  $M_{ee}$ . Under the new paradigm, we can still make use of the original modes to reduce the current model, but we must augment the modal stiffness and mass updating algorithm:

$$[K_{gg}]_M = AK_{ee_{fixed}} + A \sum_j \sum_i P_{ij} K_{i_{fact}} V_j + AK_{ee_{nl}} \quad (4.4.3)$$

where  $A$  denotes an operator for matrix assembly, the first two terms represent the original (factored) design variables stiffness matrices associated with the nonlinear design variables (Ref 18), and the  $P_{ij}$  represent the ASTROS design variable linking coefficients.

During the first design iteration, we can compute and save

$$\left. \frac{\partial K_{hh}}{\partial v_i} \right|_{fact} = \phi_{gh}^T \left[ AK_{ee_{fixed}} + A \sum_j \sum_i P_{ij} K_{i_{fact}}^i \right] \phi_{gh} \quad (4.4.4)$$

Then the  $[K_{hh}]_M$  can be directly computed on all subsequent design iterations as:

$$[K_{hh}]_M = \sum \left[ \frac{\partial K_{hh}}{\partial v_i} \right]_{fact} v_i + \phi_{gh}^T [A K_{ee_{fixed}}] \phi_{gh} \quad (4.4.5)$$

where the second term is relatively inexpensive to compute since  $AK_{ee_{fixed}}$  is typically very sparse.  $\phi_{gh}$  represents the original modal matrix and  $[M_{hh}]_M$  follows in an identical manner.

To complete the update of the system, new first order modal system matrix sensitivities are needed. In the absence of nonlinear design variables, the sensitivities require no update and are identical to those of the first design iteration. However, the nonlinear design variables introduce an additional term:

$$\left[ \frac{\partial K_{hh}}{\partial v_i} \right]_M = \left[ \frac{\partial K_{hh}}{\partial v_i} \right]_{fact} + \phi_{gh}^T \left[ A \sum_j P_{ij} \frac{\partial K_{ee}}{\partial t_i} \right] \phi_{gh} \quad (4.4.6)$$

where  $\partial K_{ee} / \partial t_i$  is the finite-difference sensitivity of the elemental stiffness to the nonlinear, local design parameter,  $t_i$ .  $\phi_{gh}$  again are the original modal matrix. The mass sensitivities follow directly.

For the traditional ASTROS disciplines STATICS and static aeroelasticity (SAERO), the current ASTROS approaches will be used. The processing will be unaffected by the modal reduction scheme used in the ASE analysis. For the MODES analysis, the reduced  $K_{hh}$  and  $M_{hh}$  will be used to compute updated eigenvalues for purposes of ASTROS frequency constraints. If no frequency constraints exist, the MODES analyses will not be performed after the first design iteration.

#### 4.5 Control Model

Construct the s-domain transfer function matrix  $[T(s)]$  that relates actuator outputs to sensor inputs:

$$\{\delta(s)\} = [T(s)] \{y(s)\} \quad (4.5.1)$$

Input:

(a) Actuator transfer functions of the form:

$$\frac{\delta_i(s)}{u_{ac_i}(s)} = \frac{a_{i0}}{s^3 + a_{i2}s^2 + a_{i1}s + a_{i0}} \quad (4.5.2)$$

The order difference between the numerators and denominators is 3 to allow for the appearance of  $\delta_i$ ,  $\dot{\delta}_i$ , and  $\ddot{\delta}_i$  as independent states, and to allow for direct connection to acceleration sensors. A high order actuator can be defined by adding cascade transfer function in (c) below.

(b) Sensor transfer function.

(c) Additional filters expressed in either s-domain transfer function or state-space form.

Output:

The terms of  $[T(s)]$ , each expressed as a series of s-domain transfer functions.

### Method:

Most of the processing is just relating the input data to the individual terms of  $[T(s)]$ . State-space filter components are converted to polynomial form.

### New Bulk Data Entries:

The introduction of the control model requires an interface between the ASE module and the user. Four new bulk data entries are defined and described as follows:

- **Input data entry: SENSOR**

Description: Define sensor location and sensor dynamics.

#### Format and Example

1	2	3	4	5	6	7	8	9	10
SENSOR	IDSEN	BID	GD	CD	ITYPE	IORD	IDYNSSET		
SENSOR	1000	1	13	3	1	0	7		

#### Field:

IDSEN            Sensor ID  
BID             Boundary condition ID  
GD              Grid ID  
CD              Component ID  
ITYPE           Integer indicating whether sensor measures linear or angular motion  
                 = 0 determined by CD  
                 = 1 linear motion  
                 = 2 angular motion  
IORD            = 0 position sensor  
                 = 1 rate sensor  
                 = 2 acceleration sensor  
IDYNSSET       ≠ 0 DYNSET set ID in which the coefficients of the numerator and  
                 denominator polynomial are specified  
                 = 0 perfect sensor, do not include sensor dynamics

- **Input data entry: DYNSET**

Description: Define the values of the numerator and the denominator polynomials of transfer function.

#### Format and Example

1	2	3	4	5	6	7	8	9	10
DYNSET	ID	NUM	NDE	AN(1)	AN(2)	...	...	...	+ABC
DYNSET	31	6	8	0.1	2.0				

1	2	3	4	5	6	7	8	9	10
DYNSET	AN(NUM)	AD(1)	AD(2)	...	...	...	AD(NDE)		
+ABC	1.9	3.1	0.0				0.5		

#### Field:

ID               set ID of DYNSET  
NUM             order of numerator  
NDE             order of denominator  
AN(i)           coefficient of polynomial for numerator  
AD(i)           coefficient of polynomial for denominator

#### Remarks:

(1) The transfer function between input  $X$  and output  $Y$  is defined as:

$$\frac{Y}{X} = \frac{AN(1) + AN(2)s + \dots + AN(NUM)s^{NUM-1} + s^{NUM}}{AD(1) + AD(2)s + \dots + AD(NDE)s^{NDE-1} + s^{NDE}}$$

(2) NUM must be less than or equal to NDE.

• **Input data entry: ACTUAT**

Description: Define actuator dynamics

Format and Example

1	2	3	4	5	6	7	8	9	10
ACTUAT	ID	LABEL	AD (1)	AD (2)	AD (3)				
ACTUAT	101	ELEV	0.0	0.1	0.5				

Field:

ID Actuator ID  
 LABEL Aerodynamic control surface label defined in AESURF to which the actuator is attached  
 AD (1), Denominator coefficients  
 AD (2),  
 AD (3)

Remarks:

The transfer function of the actuator is defined as 
$$\frac{Y}{X} = \frac{AD(1)}{AD(1) + AD(2)s + AD(3)s^2 + s^3}$$

• **Input data entry: FILTER**

Description: Define type of filter for compensation of the signals from the sensors prior to sending them to the actuators.

Format and Example

1	2	3	4	5	6	7	8	9	10
FILTER	IDFTR	ITYPE	A1	A2					
FILTER	10	3	10.0	0.01					

Field:

IDFTR ID of FILTER

ITYPE = 1 notch filter: 
$$\frac{1 + (s^2/A1^2)}{1 + 2s(A2/A1) + (s^2/A1^2)}$$
  
 = 2 integral filter:  $A1/s$   
 = 3 lead-lag (lag-lead) filter:  $\frac{1 + (A1)s}{1 + (A2)s}$   
 < 0 polynomial filter 
$$\frac{Y}{X} = \frac{AN(1) + AN(2)s + \dots + AN(NUM)s^{NUM-1} + s^{NUM}}{AD(1) + AD(2)s + \dots + AD(NDE)s^{NDE-1} + s^{NDE}}$$
  
 [ITYPE] represents the set ID of a DYNSET entry which defines the numerator and denominator polynomials of the polynomial filter  
 A1, A2 values used for IDFTR = 1, 2, or 3

## 4.6 Rational Aerodynamic Approximation

Approximates the combined generalized unsteady aerodynamic force coefficient matrix:

$$[Q(ik)] = \begin{bmatrix} Q_{hh} & Q_{hc} & Q_{hg} \\ Q_{Lh} & Q_{Lc} & Q_{Lg} \end{bmatrix} \quad (4.6.1)$$

by a rational function of  $ik$  which has the form:

$$[\tilde{Q}(ik)] = [A_0] + [A_1](ik) + [A_2](ik)^2 + [D]([I](ik) + [R])^{-1}[E](ik) \quad (4.6.2)$$

where the coefficient matrices are real.

Input:

- (i) Generalized matrices generated in block 2.1.
- (ii) Actuator transfer function from block 2.2.
- (iii) Type of data weighting and design flight conditions if physical weighting is used.
- (iv) Approximation order and constraints.
- (v) The diagonal  $[R]$ .
- (vi) Initial guess of  $[D]$  and number of approximation iterations.

Output:

- (i)  $[A_0]$ ,  $[A_1]$ ,  $[A_2]$ ,  $[D]$ ,  $[E]$ , and  $[R]$  of Eq (4.6.2). Partitions of  $[A_i]$  are as in Eq (4.6.1), partitions of  $[D]$  are  $\begin{bmatrix} D_h \\ D_L \end{bmatrix}$ , and partitions of  $[E]$  are  $[E_h \ E_c \ E_g]$ .
- (ii) Table of maximum weight assigned to each term of  $[\tilde{Q}(ik)]$ .

Method:

The minimum-state rational approximation method with physical weighting and constraints is described in detail in (Refs 41 and 42). The approximation process is based on a series of weighted lease-square solutions:

$$\left( \sum_l [A^*]_l^T [W^*]_l^2 [A^*]_l \right) \{x^*\} = \sum_l [A^*]_l^T [W^*]_l^2 [b^*]_l \quad (4.6.3)$$

where  $\{x^*\}$  is a vector of unknown coefficients,  $[b^*]$  is based on the aerodynamic tabulated data associated with  $k_l$ , and  $[W^*]_l$  is a diagonal matrix with weights associated with the data terms in  $[b^*]_l$ . When no constraints are applied, the process starts with an initial  $[D]$  and solves  $[A_0]$ ,  $[A_1]$ ,  $[A_2]$ , and  $[E]$ , column by column, by applying Eq (4.6.3) with

$$[A^*]_l = \begin{bmatrix} I & 0 & -k_l^2 I & k_l^2 [D] (k_l^2 [I] + [R]^2)^{-1} \\ 0 & k_l I & 0 & -k_l [D] (k_l^2 [I] + [R]^2)^{-1} [R] \end{bmatrix},$$

$$\{x^*\} = \begin{Bmatrix} A_{0j} \\ A_{1j} \\ A_{2j} \\ E_j \end{Bmatrix}, \quad \{b^*\}_l = \begin{Bmatrix} F_j(k_l) \\ G_j(k_l) \end{Bmatrix} \quad (4.6.4)$$

where  $\{F_j(k_l)\}$  and  $\{G_j(k_l)\}$  are real and imaginary parts of the  $j$ -th column of the tabulated matrix  $[\tilde{Q}(ik_l)]$ . The resulting  $[E]$  is used to calculate  $[A_0]$ ,  $[A_1]$ ,  $[A_2]$ , and  $[D]$ , row by row, by solving Eq (4.6.2) with

$$[A^*]_l = \begin{bmatrix} I & 0 & -k_l^2 I & k_l^2 E^T (k_l^2 [I] + [R]^2)^{-1} \\ 0 & k_l I & 0 & -k_l E^T (k_l^2 [I] + [R]^2)^{-1} [R] \end{bmatrix},$$

$$\{x^*\} = \begin{Bmatrix} A_{0j}^T \\ A_{1j}^T \\ A_{2j}^T \\ D_j^T \end{Bmatrix}, \quad \{b^*\}_l = \begin{Bmatrix} F_j^T(k_l) \\ G_j^T(k_l) \end{Bmatrix} \quad (4.6.5)$$

These  $[D] \rightarrow [E] \rightarrow [D]$  iterations are repeated until convergence is obtained.

The users will have the option to use Roger's approximation which can be posed as a special case of Eq (4.6.2), see (Ref 42).

Each column of  $[\tilde{Q}(ik_l)]$  will be approximated with up to 3 approximation constraints selected from the following:

- (i) Steady aerodynamic match at  $k = 0$ .
- (ii) Either a real-part data-match constraint at a non-zero  $k_l$  value or a  $\{A_{2j}\} = 0$  constraint.
- (iii) An imaginary-part data-match constraint at a nonzero  $k_l$  value.

There will be three weighting options:

- (i) Uniform weighting,  $[W^*]_l = [I]$  (4.6.6)

- (ii) Data-normalization weighting  $W_{ij} = \frac{\epsilon}{\max_l \{|Q_{ij}(ik_l)|, \epsilon\}}$  (4.6.7)  
where  $\epsilon$  is a user-defined small positive parameter.

- (iii) Physical weighting, as detailed in (Refs 41, 47).

When option (iii) is selected, the weights of the  $h$  column partition in Eq (4.6.1) are based on derivatives of the system matrix in the left hand side of Eq (4.4.1). The weights of the  $c$  column partition of Eq (4.6.1) are based on Nyquist return signals with the control system assumed to be represented by the actuator transfer functions, Eq (4.5.2). The weights assigned to the gust columns are based on a selected response to Dryden's gust spectrum.

The physical weighting assigns measures of aeroelastic importance that can be used to select modes for residualization or truncation.

#### New Bulk Data Entries:

One new bulk data entry is required to define the input parameters for the minimum state technique and is described as follows:

- **Input data entry: MIST**

Description: Define parameters for rational approximation of unsteady aerodynamic forces by minimum state technique.

#### Format and Example

1	2	3	4	5	6	7	8	9	10
MIST	ID	KLIST	M	NKF	ITMAX	IWE	WCUT	NWD	+ ABC
MIST	1	2	3	1	50	1	1.0	2	

1	2	3	4	5	6	7	8	9	10
MIST	R(1)	R(2)	...	R(M)					
+ ABC	-1.0	-0.2		-1.0	0				

**Field:**

ID ID number  
 KLIST ID number of AEFACT entry specifying a list of hard point reduced frequencies  
 M Number of approximation roots  
 NKF = 1 all real and imaginary parts of generalized forces are matched at the last hard point reduced frequency list in FEFACT entry  
 > 1 all real and imaginary parts matched at the NKF'th reduced frequency listed in AEFACT entry  
 = 0 real parts are matched at the last hard point reduced frequency and imaginary parts at K(2)  
 ITMAX < 0  $[A_2]=0$ , imaginary parts are matched at k(-NKF) number of D → E → D iterations  
 IWE = 1 use weight matrices from a previous run  
 = 2 calculate weight matrices based on physical weighting  
 = 3 calculate weight matrices by data-normalization  
 WCUT Minimal maximum absolute value of weighted aerodynamic term (0.0 < WCUT < 1.0)  
 NWD Number of weight-peak widening cycle  
 R(i) M number of approximated roots (distinct negative values)

## 4.7 Control Margins

Calculates gain margins, phase margins, and singular values of the MIMO aeroservoelastic system.

**Input:**

- Retrieve generalized structural matrices of Eq (4.4.1) from block 2.1.
- Control transfer function from block 2.2.
- Modal displacements of sensor inputs  $[\phi_{sh}]$ .
- Definition of the control design variables.
- Rational approximation of  $[\tilde{Q}(ik)]$ , Eq (4.6.2) from block 2.3.

**Output:**

- Gain margins, phase margins and minimum singular values in the user-defined frequency range.
- Derivatives of these control margins with respect to structural and control design variables.

**Method:**

The aeroelastic plant in Eq (4.4.1) is expanded to include the diagonal matrix of actuator transfer functions  $[T_{ac}(s)]$  and the diagonal matrix of sensor transfer functions  $[T_s(s)]$ . The resulting transfer function of the plant, from actuator input to sensor output is

$$[G(s)] = [T_s(s)][\phi_{sh}][C_{hh}(s)]^{-1} (q_{\infty}[\tilde{Q}_{hc}(s) - s^2[M_{hc}]] [T_{ac}(s)]) \quad (4.7.1)$$

The remaining control feedback system  $[k(s)]$ , which relates actuator inputs  $\{u_{ac}\}$  to command error  $\{\varepsilon\}$  is based on the filters defined in block 2.2. The MIMO control aeroservoelastic system block diagram is given in Figure 4.7.1.



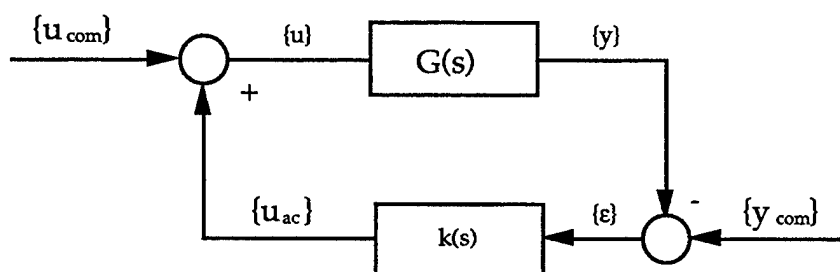


Figure 4.7.1 Block Diagram of the MIMO ASE System.

The command errors are defined as  $\{\varepsilon\} = \{y_{com}\} - \{y\}$ . To analyze the system stability, it is assumed that  $\{y_{com}\} = 0$  such that the input return signal is  $\{u_{ac}\} = -[k][G]\{u\}$  and the input return-difference matrix is  $[I + KG]$ . As suggested by Ref 48, the minimum singular values of  $[I + KG]$ , denoted by  $\sigma(I + KG)$ , and those of the inverse return-difference matrix  $\sigma(I + (KG)^{-1})$ , will be used as measures of guaranteed simultaneous stability margin. The  $s$  values will be calculated over a range of  $s = i\omega$  values. Singular-value constraints at several frequency points and calculated derivatives of  $\sigma(i\omega)$  at these frequencies with respect to the structural and control design variables will be included in the optimization process.

To conform with more classical control design requirements, gain and phase margins and their sensitivities will be calculated by Nyquist-type analyses with the control loops opened one at a time at the actuator inputs.

#### New Bulk Data Entries:

Block 2.4 allows the user to define constraints of the ASE system in terms of gain margins, phase margins, and singular values. Three new bulk data entries are defined and described as follows:

- **Input data entry: DCONMAR**

**Description:** Define the gain margin constraint of the ASE system with the control loops opened one at a time at the specified actuator inputs.

#### Format and Example

1	2	3	4	5	6	7	8	9	10
DCONMAR	CTSET	CTYPE	IDACT	RMAR	IFREQ				
DCONMAR	1	UPPER	31	3.0	10				

#### Field:

CTSET            Constraint set identification  
CTYPE           Constant type, either UPPER for upper bound or LOWER for lower bound (Text, default = LOWER)  
IDACT           Actuator ID  
RMAR           Required gain margin value (dB)  
IFREQ           Frequency set identification number of bulk data FREQ, FREQ1, or FREQ2

#### Remarks:

The frequencies listed in IFREQ represent the frequency points at which the gain margins cannot exceed the constraint value RMAR.

- **Input data entry: DCONPHS**

**Description:** Define the phase margin constraint of the ASE system with the control loops opened one at a time at the specified actuator inputs.

#### Format and Example

1	2	3	4	5	6	7	8	9	10
DCONPHS	CTSET	CTYPE	IDACT	RPHS	IFREQ				
DCONPHS	2	UPPER	31	30.0	10				

**Field:**

CTSET            Constraint set identification  
CTYPE            Constraint type either UPPER for upper bound or LOWER for lower bound. (Text, Default = Lower)  
IDACT            Actuator ID  
RPHS             Required phase margin value (degrees)  
IFREQ            Frequency set identification number of bulk data FREQ, FREQ1, or FREQ2

**Remarks:**

The frequencies listed in IFREQ represent the frequency points at which the phase margins cannot exceed the constraint value RPHS.

• **Input data entry: DCONSIN**

Description:    Define the singular value constraint of the ASE system in a specified frequency range.

**Format and Example**

1	2	3	4	5	6	7	8	9	10
DCONSIN	CTSET	CTYPE	SING	IFREQ					
DCONSIN	1	0	0.3	10					

**Field:**

CTSET            Constraint set identification  
CTYPE            = 0   singular value of return-difference matrix  
                  = 1   singular value of inverse return-difference matrix  
SING             Required minimum singular value (positive)  
IFREQ            Frequency set identification number of bulk data entry FREQ, FREQ1, or FREQ2

**Remarks:**

The frequency listed in IFREQ represent the frequency points at which the frequency points at which the singular value must be greater than SING.

## 4.8    State - Space ASE Model

Constructs the ASE state-space model for flutter and gust-response analyses and export for control analyses.

**Input:**

- (i) Generalized structural matrices of Eq (4.4.1) from block 2.1.
- (ii) Control transfer functions and/or state-space matrices from block 2.2.
- (iii) Rational approximation of  $[Q(ik)]$ , Eq (4.6.2), from block 2.3.

**Output:**

- (i) State-space  $[A_{ae}]$ ,  $[B_{ae}]$ , and  $[C_{ae}]$  matrices describing the aeroelastic system (plant + actuators + sensors).
- (ii) State-space  $[A_c]$ ,  $[B_c]$ ,  $[C_c]$ , and  $[D_c]$  matrices describing the control system.
- (iii) Closed-loop control-augmented system matrix  $[\bar{A}]$ .
- (iv) Output matrix for gust response analysis.
- (v) Sensitivities of the above matrices.

**Method:**

The open-loop state-space equation of motion of the aeroelastic system excited by a control surface is

$$\{\dot{x}_p\} = [A_p] \{x_p\} + [B_p] \{u_p\} \quad (4.8.1)$$

where

$$\{x_p\} = \begin{Bmatrix} \xi \\ \dot{\xi} \\ \ddot{\xi} \\ x_a \end{Bmatrix} \quad \{u_p\} = \begin{Bmatrix} \delta \\ \dot{\delta} \\ \ddot{\delta} \\ \delta \end{Bmatrix}$$

$$[A_p] = \begin{bmatrix} 0 & , & [I] & , & 0 \\ -[\bar{M}]^{-1} [K_{hh} + qA_{hho}] & , & -[\bar{M}]^{-1} \left[ B_{hh} + \frac{q_\infty b}{V_\infty} A_{hh1} \right] & , & -q_\infty [\bar{M}]^{-1} [D_h] \\ 0 & , & [E_h] & , & \frac{V_\infty}{b} [R] \end{bmatrix}$$

$$[B_p] = \begin{bmatrix} 0 & , & 0 & , & 0 \\ -q_\infty [\bar{M}]^{-1} [A_{hc0}] & , & \left[ -\frac{q_\infty b}{V_\infty} [\bar{M}]^{-1} A_{hcl} \right] & , & -[\bar{M}]^{-1} \left[ M_{hc} + \frac{q_\infty b^2}{V_\infty^2} A_{hc2} \right] \\ 0 & , & [E_c] & , & 0 \end{bmatrix}$$

and  $[\bar{M}] = [\bar{M}_{hh}] + \frac{q b^2}{V^2} [A_{hh2}]$ . Here,  $\{\xi\}$  is the vector of generalized structural displacements and  $\{\delta\}$  is the vector of control surface command deflections. The plant output equation, based on the sensor modal deflections  $[\phi_{sh}]$  is described in the form:

$$\{y_p\} = [C_p] \{x_p\} + [D_p] \{u_p\} \quad (4.8.2)$$

where  $[C_p]$  and  $[D_p]$  depend on the type of the sensor (displacement, velocity, or acceleration).

The actuator of Eq (4.5.2) is modeled in state-space form as

$$\{\dot{x}_{ac_i}\} = \begin{bmatrix} 0 & 1 & 0 \\ 0 & 0 & 1 \\ -a_{io} & -a_{il} & -a_{i2} \end{bmatrix} \{x_{ac_i}\} + \begin{Bmatrix} 0 \\ 0 \\ a_{io} \end{Bmatrix} u_{ac_i} \quad (4.8.3)$$

where

$$\{x_{ac_i}\} = \begin{Bmatrix} \delta_i \\ \dot{\delta_i} \\ \ddots \\ \delta_i \end{Bmatrix}$$

Several actuators can be grouped together for the general form

$$\{\dot{x}_{ac}\} = [A_{ac}] \{x_{ac}\} + [B_{ac}] \{u_{ac}\} \quad (4.8.4)$$

Augmentation to the plant Eqs (4.8.1) and (4.8.2) yields

$$\begin{Bmatrix} \dot{x}_p \\ \dot{x}_{ac} \end{Bmatrix} = \begin{bmatrix} [A_p] & [B_p] \\ 0 & [A_{ac}] \end{bmatrix} \begin{Bmatrix} x_p \\ x_{ac} \end{Bmatrix} + \begin{bmatrix} 0 \\ [B_{ac}] \end{bmatrix} \{u_{ac}\} \quad (4.8.5)$$

since  $\{x_{ac}\} = \{u_p\}$ , and the output (sensor measurement) equation becomes

$$\{y\} = \begin{bmatrix} [C_p] & [D_p] \end{bmatrix} \begin{Bmatrix} x_p \\ x_{ac} \end{Bmatrix} \quad (4.8.6)$$

A general transfer function of a control component is

$$T(s) \equiv \frac{y_c(s)}{u_c(s)} = \frac{b_0 s^n + b_1 s^{n-1} + \dots + b_n}{s^n + a_1 s^{n-1} + \dots + a_n} \quad (4.8.7)$$

The controller canonical form realization of this transfer function is

$$\begin{aligned} \{\dot{x}_c\} &= [A_c] \{x_c\} + \{B_c\} \{u_c\} \\ y_c &= [C_c] \{x_c\} + [D_c] \{u_c\} \end{aligned} \quad (4.8.8)$$

where

$$[A_c] = \begin{bmatrix} 0 & 1 & & 0 \\ & \ddots & \ddots & \\ 0 & & 0 & 1 \\ -a_n & -a_{n-1} & \dots & -a_1 \end{bmatrix} \quad \{B_c\} = \begin{Bmatrix} 0 \\ \vdots \\ 0 \\ 1 \end{Bmatrix}$$

$$[C_c] = [(b_n - b_0 a_n) \ (b_{n-1} - b_0 a_{n-1}) \ \dots \ (b_1 - b_0 a_1)]$$

$$D_c = b_0$$

Application of Eq (4.8.8) to the sensor transfer functions and augmentation with Eq (4.8.5) yield the state space equations of the aeroelastic system

$$\begin{aligned} \{\dot{x}_{ae}\} &= [A_{ae}] \{x_{ae}\} + [B_{ae}] \{u_{ae}\} \\ \{y_{ae}\} &= [C_{ae}] \{x_{ae}\} \end{aligned} \quad (4.8.9)$$

Finally, the state-space equations of the control filters can be grouped in the form

$$\begin{aligned}\{\dot{x}_c\} &= [A_c] \{x_c\} + [B_c] \{u_c\} \\ \{y_c\} &= [C_c] \{x_c\} + [D_c] \{u_c\}\end{aligned}\quad (4.8.10)$$

Augmentation of Eq (4.8.10) to Eq (4.8.9) with  $\{u_c\} = \{y_{ae}\}$  yields the general open-loop control form

$$\begin{aligned}\{\dot{x}\} &= [A] \{x\} + [B] \{u\} \\ \{y\} &= [C] \{x\}\end{aligned}\quad (4.8.11)$$

Connection of the inputs  $\{u\}$  to the outputs  $\{y\}$  through a gain matrix,  $\{u\} = [G] \{y\}$ , yields the closed-loop equation

$$\{\dot{x}\} = [\bar{A}] \{x\} \quad (4.8.12)$$

where

$$[\bar{A}] = [A] + [B][G][C]$$

The block 2.5 assembly of the state-space ASE system matrix sensitivities with respect to structural and controller design parameters must be evaluated if any constraints associated with the ASE analyses are retained as active. With the advent of design variables associated with the control law, the derivatives must account for both FE matrix perturbations (which are well understood and have been extended to support the iterative formation of a generalized modal and its first order derivative) and control parameter perturbations. The control parameters include gains and the coefficients of the polynomials for each actuator/sensor. The user will describe which of these parameters is available for design and its range of values  $[v_{min}, v_{max}]$ .

The sensitivities of the ASE constraints (or the objective function) will be solved analytically based on the sensitivities of the state-space  $[A_{ae}]$ ,  $[B_{ae}]$ , and  $[C_{ae}]$  matrices describing the system and of the state-space controller matrices  $[A_c]$ ,  $[B_c]$ ,  $[C_c]$  and  $[D_c]$ . It will be assumed that the structural design parameters affect only  $[K]$  and  $[M]$  and the controller design parameters do NOT affect  $[K]$  and  $[M]$  or the rational aerodynamic approximation. Traditional ASTROS constraints will not be affected except that the vector of design variables must be kept separated in the structural and controller parameters.

$$\{v\} = \begin{Bmatrix} v_s \\ v_c \end{Bmatrix}$$

The cross-sensitivities will be ignored for purposes of sensitivity calculation.

#### New Bulk Data Entries:

- **Input data entry: GAIN**

Description: Define gain of a control-sensor pair.

Format and Example

1	2	3	4	5	6	7	8	9	10
GAIN	ID	LABEL	IDSEN	GN	PHASE	IDFTR			
GAIN	4	ELEV	20	0.7	0	10			

**Field:**

CTSET ID of gain  
 LABEL Alphanumeric string for aerodynamic control surface defined in input data entry  
 AESURF  
 IDSEN Sensor ID number defined in input data entry SENSOR  
 GN Value of gain  
 PHASE Phase error (degrees) in transfer function  
 IDFTR ID of filter associated with the current control-sensor pair

- **Input data entry: DESGAIN**

Description: Define gain value of a control-sensor pair as a design variable.

**Format and Example**

1	2	3	4	5	6	7	8	9	10
DESGAIN	DVID	GID	VMIN	VMAX	VINIT	LABEL			
DESGAIN	3	4	0.1	0.3	0.2	GAIN1			

**Field:**

DVID Design variable identification  
 GID ID of data entry GAIN  
 VMIN Minimum allowable value of the design variable  
 VMAX Maximum allowable value of the design variable  
 VINIT Initial value of the design variable (VMIN < VINIT < VMAX)  
 LABEL Optional user-supplied label to define the design variable (text)

- **Input data entry: DESCOEF**

Description: Define a coefficient of the polynomials associated with the transfer function of a control filter as a design variable.

**Format and Example**

1	2	3	4	5	6	7	8	9	10
DESCOEF	DVID	IDFTR	ITYPE	N	VMIN	VMAX	VINIT	LABEL	
DESCOEF	1	2	1	3	0.1	0.3	0.2	COE1	

**Field:**

DVID Design variable identification  
 IDFTR ID of bulk data entry FILTER  
 ITYPE = 1 define the coefficient A1 as design variable for notch, integral, proportional plus derivative, or lead-lag filter  
 = 2 same as ITYPE = 1 but for A2  
 = 3 define one of the coefficients of the numerator polynomial as a design variable  
 = 4 same as ITYPE = 3 but for the denominator polynomial  
 N The N-th coefficient of the numerator or denominator (Used only for ITYPE = 3 or 4)  
 VMIN Minimum allowable value of the design variable  
 VMAX Maximum allowable value of the design variable  
 VINIT Initial value of the design variable (VMIN < VINIT < VMAX)  
 LABEL Optional user-supplied label to define the design variable (text)

## 4.9 Flutter

Calculates flutter velocity and the same flutter constraints as in ASTROS Version 11, but based on a state-space formulation, with or without a control system.

**Input:**

- Closed-loop system matrix from block 2.5.

**Output:**

- Flutter speed.
- Damping constraints and their sensitivities.

#### Method:

The flutter analysis is based on the eigenvalues of the closed-loop system matrix  $[\bar{A}]$  of Eq (4.8.12) or the open-loop matrix  $[A_p]$  of Eq (4.8.1) when there is no control system. Root locus analysis is performed for the flutter velocity with fixed density or for the flutter density with fixed velocity. The definition of the damping constraints and the sensitivities of the active constraints will be similar to those in Version 11, based on the eigenvectors of  $[\bar{A}]$  or  $[A_p]$  at the required constraint points.

### 4.10 Gust Model

Constructs a state-space model where the input signal represents a white noise process and the output signal represents Dryden's or von Karman's continuous gust velocity.

#### Input:

- User input parameters for either Dryden's or von Karman's power spectral density (PSD) functions.

#### Output:

State-space gust matrices  $[A_g]$ ,  $[B_g]$ , and  $[C_g]$ .

#### Method:

The construction of the gust model is based on (Ref 49). Either Dryden's or von Karman's gust PSD functions are represented by a Laplace domain transfer function, from white noise signal  $w$  to gust velocity  $w_g$ . The order of the transfer function denominator is larger than that of the numerator. The resulting gust model has the form

$$\begin{aligned} \{x_g\} &= [A_g] \{x_g\} + \{B_w\} w \\ \{y_g\} &= [C_g] \{x_g\} \end{aligned} \quad (4.10.1)$$

with three states for Dryden's gust and four states for von Karman's gust.

#### New Bulk Data Entries:

One new bulk data entry is defined for the continuous gust input.

- **Input data entry: GUST1**

Description: Defines Dryden's or von Karman's gust PSD functions for ASE gust analysis.

#### Format and Example

1	2	3	4	5	6	7	8	9	10
GUST1	SID	SYMXY	ITYPE	MIST	WG	XO	V		
GUST1	1	1	1	10	1.0	10.0	1000.0		

#### Field:

SID            Gust set identification number  
SYMXY        = 1 vertical gust  
               = 2 lateral gust  
ITYPE        = 1 von Karman's gust PSD function  
               = 2 Dryden's gust PSD function  
MIST         ID of bulk data entry MIST for rational approximator of the harmonic gust forces

WG	Scale factor of the gust velocity
XO	Location of reference plane in aerodynamic coordinates
V	Velocity of vehicle

#### 4.11 Gust Response

Calculates the Root-Mean-Square (RMS) values of gust response parameters and their sensitivities.

##### Input:

- Closed-loop system matrix from block 2.5.
- State-space gust matrices from block 2.7.
- Rational approximation matrices from block 2.3.
- Sensitivities of the system matrices from block 2.5.

##### Output:

- Gust response constraints and their sensitivities.

##### Method:

The gust matrices of Eq (4.10.1) are augmented to either the plant matrix  $[A_p]$  of Eq (4.8.1) or the closed-loop matrix  $[A]$  of Eq (4.8.12), as detailed in (Ref 8). The resulting system has the form

$$\begin{aligned}\{\dot{x}\} &= [A] \{x\} + \{B_w\} w \\ \{y\} &= [C] \{x\}\end{aligned}\tag{4.11.1}$$

The root-mean square values of the response parameters are based on the state covariance matrix  $[X] \equiv E[\{x\} \{x\}^T]$ . When Eq (4.11.1) is excited by a unit intensity white noise,  $[X]$  satisfies the matrix Lyapunov equation

$$[A][X] + [X][A]^T = -\{B_w\} \{B_w\}^T\tag{4.11.2}$$

The covariance matrix associated with  $\{y\}$  of Eq (4.11.1) is

$$[Y] \equiv E[\{y\} \{y\}^T] = [C][X][C]^T\tag{4.11.3}$$

The diagonal of  $[Y]$  contains the mean-square output response parameters  $\sigma_y^2$ . The differentiation of Eq (4.11.2) with respect to a design variable  $v_i$ , using  $\frac{\partial \{B_w\}}{\partial v_i} = 0$ , yields another Lyapunov equation

$$[A] \frac{\partial [X]}{\partial v_i} + \frac{\partial [X]}{\partial v_i} [A]^T = -\frac{\partial [A]}{\partial v_i} [X] - [X] \frac{\partial [A]^T}{\partial v_i}\tag{4.11.4}$$

which can be solved for  $\frac{\partial [X]}{\partial v_i}$ . A new solution is required for each design variable, but they can

all be based on the same decomposition used in solving for  $[X]$  by Eq (4.11.2). The differentiation of Eq (4.11.3) yields the response sensitivity derivatives



$$\frac{\partial[Y]}{\partial v_i} = [C] \frac{\partial[X]}{\partial v_i} [C]^T + \frac{\partial[C]}{\partial v_i} [X] [C]^T + [X] [X] \frac{\partial[C]^T}{\partial v_i} \quad (4.11.5)$$

where the diagonal terms  $\frac{\partial \sigma_y^2}{\partial v_i}$  are usually the only derivatives of interest.

#### New Bulk Data Entries:

Two new bulk data entries are introduced for the gust response constraints of the RMS value of a group of aerodynamic components and the RMS displacements, velocities and accelerations of grid point.

##### • **Input data entry: DCONACD**

Description: Defines the gust response constraint of a group of aerodynamic components in terms of forces and moments.

##### Format and Example

1	2	3	4	5	6	7	8	9	10
DCONACD	SID	IACORD	ITYPE	RMS	IGUST				
DCONACD	3	10	1	100.	1				

##### Field:

SID Constraint set identification number  
IACORD Identification number of the ACORD bulk data entry in which a group of aerodynamic components is defined  
ITYPE = 1, 2, or 3 : force along x, y, or z direction  
= 4, 5, or 6 : moment about x, y, or z axis  
RMS Constraint in term of RMS value  
IGUST Identification number of GUST1 bulk data entry where the gust input is defined

##### Remarks:

The moment axis is defined by XMCNT, YMCNT, and ZMCNT in ACORD data entry.

##### • **Input data entry: DCONRMS**

Description: Defines the displacement, velocity or acceleration constraint in terms of RMS value in response to a gust input.

##### Format and Example

1	2	3	4	5	6	7	8	9	10
DCONRMS	SID	DTYPE	IGUST	GID	C	DALL	CTYPE		
DCONRMS	1	1	1	73	1	2.0	UPPER		

##### Field:

SID Constraint set identification numbers  
DTYPE = 1 displacement constraint  
= 2 velocity constraint  
= 3 acceleration constraint  
IGUST Identification number of GUST1 bulk data entry where the gust input is defined  
GID Grid ID  
C Component ID  
DALL Allowable value  
CTYPE Either UPPER or LOWER bound (Text, default = UPPER)

## SECTION 5

### MODIFICATION OF ASTROS FOR ZAERO AND ASE INTEGRATION

#### 5.1 Integration Overview

The purpose of the ASE capabilities in ASTROS is to facilitate the structural optimization of an aeroservoelastic system with respect to objective and constraint functions associated with ASE Stability and Response (Gust) analyses. The parameters used to effect improvements will be the usual ASTROS structural parameters and with the addition of gains and polynomial coefficients of the control system. The control system architecture is fixed.

It is important to note, however, that the proposed ASE capabilities extend beyond the straight forward (black-box) implementation of automated design subject to constraints on ASE analysis responses. Rather, the proposed enhancements are intended to make ASTROS useful in the process of designing a flight vehicle in which the designer wants to find the "best" design by exploiting the complex synergies between the structural behavior and the MIMO control system.

Out of necessity, this is an interactive process that is dominated by perturbation of mathematical models described by parameters that cannot be updated automatically. For example, the sensor and actuator locations, filters and other components of the control laws do not readily lend themselves to the automated design techniques of traditional structural optimization. The proposed extension of ASTROS will enable the design team to assemble ASE models, optimize them with respect to stability, control, and strength requirements and to compare the optimal designs to one another to gain insight into the system's characteristics. Because many components of the ASE models can be shared and are computationally intensive to produce, many of the proposed enhancements deal with their creation, assembly, management, and use of these components.

The proposed ASE analysis approach, minimum state rational approximation based on modal system matrices, requires an initialization phase in ASTROS to create the modal system matrices. The rational approximation and the generation of the state-space model of the ASE system will then be performed for each analysis case. The controller and the aerodynamics may be different from case to case; e.g. symmetric flutter at  $M = 0.9$  in one case and antisymmetric gust response at  $M = 1.5$  in another. Each of the analysis cases could have different control laws as well: to handle, for example, separate low- $\bar{q}$  and high- $\bar{q}$  systems.

Since the generation of the ASE model for a given analysis case is computationally intensive and may call for user intervention, a requirement of this integration activity is that ASTROS produce "archival" models at each stage of the process for

- 1) subsequent re-use in ASTROS ASE
- 2) export to other state-space ASE tools, e.g., MATLAB and MATRIX x.

As part of the improvements to generalized unsteady aerodynamic influence coefficients in the ZAERO module, ASTROS will support the generation and archiving of a very general set of aerodynamics that will provide the ASE analyses with their required aerodynamic influence coefficients. The other remaining activities to support the assembly of an ASE module are the creation and archival of modal representations of the basic structural system matrices,  $K_{hh}$ ,  $M_{hh}$ ,  $B_{hh}$  and of the response matrices,  $s = S_h u_h$ ; (where  $S_h$  is the modal stress or strain displacement) and the generation of a rational aerodynamic approximation in the s-domain. Each of these two steps have implications with respect to the current ASTROS paradigm.

To create the rational aerodynamic approximation, the raw AIC data for a given set {Mach number, symmetry, method, modal} need to be fit with the help of user input to control the fitting process. The input to this process includes:

- 1)  $M_{hh}$ ,  $K_{hh}$ , and  $B_{hh}$
- 2)  $Q_{hh}(ik)$ , aerodynamic geometry & control surfaces
- 3) control system definition
- 4) algorithm control parameters

As part of this process, the structural equations of motion for the open-loop system must be assembled and solved. Also, at this time, the archived AIC matrix, the archived aerodynamic geometry and control surfaces along with the particular disciplinary parameters describing the analysis subcase (flight condition, gust form and reference data, etc.) are used to produce the  $\phi_{kc}$ ,  $\phi_{Lg}(ik)$  and  $\phi_{kL}$  as needed. This process is not computationally intensive and is a function of parameters which the user may want to vary as part of a trade study. Thus, these data are NOT archived as part of the aerodynamic model. The results are a set of coefficient matrices fitting the aerodynamics.

The quality of this fit may need to be checked for the set of responses that are deemed important in the current analysis. This activity may need to be performed off-line and the fit may need to be modified. Finally, the fitting coefficient matrices may be archived for reuse. They constitute a particular system representation that includes

- 1) structural geometry and element properties & design variables "the FE model"
- 2) AIC matrix for a particular aerodynamic model at a particular {Mach, number, symmetry, method, modal}.
- 3) a spline model that connects 1) and 2)
- 4) a particular control law that includes
  - actuators
  - sensors
  - filters

This archived approximation, while computed based on the current design point, will be re-used during the subsequent ASTROS design iterations, with the user free to update the fit at any point.

The final activity to complete the assembly of the ASE module is the generation and archiving of the modal representations of the FE model. The typical modal parameters:  $\{\lambda\}$ ,  $[\phi_{gh}]$ ,  $[M_{hh}]$ ,  $[K_{hh}]$ , and  $[B_{hh}]$  are straight forward. However, they introduce some complexity in that the particular modes  $[\phi_{gh}]$  may need to be extracted from a larger archived pool of modes that have been computed. They do not necessarily represent all the modes in the frequency range  $[\lambda_{min}, \lambda_{max}]$  from the archived modal analysis. In other words, to support ASE, ASTROS will allow the archival of

$$[K_{ii}], [M_{ii}] \text{ and } [B_{ii}]$$

and the associated  $[\lambda_1, \lambda_2 \dots \lambda_i]$  that are produced by normal modes analysis. They are associated with a particular structural FE model and a particular boundary condition (symmetric, antisymmetric). The ASE disciplines will be developed such that they "import" these data for use. The assembly of the  $h$ -set matrices for ASE is then the process of extracting the desirable

subset of  $[\lambda, \dots \lambda_i]$  and the augmentation of the model with additional generalized coordinates (extra points, residual vectors, etc.).

## 5.2 ASE Design Overview

In design optimization, the concept of re-using the archived modal representation of the FE model becomes more complex. The aerodynamic model is completely reusable, apart from some considerations with respect to the rational approximation and the generalized aerodynamic model. Also, the generation and use of the approximate optimization problem in ASTROS has some implication with respect to the implementation of Blocks 2.1, 2.5, 2.6 and 2.8.

## 5.3 Solution Control

ASTROS' solution control will be enhanced in a number of ways to support the proposed ASE features. These enhancements fall into seven categories (in order of dependence):

- 1) Definition of one or more unsteady aerodynamic cases
- 2) Archival/Import of aerodynamic models
- 3) Definition of one or more rational aerodynamic approximations (RAA)
- 4) Archival/Import of RAA data
- 5) Definition of one or more control margin analyses
- 6) Definition of one or more state-space flutter analyses
- 7) Definition of one or more state-space gust analyses

There will be five new analysis disciplines to create aerodynamic data or to use aerodynamics to perform response analyses:

- ZAERO: generates  $[A_{JJ}]$  matrices and geometry for a given method and model and for a series of  $\{M, k, \text{symmetry}\}$  triplets where the model is a named collection of CAERO<sub>i</sub> bulk data representing a configuration and the method is selected from
- |   |         |     |
|---|---------|-----|
| { | ZONA6   | CPM |
|   | ZONA7   | DLM |
|   | ZTAIC   |     |
|   | ZONA51U |     |
- MIST: Minimum state approximation to fit aerodynamic data for one or more Mach numbers of a ZAERO case.
- This analysis discipline either imports an archived ZAERO case or refers to a previously defined case in the current run.
  - Imports or refers to a MODES case for structural modes.
- MARGIN: Computes gain and phase margins and singular values of a MIMO system, for a given set of Mach number, boundary conditions, method, and model.
- This analysis discipline either imports an archived MIST case or refers to a previously defined MIST case in the current form.
  - In optimization, constraints (upper and lower bounds) may be placed on some or all the margins and singular values.
- ASEFLUT: Performs state space flutter analysis
- Refers to a MIST case or imports an archived MIST case.
  - In optimization, constraints can be placed on flutter damping.
- GUST: Perform a state space gust response analysis for a given set of Mach number, boundary conditions, method, and model for a particular gust spectrum.
- Refers to a MIST case or imports one.
  - In optimization, constraints can be placed on

- 1) RMS  $\{u\}$ ,  $\{\dot{u}\}$ , or  $\{\ddot{u}\}$  of structural points.
  - 2) RMS section loads (forces and moments) of a group of aerodynamic components such as a wing with a tip missile.
  - 3) RMS control command  $\{\dot{\delta}\}$ ,  $\{\delta\}$ , or  $\{\ddot{\delta}\}$ .
- Triggers the computation of  $\phi_g(ik)$  and  $\phi_{kL}$  for the gust and load modes.

In the ZAERO and MIST cases, the user can archive a pre-defined collection of data that will enable the downstream (or dependent) analysis cases to import previously computed data. This allows the output from the computationally intensive ZAERO and MIST steps to be used repeatedly. The MIST step will further support an export option to output the ASE model to MATLAB or MATRIX x.

The current ASTROS MODES discipline will be enhanced to allow the normal modes to be archived for re-use as well. This will preserve the normal modes for the generalized model update. Similar to the current ASTROS capability, the use of more than one set of MODES in a single boundary condition will not be allowed. Under the proposed effect, there will be no provision for combining symmetric and antisymmetric modal models to create an asymmetric system.

All other existing solution control commands will be supported without change. The existing flutter analysis features will continue to be supported, but will not make use of any of the enhancements presented in this proposal regarding controls. The feature will, however, be modified to import ZAERO and modal data to take advantage of those new features.

#### 5.4 MAPOL Modifications

The basic structure of the ASTROS MAPOL sequence will be retained under the proposed enhancements. That structure is shown in Fig (5.4.1) as follows:

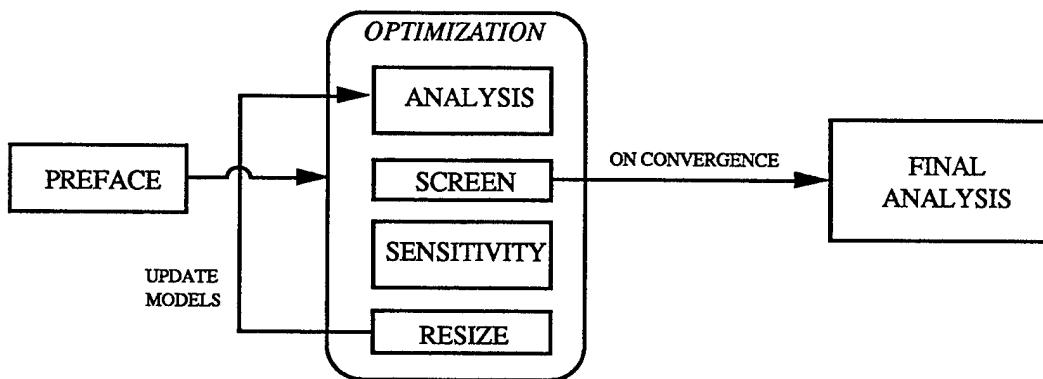


Figure 5.4.1 Basic Structure of the ASTROS MAPOL Sequence.

One of the proposed new disciplines will occur in the PREFACE section (ZAERO) while the remaining four will be supported within the analysis phase of both the optimization and the analysis segments (Ref 13). Support of the MIST case within the optimization segment will require some special code in MAPOL to avoid re-computing the minimum state approximation after the first design iteration. Note that, if the ASEFLUT, MARGIN, or GUST disciplines use imported RAA data, the MIST case need not appear in the OPTIMIZE packet of the solution control. This represents the anticipated scenario in which the ZAERO, MODES, and MIST steps

are performed in the ANALYSIS segment of an earlier ASTROS execution and archived for use in optimization.

The ASEFLUT, MARGIN, and GUST disciplines must be coded differently in the OPTIMIZATION segment than in the ANALYSIS segment to accommodate the generation of a new set of generalized matrix data for K and M using the original normal modes. The MIST output data are assumed to be design invariant and will not be updated either due to changes in the plant model or the controller model. In addition, the MAPOL support of the MODES discipline must be enhanced in the optimization phase to

- 1) Avoid recomputing modes unless the following disciplines are present
  - a) flutter
  - b) modal frequency
  - c) modal transient
  - d) a MODES case with applied frequency constraints
- 2) If the MODES discipline must be recomputed, the  $[K_{hh}]_M$  and  $[M_{hh}]_M$  matrices should be used rather than the updates  $[K_{dd}]$ , and  $[M_{dd}]$ . This makes the MODES discipline very inexpensive on subsequent design iterations.

The response analyses, ASEFLUT, MARGIN, and GUST will be decomposed into a series of discrete modules that will be called within either the OPTIMIZATION or ANALYSIS segments. Since the ASEFLUT and GUST disciplines share input, the modules creating those matrices will be separately addressable from MAPOL to maximize code re-use. As part of the proposed effort, a more detailed study of the computational steps will be performed to determine the appropriate decomposition for the MAPOL modules supporting these disciplines.

The ZAERO cases, whether in the OPTIMIZE or ANALYZE packets, will be handled in the PREFACE. This is similar to the current ASTROS' handling of DLM and CPM matrix generation, except that, under the proposed effort, the user will have to call a ZAERO discipline to compute the unsteady AIC's as opposed to the current approach where the dependent analysis (e.g. FLUTTER) triggers the computation of the required data. The current ASTROS methodology is incompatible with the ARCHIVE/IMPORT concepts.

For sensitivity analysis, the proposed enhancements require a substantial number of changes. Most importantly, the set of design parameters has been extended to include design variables that have no stiffness or mass sensitivity. ASTROS must be modified accordingly to only compute the appropriate elemental sensitivities.

The new design constraint functions generated by the ASEFLUT, MARGIN and GUST disciplines must have the appropriate modules written to compute the first derivatives of the response in the sensitivity phase of the optimization segment. As for the case of the analyses, a study will be performed to determine the best module decomposition to use in supporting the sensitivities of the related system matrices. Further changes in the sensitivity analysis are required to support the concept that the original normal modes (rather than the current modes) are the generalized coordinates.

The DESIGN module will need to be enhanced to support the new design constraints and design variables. Also, the constraint screening modules ACTCON and ABOUND will need to be extensively modified to support both, the new constraints and the new design variables.

## SECTION 6

### FUTURE RESEARCH AND DEVELOPMENT

The success of the Phase I contractual performance leads to the follow-up action of planning the Phase II activity. Under the Air Force's STTR invitation, a Phase II proposal is in preparation to be submitted to the Air Force shortly. In the Phase II proposal, the ZONA Team proposes to complete the research begun in Phase I and fully develop the ZAERO module and the ASE module in ASTROS. Seamless integration of these modules into ASTROS would be the next major task. ZONA believes that its ZAERO module would adequately support the ASTROS/ASE module for a wide range of applications in the ASTROS design and analysis environment. In the course of current and future developments of ASTROS, ZONA intends to play a major role in the enhancement support and maintenance of ASTROS/ZAERO module and consequently the ASE module. Once the seamless integration of ASTROS/ZAERO is completed in this phase, its commercialization can be carried out readily by a tentative ZONA/UAI partnership. Since both parties have established a customer base for codes in ZAERO and for ASTROS, a fruitful outcome of the initial commercialization effort is anticipated.

#### 6.1 Anticipated Successful Results of Phase II

##### (a) ASTROS/ZAERO

- i) Full development of the ZAERO module together with the AGM module.
- ii) Seamless-Integration of ASTROS/ZAERO (with AGM) will be accomplished.
- iii) Full documentation of ASTROS/ZAERO: ZONA will deliver four manuals, namely, the User's Manual, the Theoretical Manual, the Applications Manual and the Programmer's Manual.
- iv) Commercialization of the ASTROS/ZAERO will be initiated by a tentative partnership between ZONA and UAI, following the incremental development of the ZAERO model proposed in Phase II.

##### (b) ASTROS/ASE

- i) Completion of the research phase of the ASTROS/ASE development. Data retrieval (UAIC/USDA) by ASE module from ZAERO module.
- ii) ASTROS/ASE pilot software created and tested. Proposed scenario cases and industry-supplied realistic cases will be tested and demonstrated for the capability of ASTROS/ASE.
- iii) Full documentation of ASTROS/ASE. ZONA will deliver four manuals (same as those in section (a) part (iii) above).

Under the Phase II support, ZONA realizes that the provided funding could only be budgeted to accomplish the preparation for commercialization of ASTROS/ZAERO. There appears to be inadequate budget for performing the Seamless-Integration of ASTROS/ASE, thus prohibiting its immediate commercialization after Phase II. However, ZONA believes that funding from the private sector can be obtained from the aerospace industry under Phase III solicitation. The completion of the ASE as a documented code and its commercialization will be discussed next.

#### 6.2 Plans for Phase III

- (a) Full commercialization of ASTROS/ZAERO: Further improvement of the commercialized packaging of ASTROS/ZAERO, which includes the consolidation of software licensing, maintenance user serve policies and the refinement of the documentation package.
- (b) Enhance co-marketing activities between ZONA and UAI.

- (c) Seek private funding support from aerospace industry for further development of ASTROS/ASE:
  - i) Seamless Integration of ASTROS/ASE.
  - ii) Link up with the aerospace industry for ASE applications to ongoing projects (e.g. AAW, HSCT, JAST, etc.)
  - iii) In this regard, ZONA has obtained a number of supportive letters on the ASTROS/ASE development from potential users. The likelihood of funding support is evidenced by these responses from the aerospace community.

### **6.3 Significance and Impact of Phase II on Phase III**

- a) The successful results of Phase II will enhance the confidence from potential users in the aerospace industry. For example, Transonic/Hypersonic flutter results of ZAERO and the scenario and realistic case demonstration of the ASE capability could definitely serve this purpose.
- b) The research and development effort in Phase II is aimed at setting a firm foundation towards a unified methodology for aeroservoelasticity design/analysis, thus leading to a industrial-standard production software which would serve the aerospace community worldwide.



## SECTION 7

### POTENTIAL APPLICATIONS

#### 7.1 Potential Technical Applications

The potential areas of applications are many for ASTROS/ASE. It will provide the aerospace industry an excellent design/analysis tool for aircraft such as the High Speed Civil Transport (HSCT) or the Active Aeroelastic Wing (AAW), among other ongoing and future projects. Other gross potentials of ASTROS/ASE include its integration with Probabilistic Design Methods, Designing Smart Structures and its further inclusion of a emerging robust control technology.

#### 7.2 Potential Commercial Application

- a) As discussed in an earlier section (D.2), ZONA Technology has enjoyed the commercial success of ZONA51 since its release in 1985. Now with over 35 users worldwide, the ZONA51 code has been marketed independently by ZONA since 1985 and jointly marketed by ZONA and the MacNeal Schwendler Corporation (MSC) under MSC/NASTRAN (as Aero Option II) since 1991.

- b) The ZAERO Module

As described previously (see Fig 2.1.1), the ZAERO module contains four major unsteady aerodynamic codes covering the complete flight regime throughout the full Mach number range, a capability surpassing that of the current Aero modules in MSC/NASTRAN and in ASTROS. Specifically, ZTAIC and ZONA51U are the transonic and unified hypersonic/supersonic generalization of the lifting surface code ZONA51, respectively. ZONA6 and ZONA7 generalize the codes by including geometric complexity to wing-body combinations that can represent realistic aircraft configurations for aeroelastic applications. Further, the UAIC feature of the ZAERO allows it to be readily interfaced with the FEM model created by ASTROS. A market survey quickly reveals that none of the above features in terms of flow and geometric generalization or a unified AIC is available in any existing software. On the other hand, ZONA's market survey from responses among our ZONA code users and others in the Aerospace community indicates that a software package such as the ZAERO module is lacking presently and would be in high demand.

The built-in AGM module with ZAERO will provide any selected panel method a convenient entry to ASTROS. In this way, the flexibility of ASTROS as opposed to that of NASTRAN would be enhanced greatly, thereby generating more users for ASTROS.

- c) ASTROS/ZAERO/ASE

The Phase II products, ASTROS/ZAERO (seamlessly integrated) and ASTROS/ASE (not seamlessly integrated), should stand out as two unique software products that are cutting-edge technology for aeroelastic design/analysis and ASE design/analysis.

- d) The commercialization of ASTROS/ZAERO should resort to the code-licensing means; it could be an annual license or a one-time paid-up license. ZONA has had over ten years of experience in code licensing and UAI even more. The CREDA agreement between UAI/AF should expand further the worldwide licensing of the ASTROS/ZONA.

### **7.3 Potential Use by the Federal Government**

A fraction of the ZONA51 and ASTROS users belong to organizations in DoD and NASA (ZONA51 is used frequently by WPAFB and NASA-Langley). Aeroelasticians at Wright Laboratory have repeatedly shown strong interest in the ZONA codes (such as ZONA51 or ZONAIR) to assist them in their projects (e.g. the AAW project).

Since the AF is the sponsor of Phase II, ZONA intends to make available the executables of the ZAERO module to the appropriate divisions of WPAFB for their exclusive usage on a royalty free basis. No further rights of the ZAERO module will be transferred to the DoD/Federal Government.

## REFERENCES

1. Miller, G.D., "An Active-Flexible Wing Multi-Disciplinary Design Optimization Method," 35th AIAA/ASME/ASCE/ASC Structures and SDM conference proceeding paper, AIAA 94-4412-CP.
2. "Active Flexible Wing Design: Methodology Study," Rockwell Aerospace/North American Report No. NA94-1731, April 1995 (AF Contract No. F33657-90-D-0030-0014).
3. Adams, W.M., Jr. and Hoadley, S.T., "ISAC: A Tool for Aeroservoelastic Modeling and Analysis," AIAA-93-1421-CP, 1993.
4. Peele, E.L., and Adams, W.M., Jr., "A Digital Program for Calculating the Interaction between Flexible Structures, Unsteady Aerodynamics and Active Controls," NASA TM-80040, Jan. 1979.
5. Tinico, E.N. and Mercer, J.E., "DLEXSTAB - A Summary of the Functions and Capabilities of the NASA Flexible Airplane Analysis Computer System," NASA CR 2564, October 1974.
6. Rodden, W.P., Haper, R.L. and Bellinger, E.D., "Aeroelastic Addition to NASTRAN," NASA CR-3146, 1979.
7. Peery, B. III, Kroll, R.I., Miller, R.D. and Goetz, R.C., "DYLOFLEX: A Computer Program for Flexible Aircraft Flight Dynamic Loads Analysis with Active Controls," Journal of Aircraft, Vol. 17, No. 4, April 1980, pp. 275-282.
8. Noll, T., Blair, M. and Cerra, J., "ADAM, an Aeroservoelastic Analysis Method for Analog or Digital System, Journal of Aircraft, Nov, 1986.
9. Pitt, D.M. and Goodman, C.E., "FAMUSS: A New Aeroservoelastic Modeling Tool," AIAA Paper 92-2395-CP, April, 1992.
10. Rodden, W.P. and Johnson, E.H., "MSC/NASTRAN Aeroelastic Analysis User's Guide Version 68," The MacNeal-Schwendler Corporation publication, 1994.
11. Venkayya, V.B., Tischler, V.A. and Bharatram, G., "Multidisciplinary Issues in Airframe Design," 37th AIAA/ASME/ASCE/ASC Structures and SDM conference proceeding paper, AIAA-96-1386-CP.
12. Johnson, E.H. and Venkayya, V.B., "Automated Structural Optimization System (ASTROS), Theoretical Manual," AFWAL-TR-88-3028, Vol. 1, December 1988.
13. Neil, D.J., Johnson, E.H. and Herendeen, D.L., "Automated Structural Optimization System (ASTROS) User's Manual, AFWAL-TR-88-3028, Vol. 2, April 1988.
14. Johnson, E.H. and Neil, D.J., "Automated Structural Optimization System (ASTROS), Application Manual," AFWAL-TR-88-3028, Vol. 3, July 1988.
15. Neil, D.J., Johnson, E.H. and Hoesly, R.L., "Automated Structural Optimization System (ASTROS), Programmer's Manual," AFWAL-TR-88-3028, Vol. 4, July 1988.
16. Neill, D.J. and Herendeen, D.L., "ASTROS Enhancements, Volume I - ASTROS User's Manual," WL-TR-96-3004, May 1995.
17. Neill, D.J., Herendeen, D.L. and Hoesly, R.L., "ASTROS Enhancements, Volume II - ASTROS Programmer's Manual," WL-TR-96-3005, May 1995.
18. Neill, D.J., Herendeen, and Venkayya, V.B., "ASTROS Enhancements, Volume III - ASTROS Theoretical Manual," WL-TR-96-3004, May 1995.
19. ZONA, OU, Karpel, UAI, "Enhancement of the Aeroservoelastic Capability in ASTROS," STTR Phase I Proposal (AF95T009), April 1995.
20. ZONA, OU, Karpel, UAI, "Enhancement of the Aeroservoelastic Capability in ASTROS," STTR Phase I Final Report under STTR/AF Contract No. AF95T009, ZONA Report 96-09, May 1996.
21. Liu, D.D., Yao, Z.X., Sarhaddi, D., and Chavez, F., "Piston Theory Revisited and Further Applications," ICAS Paper 94-2.8.4, presented at the 19th Congress of the International Council of the Aeronautical Sciences, September, 1994.
22. Liu, D.D., Chen, P.C., Yao, Z.X. and Sarhaddi, D., "Recent Advances in Lifting Surface Methods," Paper No. 4, Proceedings of International Forum on Aeroelasticity and Structural Dynamics, Manchester U.K., June 1995.
23. Chen, P.C. and Liu, D.D., "A Harmonic Gradient Method for Unsteady Supersonic Flow Calculations," Journal of Aircraft, Vol. 22, No. 5, May 1985, pp. 371-379.
24. ZONAIR Theoretical Manual and ZONAIR Users Manual, ZONA 94-02/03, 1994.
25. ZONA Technology, "Aerodynamic Loads and Store Separation for Aircraft at Supersonic/Subsonic Speeds: ZONAIR and ZSTORE," ZONA Report 95-02.1, Feb 1995.
26. Chen, P.C. and Liu, D.D., "Unsteady Supersonic Computations of Arbitrary Wing-Body Configurations Including External Stores," Journal of Aircraft, Vol. 27, No. 2, February 1990, pp. 108-116.
27. Chen, P.C., Lee, H.W. and Liu, D.D., "Unsteady Subsonic Aerodynamics for Bodies and Wings with External Stores Including Wake Effect," Paper 91-060, International Forum on Aeroelasticity and Structural Dynamics, Aachen, FRG, June 3-6, 1991. Also, Journal of Aircraft, Vol. 30, No. 5, Sept.-Oct. 1993, pp. 618-628.

28. "Documentation of ZONA6 Code (Version C)," ZONA 91-8.3, October 1994.
29. "Documentation of ZONA7 Code (Version E)," ZONA 91-19.5, October 1994.
30. Albano, E. and Rodden, W.P., "A Doublet-Lattice Method for Calculating Lift Distributions on Oscillating Surfaces in Subsonic Flows," AIAA Journal, Volume 7, February 1969, pp 279-285, and Volume 7, November 1969, p 2192.
31. Liu, D.D., "Computational Transonic Equivalent Strip Method for Applications to Unsteady 3D Aerodynamics," AIAA 21st Aerospace Science Meeting, Reno, NV., January 10-13, 1983, AIAA Paper No. 83-0261.
32. Liu, D.D., Kao, Y.F. and Fung, K.Y., "An Efficient Method for Computing Unsteady Transonic Aerodynamics of Swept Wings with Control Surfaces," Journal of Aircraft, Vol. 25, No. 1, January 1988.
33. ZTES/TAIC Documentation, ZONA 93-06, September 1993.
34. Fung, K.Y. and Chung, A., "Computations of Unsteady Transonic Aerodynamics Using Prescribed Steady Pressures," Journal of Aircraft, Vol. 20, No. 12, December 1983, pp. 1058-1061.
35. Lessing, H.C., Troutman, J.L. and Menees, G.P., "Experimental Determination of the Pressure Distribution on a Rectangular Wing Oscillating in the First Bending Mode for Mach Numbers from 0.24 to 1.30," NASA TN D-33, December 1960.
36. Malone, J.B. and Ruo, S.Y., "LANN Wing Test Program: Acquisition and Application of Unsteady Transonic Data for Evaluation of Three-Dimensional Computational Methods," AFWAL-TR-83-3006, Feb. 1983.
37. Sotomayer, W.A. and Borland, C.J., "Numerical Computation of Unsteady Transonic Flow about Wings and Flaps," AIAA Paper 85-1712, 1985.
38. Scott, R.C. and Pototzky, A.S., "A Method of Predicting Quasi-Steady Aerodynamics for Flutter Analysis of High Speed Vehicles Using Steady CFD Calculations," AIAA-93-1364-CP, 1993.
39. Yates, E.C., "Agard Standard Aeroelastic Configurations for Dynamic Response I-Wing 445.6," AGARD Report No. 765.
40. Kolonay, R. Private Communication.
41. Karpel, M., "Time-Domain Aeroservoelastic Modeling Using Weighted Unsteady Aerodynamic Forces," J. Guidance, Control, and Dyn., Vol. 13, No. 1, 1990, pp. 30-37.
42. Karpel, M., and Strull, E., "Minimum-State Unsteady Aerodynamic Approximation with Flexible Constraints," International Forum on Aeroelasticity and Structural Dynamics, Manchester UK, June 1995, pp. 66.1-66.8.
43. Walters, R., Reu, T. McGrory, W., and Richardson, P., "A Longitudinally-Patched Grid Approach with Applications to High Speed Flows," AIAA Paper No. 88-0715, AIAA 26th Aerospace Sciences Meeting, Reno, Nevada, January 1988.
44. Bennet, R.M., Batina, J.T. and Cunningham, H.J., "Wing-Flutter Calculations with the CAP-TSD Unsteady Transonic Small-Disturbance Program," Journal of Aircraft, Vol. 29, No. 9, September 1989.
45. Garcia-Fogeda, P. and Liu, D.D., "Analysis of Unsteady Aerodynamics of Elastic Bodies in Supersonic Flow," Journal of Aircraft, Vol. 24, No. 12, December 1987, pp. 833-840.
46. Adams, William M., Jr.; and Tiffany, Sherwood H., "Design of a Candidate Flutter Suppression Control Law for DAST ARW-2", NASA TM-86257, 1984.
47. Karpel, M. and Hoadley, S.T., "Physically Weighted Approximations of Unsteady Aerodynamic Forces Using the Minimum-State Method," NASA Technical Paper 3025, March 1991.
48. Mukhopadhyay, V., "Control Law Synthesis and Stability Robustness Improvement Using Constrained Optimization Techniques," Control and Dynamic Systems, Vol. 32, 1990.
49. Zole, A. and Karpel, M., "Continuous Gust Response and Sensitivity Derivatives Using State-Space Models," presented at the Israel Annual Conference on Aviation and Astronautics, February 1993.

## **APPENDIX A**

### **Contractual Performance Report of STTR AF95T009:**

*(Presented to Wright Laboratory Personnel  
on March 11-12, 1996, WPAFB, Ohio)*

# ENHANCEMENT OF AEROSERVOELASTIC CAPABILITIES IN *ASTROS*

(STTR AF95T009)

ZONA\*, OU, UAI, Karpel



Presented at Wright Laboratory  
Wright-Patterson AFB, Dayton, Ohio on March 11-12, 1996

---

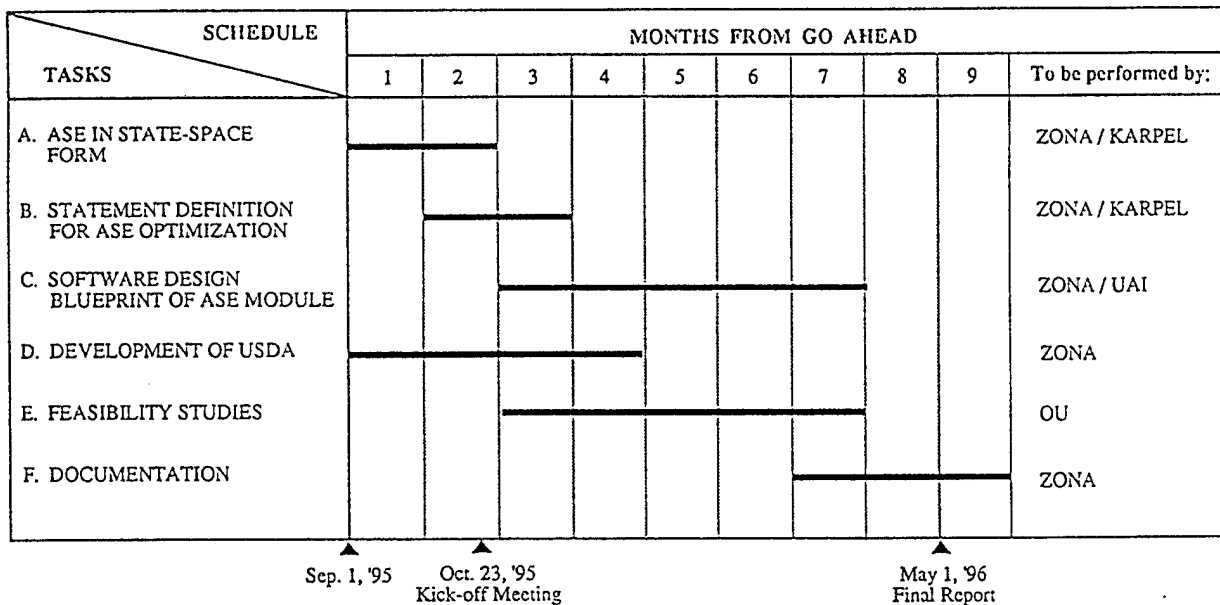
2651 W. Guadalupe Rd., Ste. B-228, Mesa, AZ 85202 Tel (602) 831-2775 / Fax (602) 820-2934 / e-mail: zonatech.com

ZTL95STTR/WLPPr021496

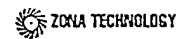
## OVERVIEW

- PROGRESS OF PHASE I
- ZONA AERO MODULE
- PROPOSED ASTROS/ASE MODULE
- PHASE II & DISCUSSION

# TASK SCHEDULE



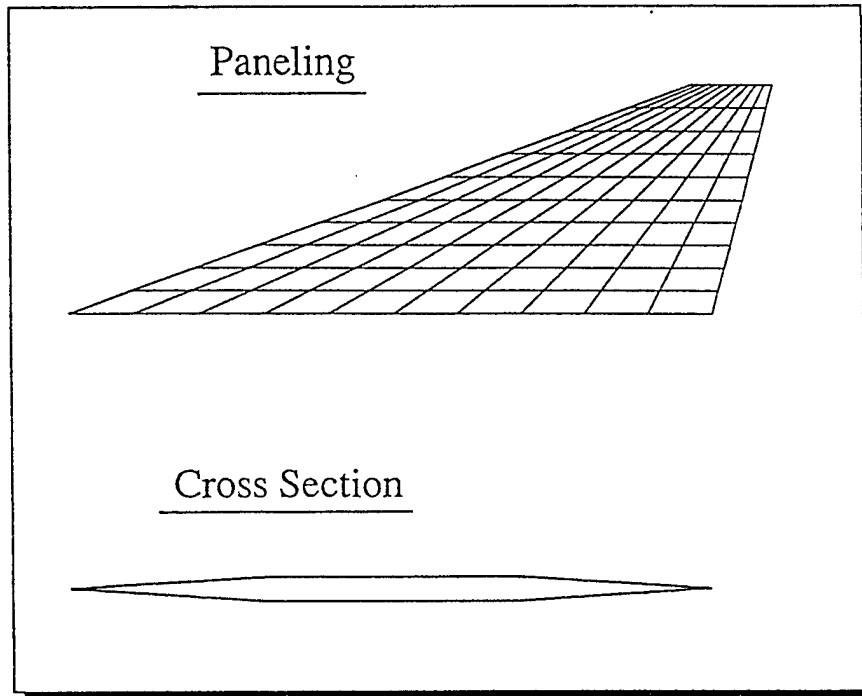
ZTL9STTR/KOM101895



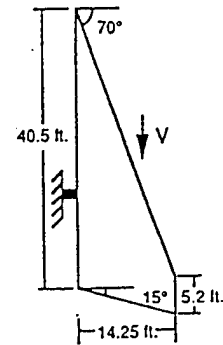
## PROGRESS OF PHASE I

- *ZONA51U*
  - NASP Demonstrator Wing
- *ZTAIC*
  - Lann Wing
  - Lessing Wing
  - 445.6 Wing
  - Modeled F-16 Wing

# AERODYNAMIC MODEL OF NASP DEMONSTRATOR WING



Wing Planform

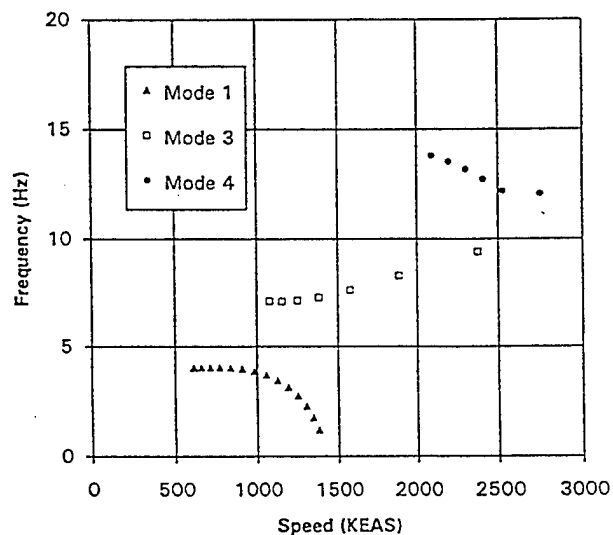
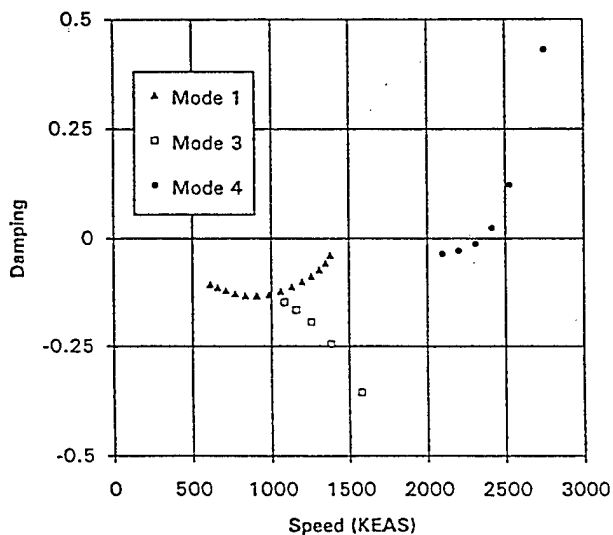


ZTL&STTR/KOM101895

ZONA TECHNOLOGY

## V-g Plot of NASP Demonstrator at $M = 5.0$

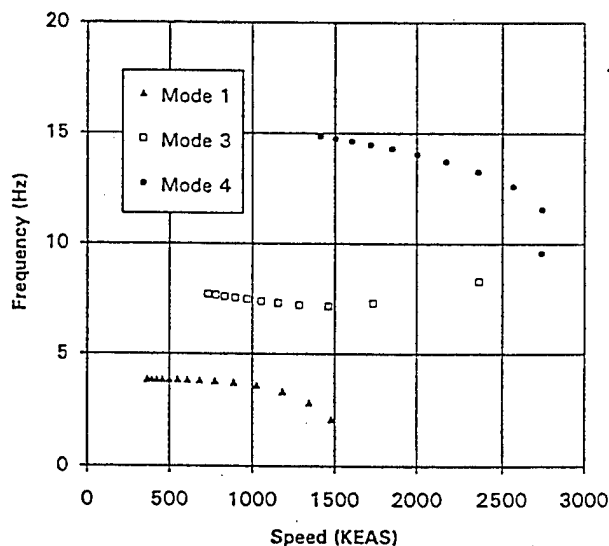
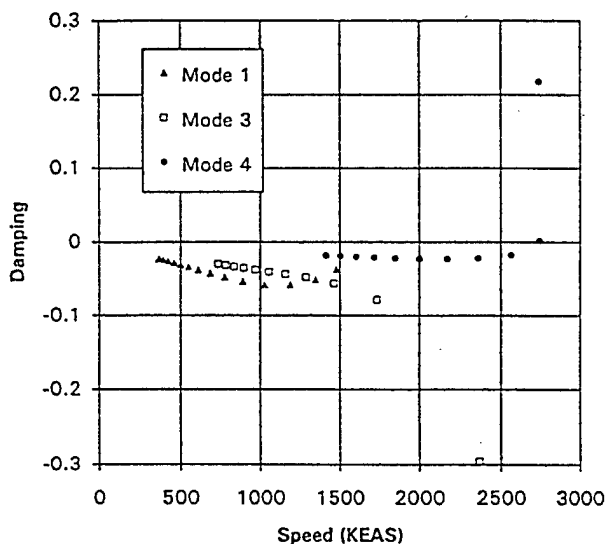
8 Modes,  $V_f = 2342$  KEAS,  $Q_f = 129$  psi,  $\omega_f = 13$  Hz on Mode 4



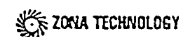


# V-g Plot of NASP Demonstrator at $M = 10.0$

8 Modes,  $V_f = 2726$  KEAS,  $Q_f = 175$  psi,  $\omega_f = 11.6$  Hz on Mode 4

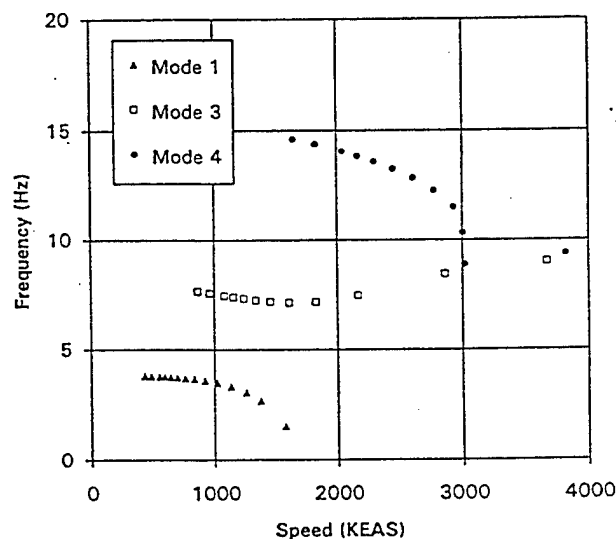
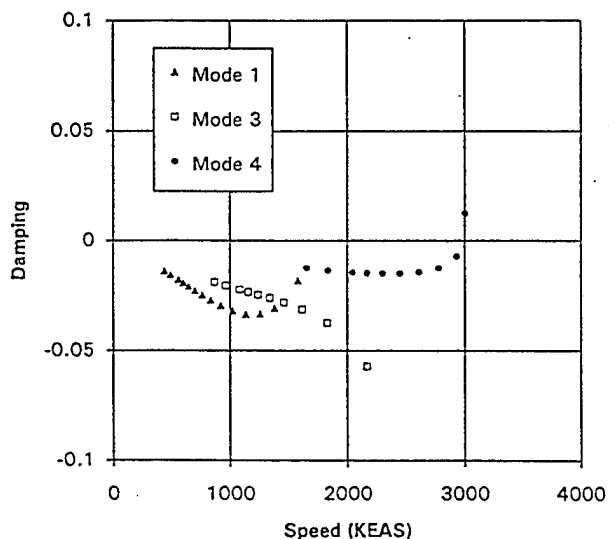


ZTLN/STTR/KOM/101895

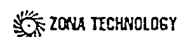


# V-g Plot of NASP Demonstrator at $M = 15.0$

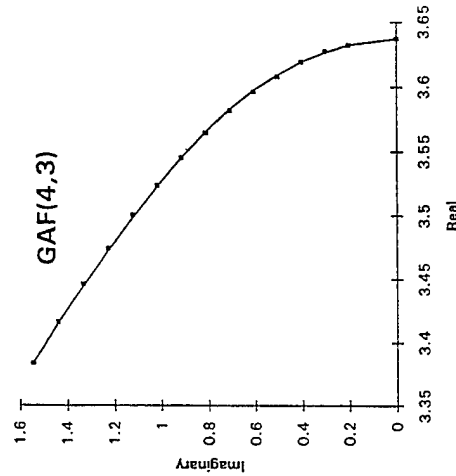
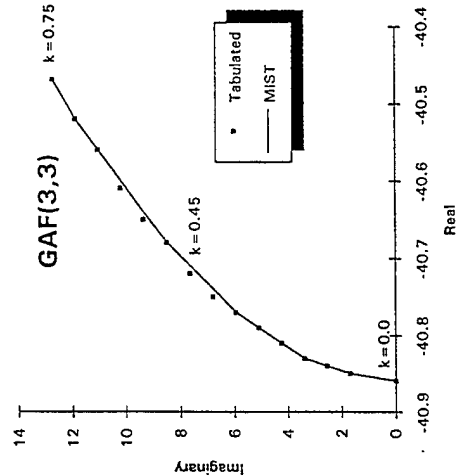
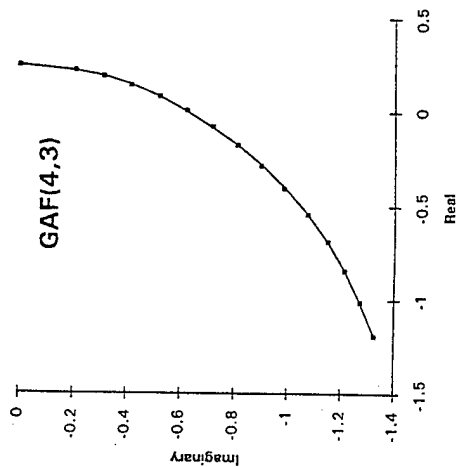
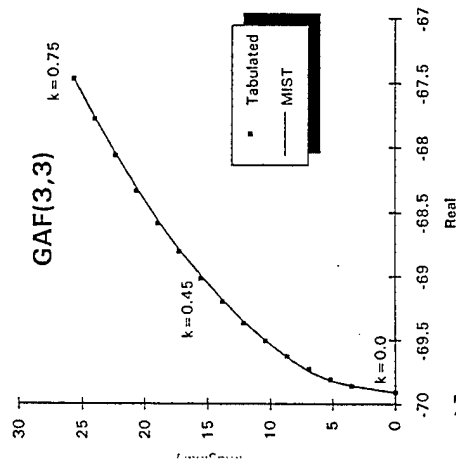
8 Modes,  $V_f = 2957$  KEAS,  $Q_f = 206$  psi,  $\omega_f = 11$  Hz on Mode 4



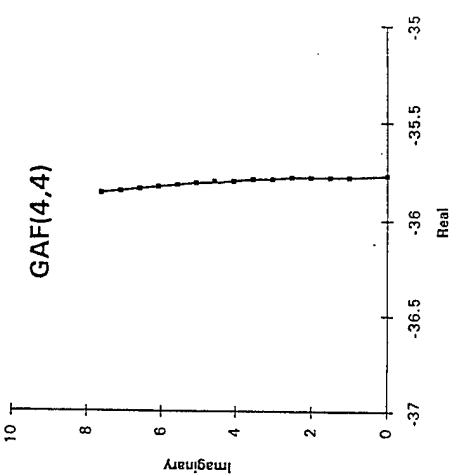
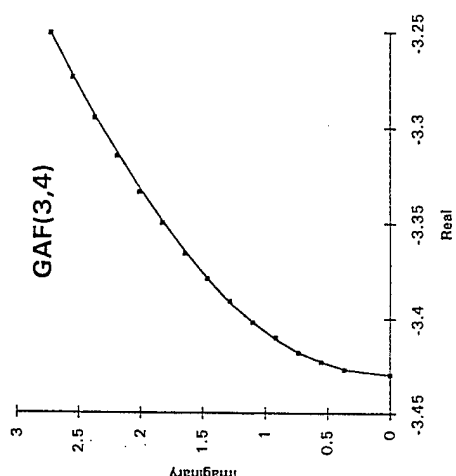
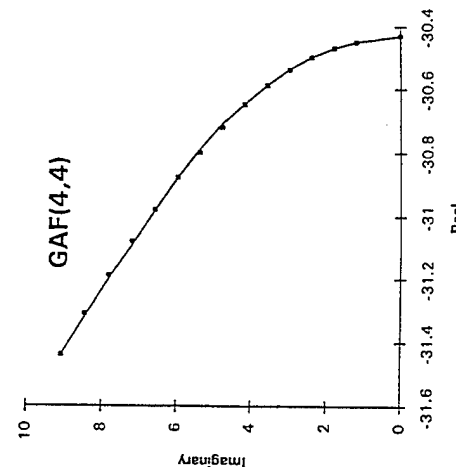
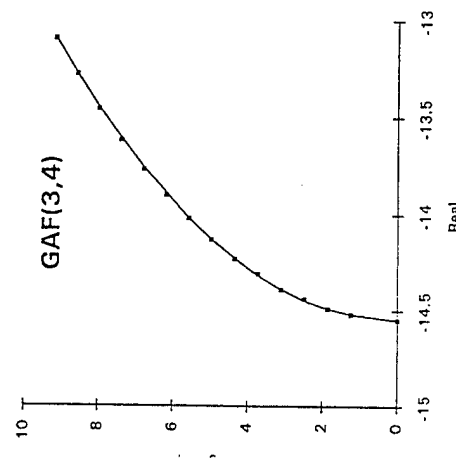
ZTLN/STTR/KOM/101895



# Minimum-State (MIST) Fit of GAF NASP Demonstrator, M = 5.0



71



ZTL5STTRKON101995



ZTL5STTRKON101995

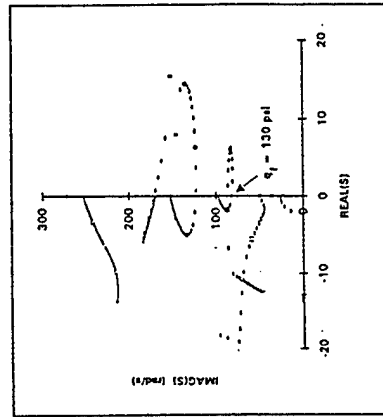
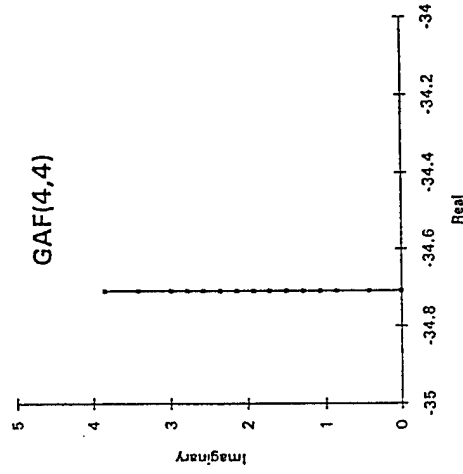
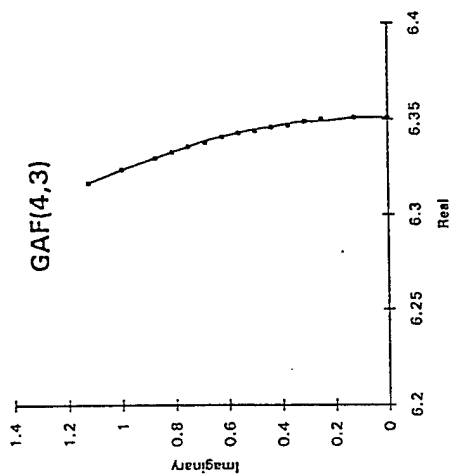
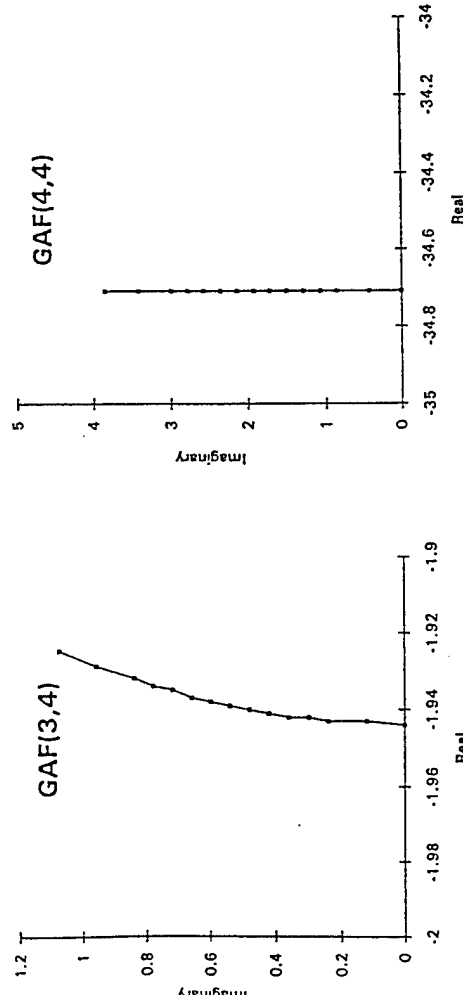
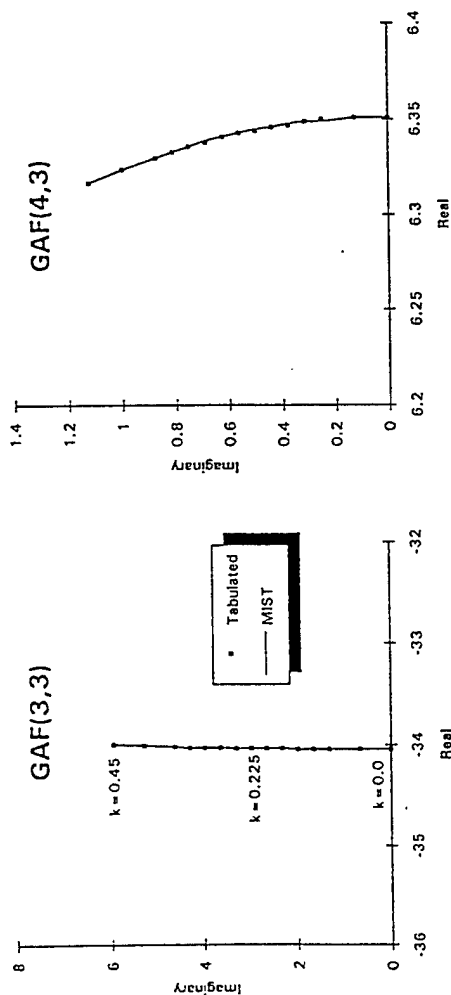


ZTL5STTRKON101995

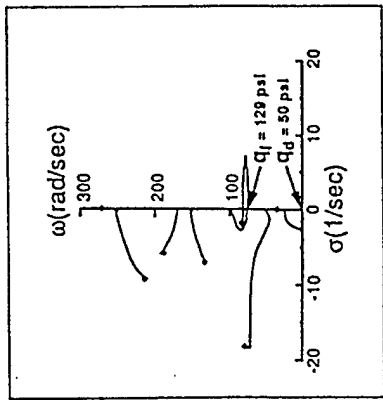
# Minimum-State (MIST) Fit of GAF NASP Demonstrator, $M = 15.0$

## Root-Locus Plots of NASP Demonstrator

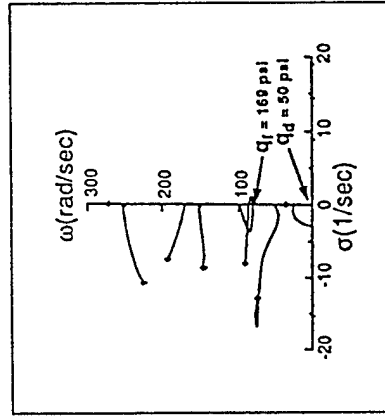
$M = 5.0$



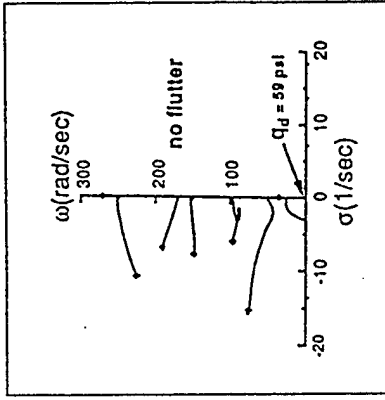
Using ZONA5IU - MIST Code Results



Using Piston Theory GAF Matrices\*



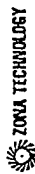
Using QSCFD 2d GAF Matrices\*



Using QSCFD 3d GAF Matrices\*

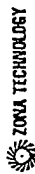
\* Plots taken from: Scott, R.C. and Pototzky, A.S., "A Method of Predicting Quasi-Steady Aerodynamics for Flutter Analysis of High Speed Vehicles Using Steady CFD Calculations," AIAA-93-1364-CP, 1993.

ZONA TECHNOLOGY



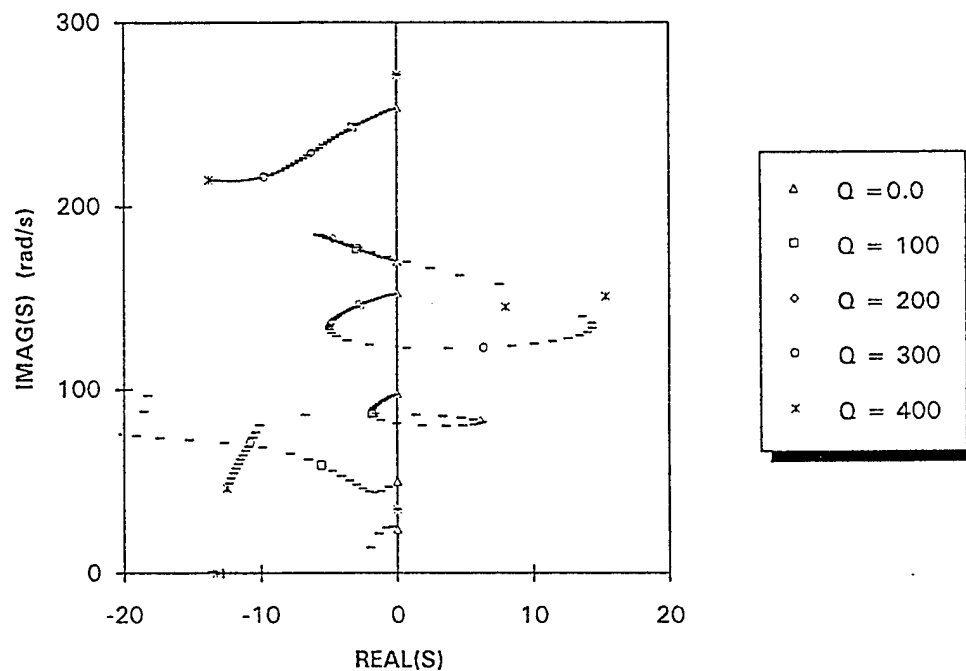
ZONA TECHNOLOGY

ZONA TECHNOLOGY



## Root-Locus Plot of NASP Demonstrator at $M = 5.0$

8 Modes,  $Q_f = 130$  psi,  $\omega_f = 82$  r/s on Mode 4

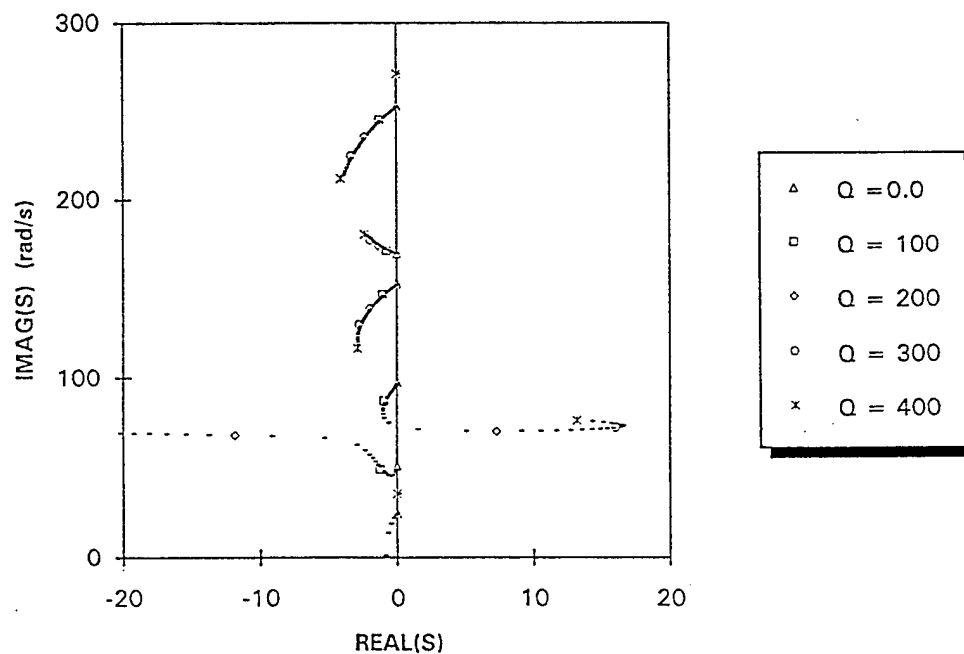


ZTL&STTR/KOM101895

ZONIA TECHNOLOGY

## Root-Locus Plot of NASP Demonstrator at $M = 10.0$

8 Modes,  $Q_f = 184$  psi,  $\omega_f = 71$  r/s on Mode 4



ZTL&STTR/KOM101895

ZONIA TECHNOLOGY

# Comparison of Flutter Results

## NASP Wing

Aerodynamic Method	Mach Number								
	5			10			15		
	$q_f$ psi	$\omega_f$ r/s	$h$ (Kft)	$q_f$ psi	$\omega_f$ r/s	$h$ (Kft)	$q_f$ psi	$\omega_f$ r/s	$h$ (Kft)
Piston Theory	129	78	18	184	78	42	250	72	51
QSCFD 2d	169	80	11	331	81	28	982	224	22
QSCFD 3d	----	----	----	330	82	28	981	224	22
ZONA51U - V-g Method	129	82	18	175	73	42	206	70	55
- S-Domain	130	82	18	184	71	41	213	68	54

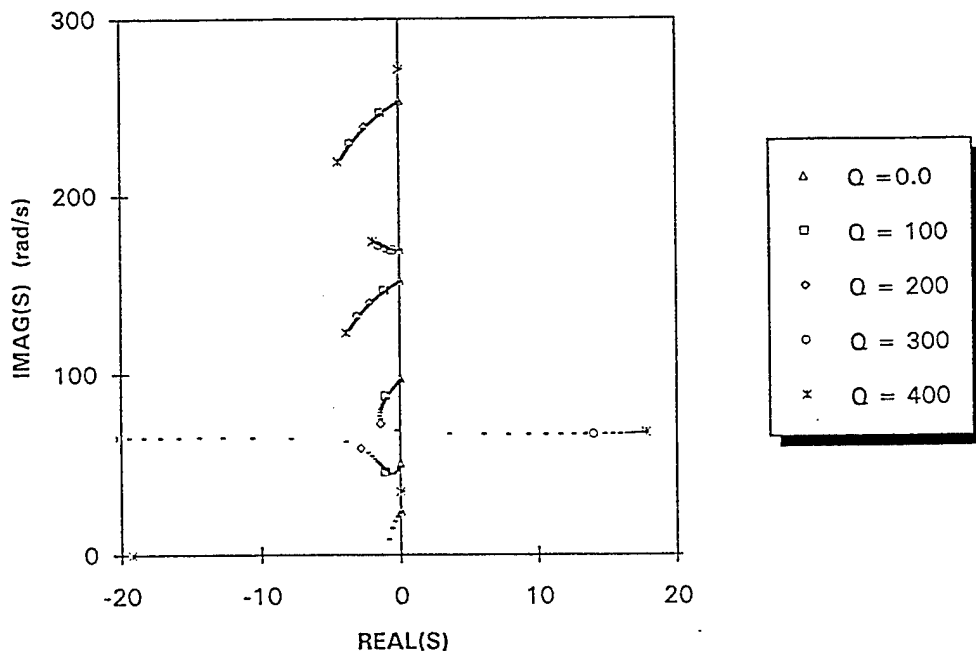
$h$  = Approximate matchpoint altitude.

Piston Theory, QSCFD 2d and QSCFD 3d data taken from:  
Scott, R.C. and Pototzky, A.S., "A Method of Predicting Quasi-Steady Aerodynamics for Flutter Analysis  
of High Speed Vehicles Using Steady CFD Calculations," AIAA-93-1364-CP, 1993.  
ZTLA-STTR/KOM101895



## Root-Locus Plot of NASP Demonstrator at M = 15.0

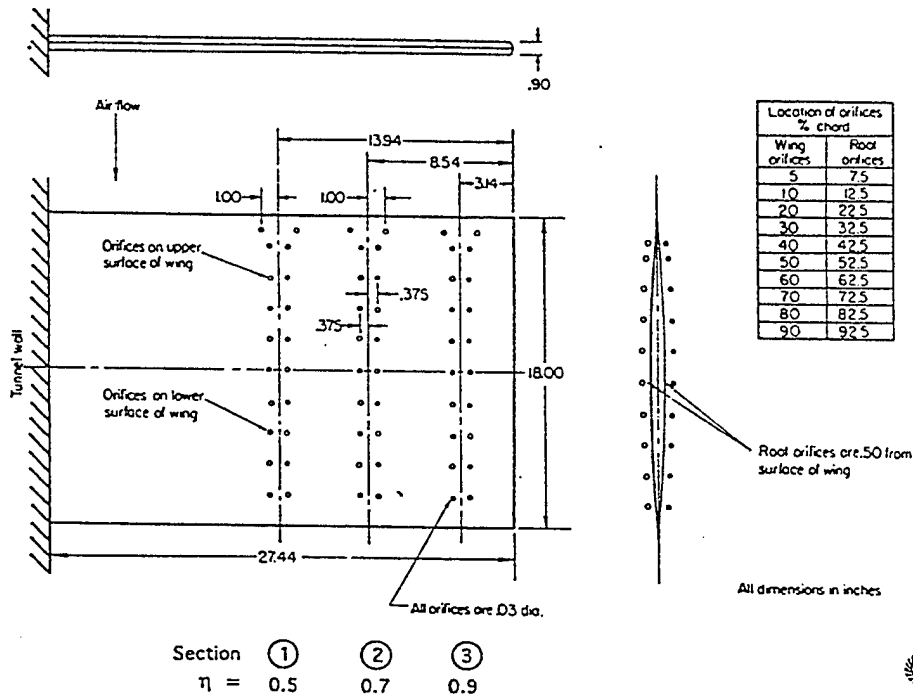
8 Modes,  $Q_f = 213$  psi,  $\omega_f = 68$  r/s on Mode 4



# THE LESSING WING

NASA TND-344 / H.C. Lessing & J.L. Troutman /  $M=0.24\sim 1.3$

AR = 3.0, 5% Parabolic Arc



ZTL8/CICFC-Occ95

ZONIA TECHNOLOGY

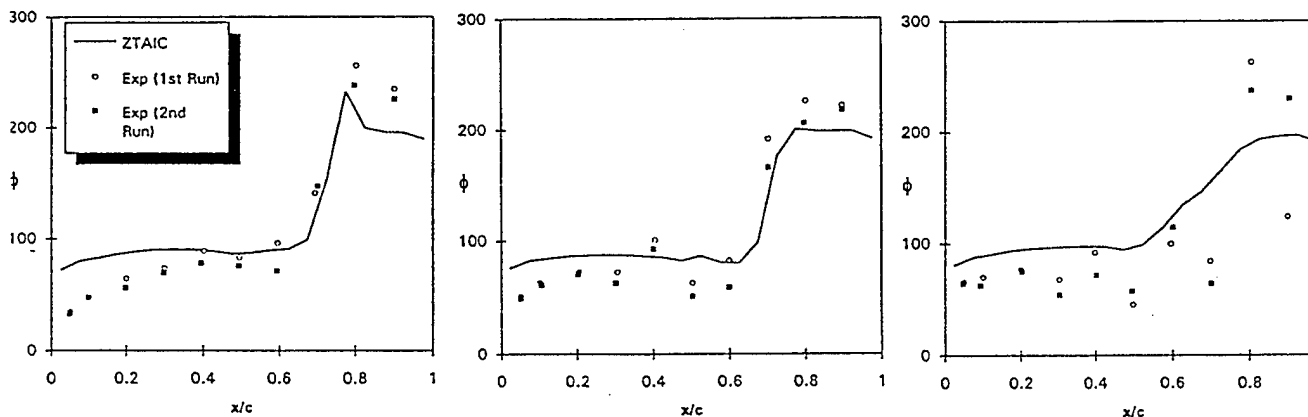
## The Lessing Wing at $M=0.9$

Phase Angle (in degrees) of First Bending at  $k = 0.13$

Section 1  
 $\eta = 0.5$

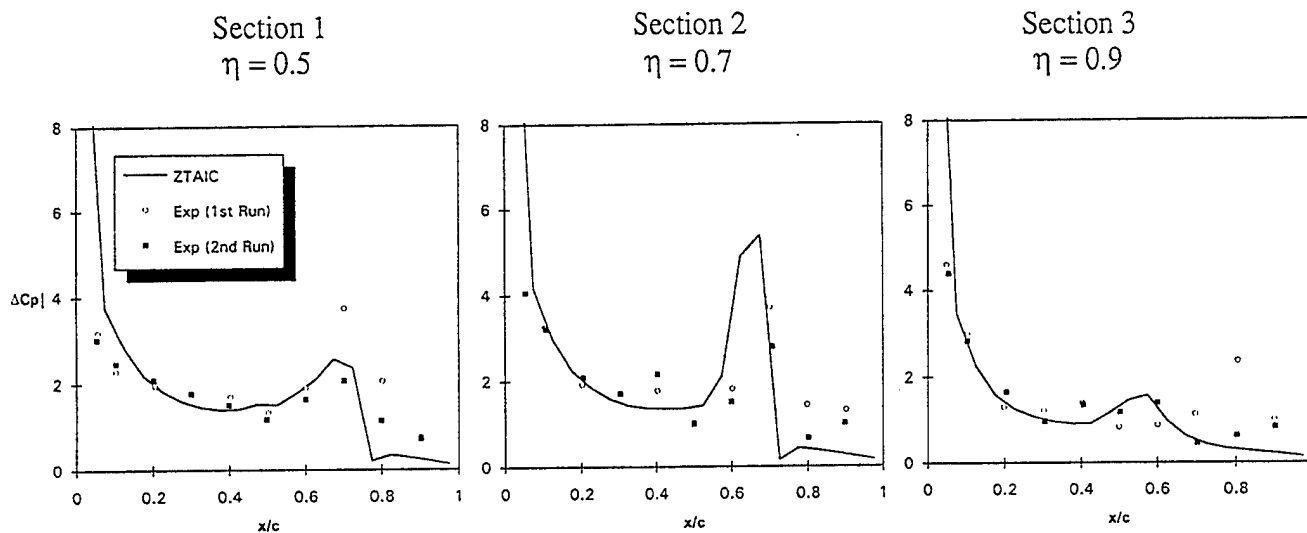
Section 2  
 $\eta = 0.7$

Section 3  
 $\eta = 0.9$



## The Lessing Wing at $M=0.9$

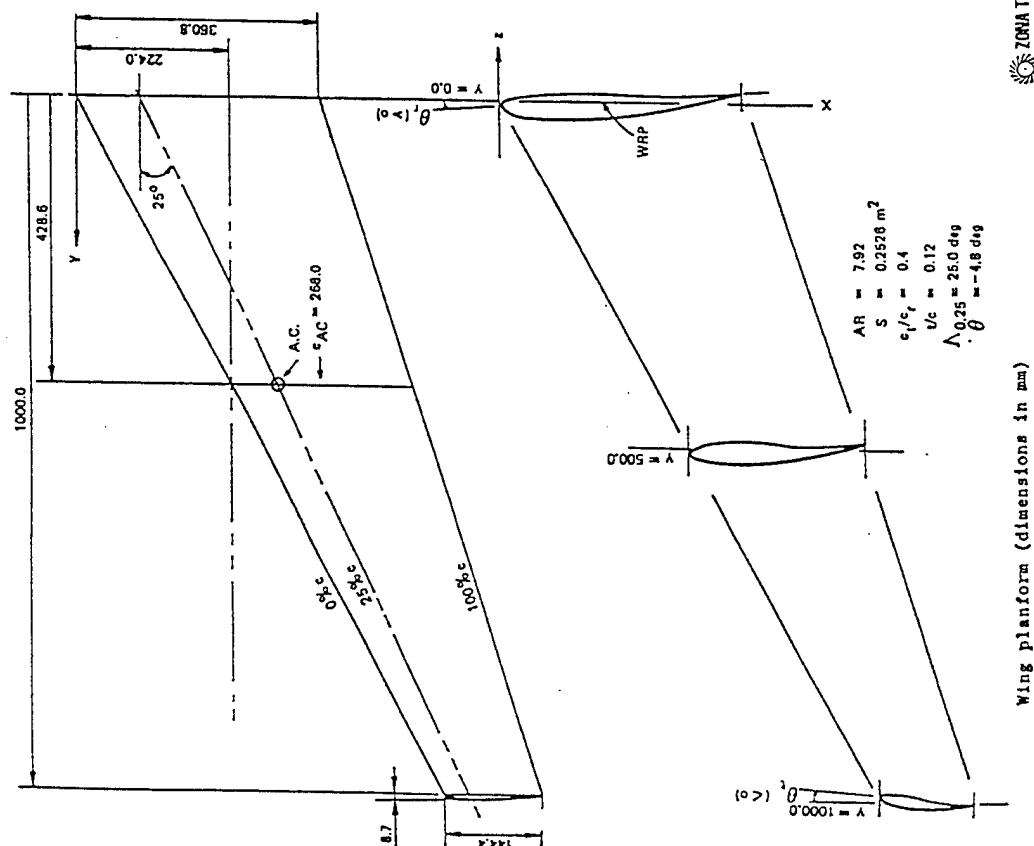
### Magnitude of First Bending at $k = 0.13$



ZILS/STTR/KOM/0189S



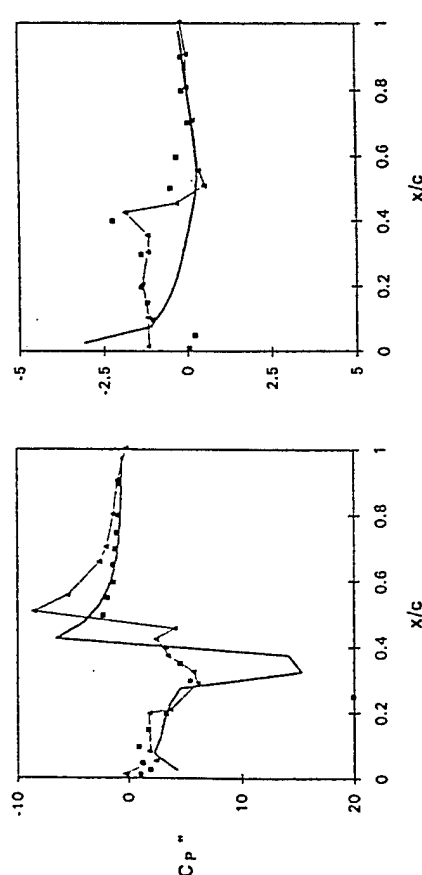
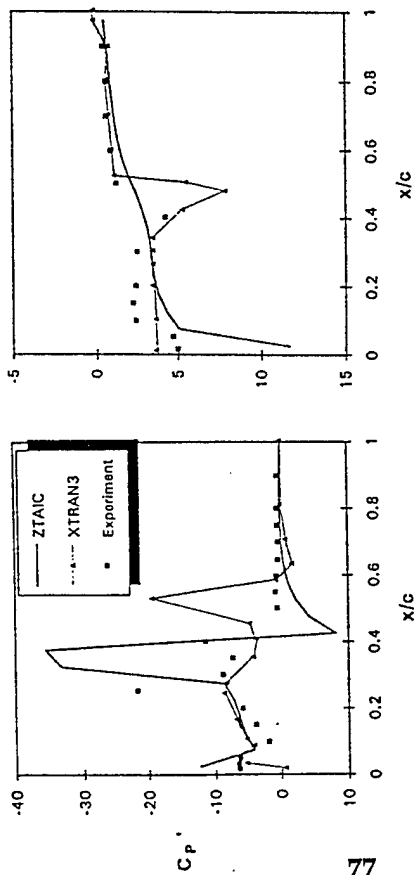
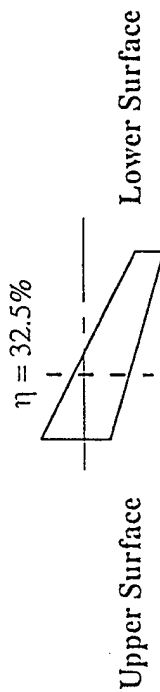
# LANN WING\* CONFIGURATION



\* AFWAL-TR-83-3050/A. STEINGA & R. HOUWINK/May 1983  
AFWAL-TR-83-3006/J.B. MALONE & S.Y. RUO/Feb 1983

# Lann Wing at M=0.82

Wing Pitching at 62% Root Chord,  $k=0.205$  &  $AOA=0.6^\circ$

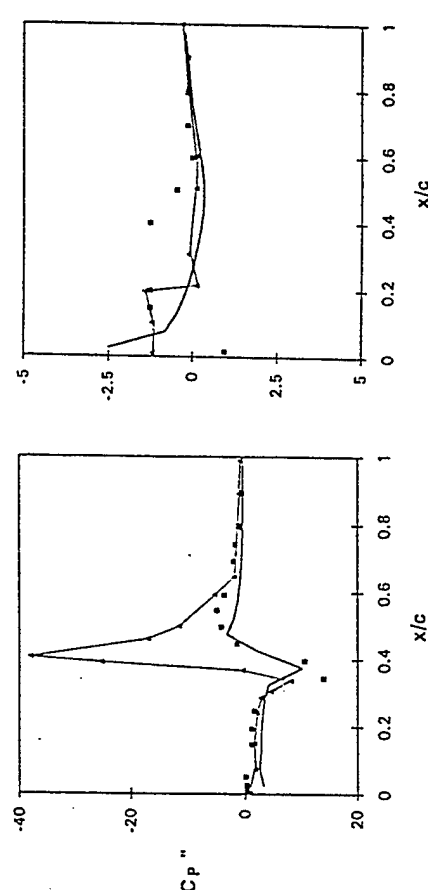
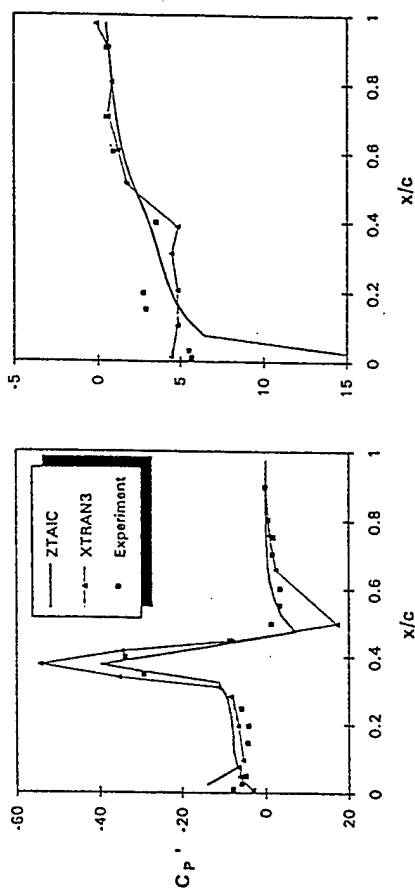
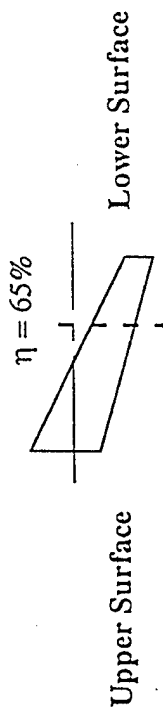


ZTLB/FCFC-0-0103

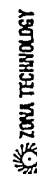


# Lann Wing at M=0.82

Wing Pitching at 62% Root Chord,  $k=0.205$  &  $AOA=0.6^\circ$



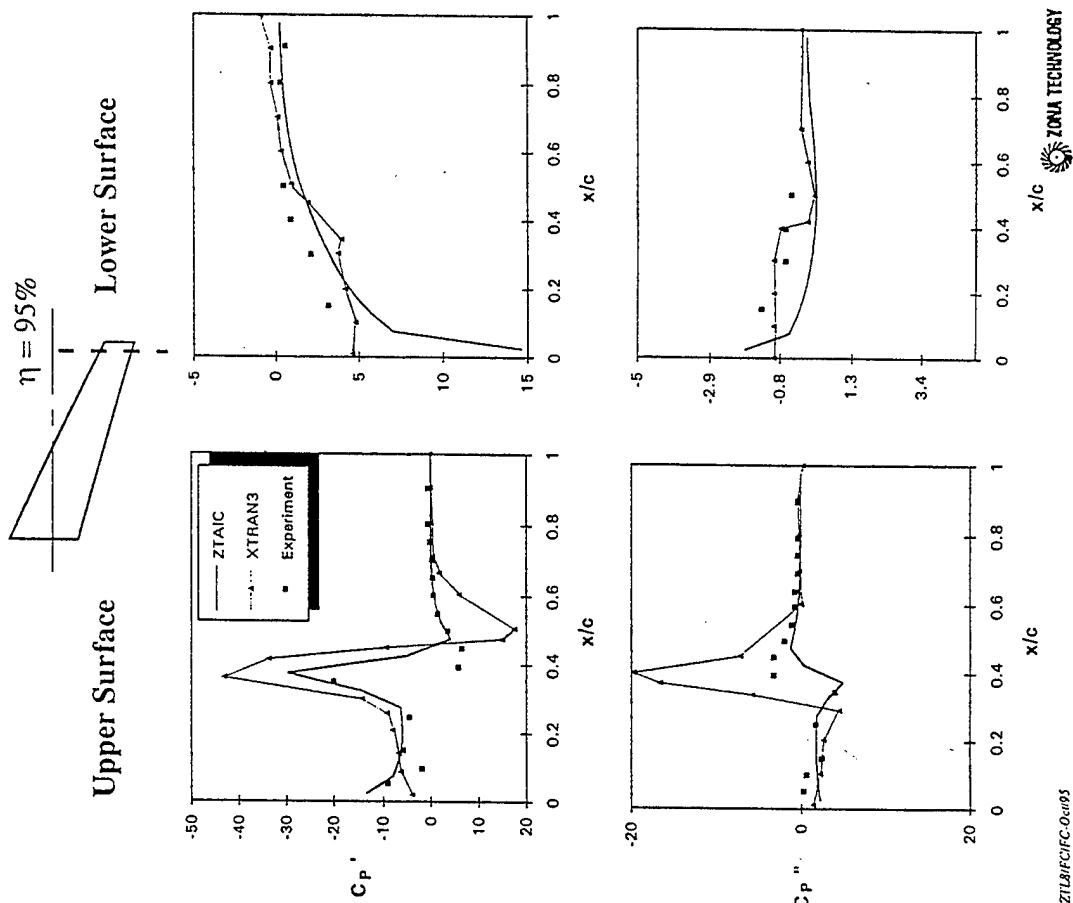
ZTLB/FCFC-0-0103





# Lann Wing at M=0.82

Wing Pitching at 62% Root Chord,  $k=0.205$  &  $AOA=0.6^\circ$



## AGARD STANDARD 445.6 WING\*

TABLE I  
MEASURED MODAL FREQUENCIES AND PANEL MASS

Model description				Frequency, cps					Panel mass, slugs
Panel span, ft	Mounting	Structure	Model	$f_{h,1}$	$f_{h,2}$	$f_{t,1}$	$f_{t,2}$	$f_a$	$\bar{m}$
1.250	Wall	Solid	1	30.40	146.00	99.10	243.00	98.77	0.02298
2.500	Wall	Solid	1	14.60	67.50	47.70	117.00	47.54	.14347
			2	14.10	69.50	50.70	127.10	50.68	.14658
2.500	Wall	Weakened	1	9.70	47.00	35.00	89.50	34.89	.13758
			2	10.10	49.00	33.80	89.00	33.69	.13605
			3	9.60	50.70	38.10	98.50	38.09	.12764
			4	9.70	51.00	38.00	98.50	37.88	.12764
			5	9.80	54.20	39.20	96.50	39.07	.12143
			6	10.00	51.20	38.90	98.50	38.77	.12826
3.750	Wall	Solid	1	8.60	40.90	32.30	79.70	32.29	.51304
1.167	Sting	Solid	Left	30.60	143.00	99.00	268.00	98.67	*.01899
			Right	31.20	143.00	97.00	251.00	96.97	*.01899

\*Calculated panel mass.

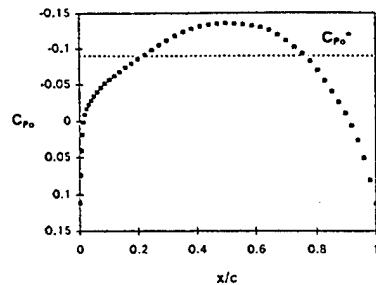
Model description		$s$ , ft	$2b_s$ , ft	$2b_t$ , ft	$\Lambda_{aa}$ , deg
Structure	Mounting				
Solid	Wall	1.250	0.917	0.604	43.15
Solid	Wall	2.500	1.833	1.208	43.15
Weakened	Wall	2.500	1.833	1.208	43.15
Solid	Wall	3.750	2.750	1.812	43.15
Solid	Sting	1.167	.856	.567	43.15

Figure 1.- Wing panel dimensions.

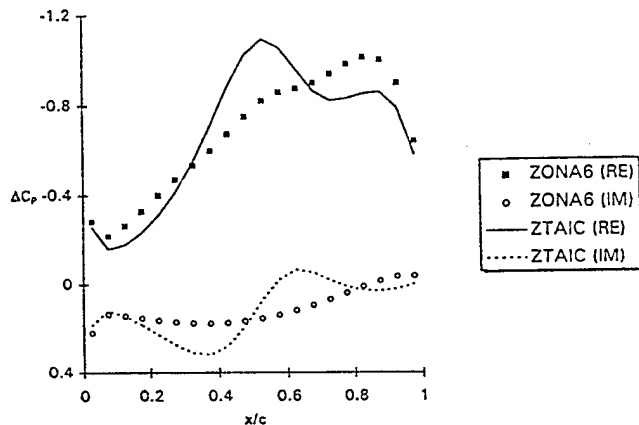
\* AGARD Report No. 765, AGARD Standard Aerodynamic Configuration for Dynamic Response I-Wing 445.6

# $\Delta C_p$ of 445.6 Weakened Wing

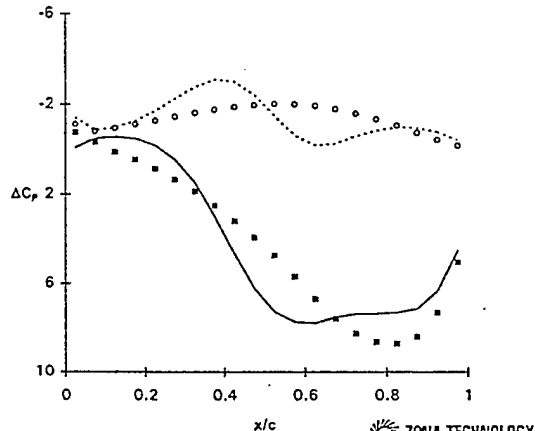
M=0.95, k=0.17, 8.22% Semi-Span Station



Mode 1



Mode 2

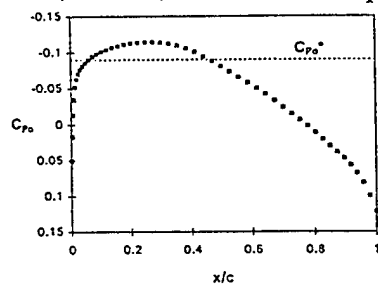


ZTL9STTR/WLPref021496

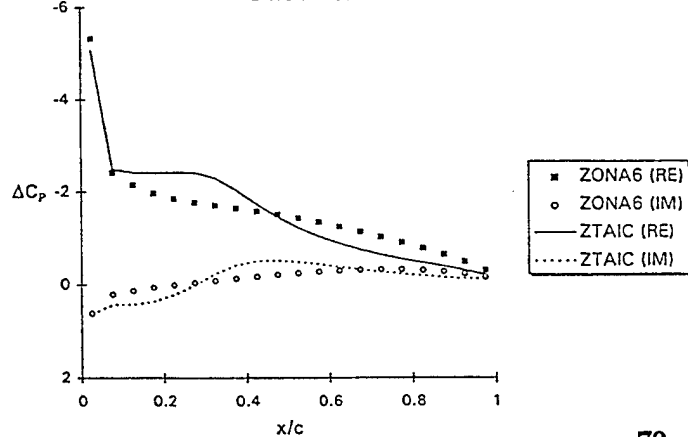
ZONIA TECHNOLOGY

# $\Delta C_p$ of 445.6 Weakened Wing

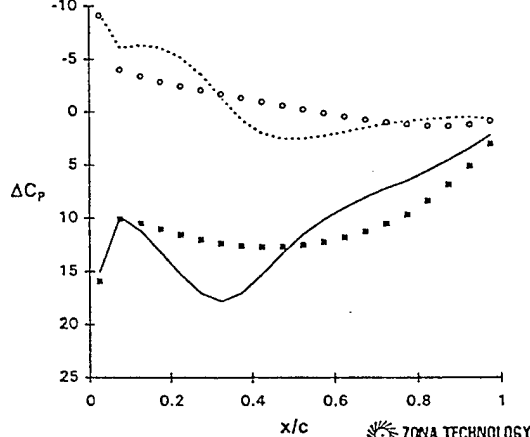
M=0.95, k=0.17, 52.45% Semi-Span Station



Mode 1



Mode 2

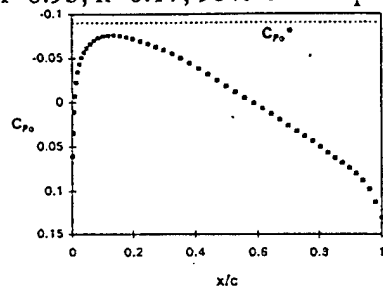


ZTL9STTR/WLPref021496

ZONIA TECHNOLOGY

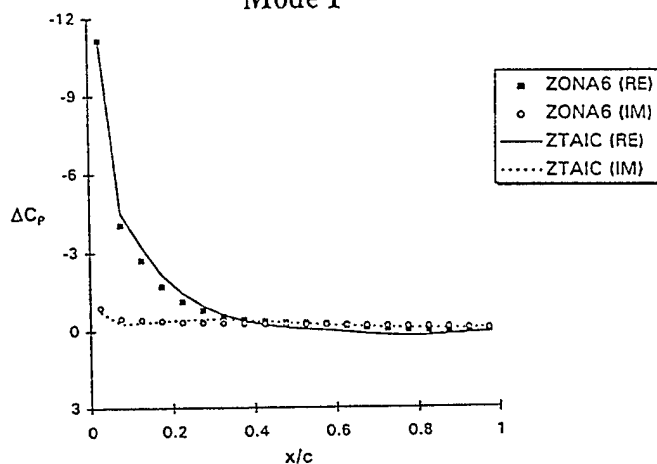
# $\Delta C_p$ of 445.6 Weakened Wing

M=0.95, k=0.17, 95% Semi-Span Station



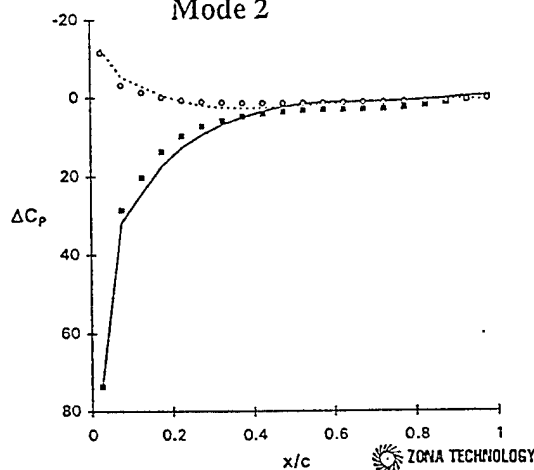
Steady  $C_p$  Computed by CAPTSD

Mode 1



ZTUA/STTR/WLP/021496

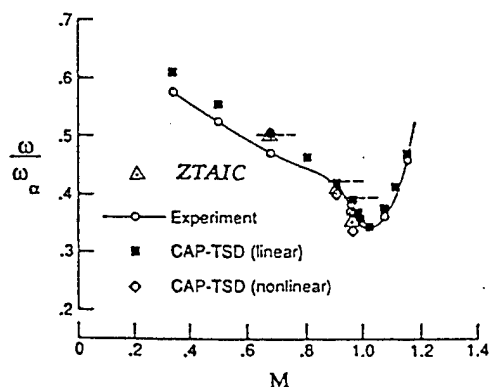
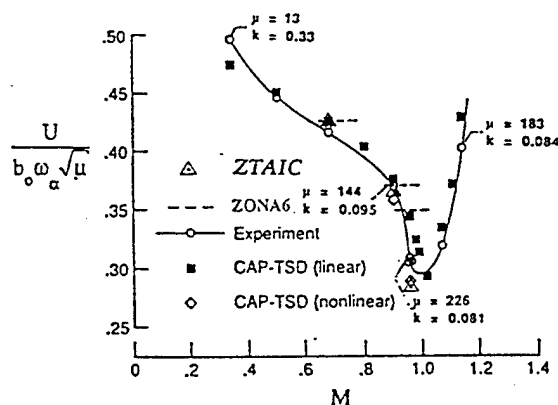
Mode 2



ZONA TECHNOLOGY

## 445.6 Weakened Wing Flutter Results

Test Cases		Wind Tunnel Data		ZONA6 --- (Linear)		ZTAIC Δ (Nonlinear)		CAPTSD ◇ (Nonlinear)	
M	$\rho$ (slug/ft <sup>3</sup> )	$\omega_f$ (Hz)	$V_f$ (ft/sec)	$\omega_f$ (Hz)	$V_f$ (ft/sec)	$\omega_f$ (Hz)	$V_f$ (ft/sec)	$\omega_f$ (Hz)	$V_f$ (ft/sec)
0.678	0.000404	17.98	759.1	19.81	766.0	19.30	761.0	19.2	768
0.900	0.000193	16.09	973.4	16.31	984.0	16.38	965.2	15.8	952
0.950	0.000123	14.50	1008.4	16.18	1192.0	13.46	944.0	12.8	956



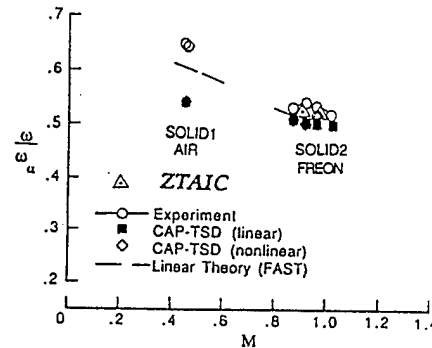
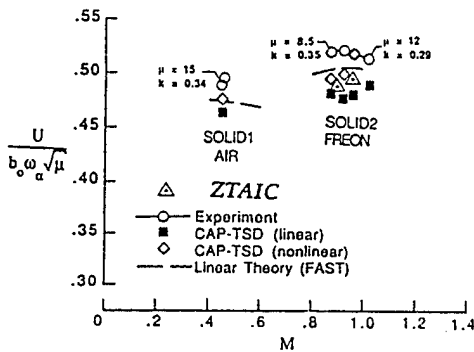
ZTUA/STTR/KOM/0101893

# 445.6 Solid Wing Flutter Results

Test Cases		Wind Tunnel Data*		ZONA6 (Linear)		ZTAIC** (Nonlinear)		CAPTSD* (Nonlinear)	
M	$\rho$ (slug/ft <sup>3</sup> )	$\omega_f$ (Hz)	$V_f$ (ft/sec)	$\omega_f$ (Hz)	$V_f$ (ft/sec)	$\omega_f$ (Hz)	$V_f$ (ft/sec)	$\omega_f$ (Hz)	$V_f$ (ft/sec)
0.90	0.00357	27.00	452.0	26.75	439.0	25.71	418.0	25.8	435.0
0.95	0.00320	26.91	479.0	26.89	462.0	25.46	450.0	26.2	472.1

\* Interpolated between Mach 0.87, 0.92 and 0.96.

\*\* Restart Run Using AIC's of Weakened Wing (1 min cpu/case).

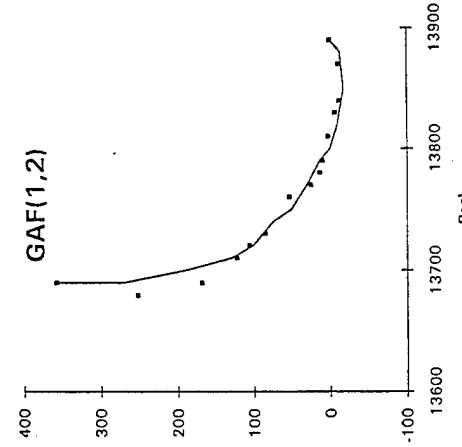
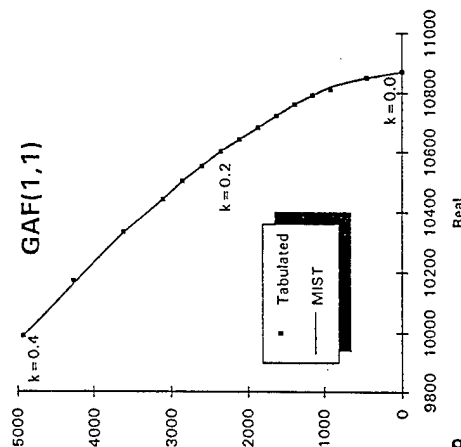
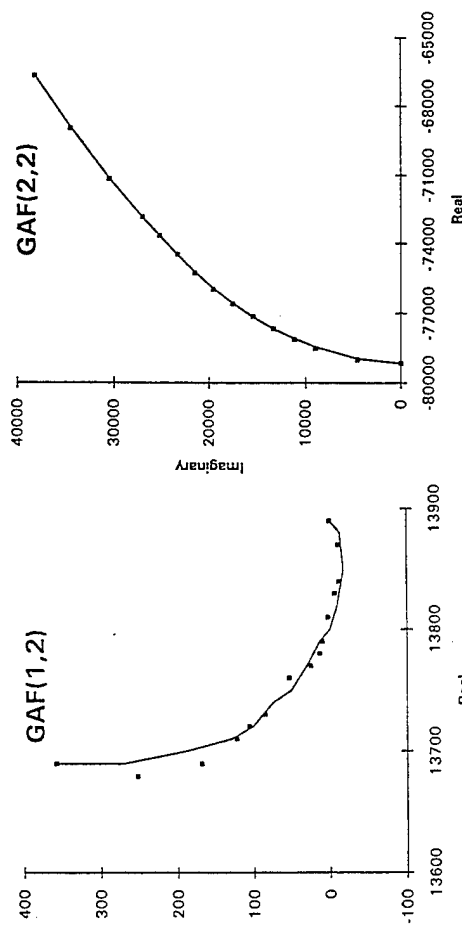
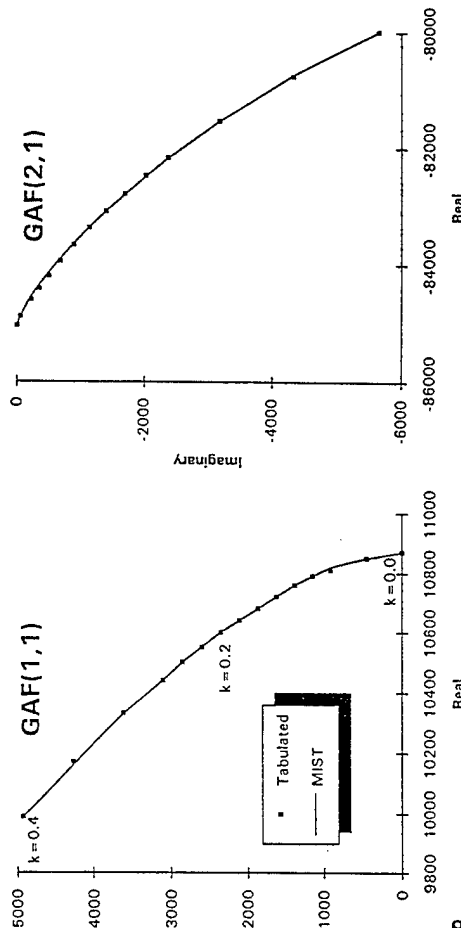


ZTLESTR/KOM101895

ZONA TECHNOLOGY

## Minimum-State (MIST) Fit of GAF 445.6 Weakened Wing, $M = 0.9$

ZTAIC Result

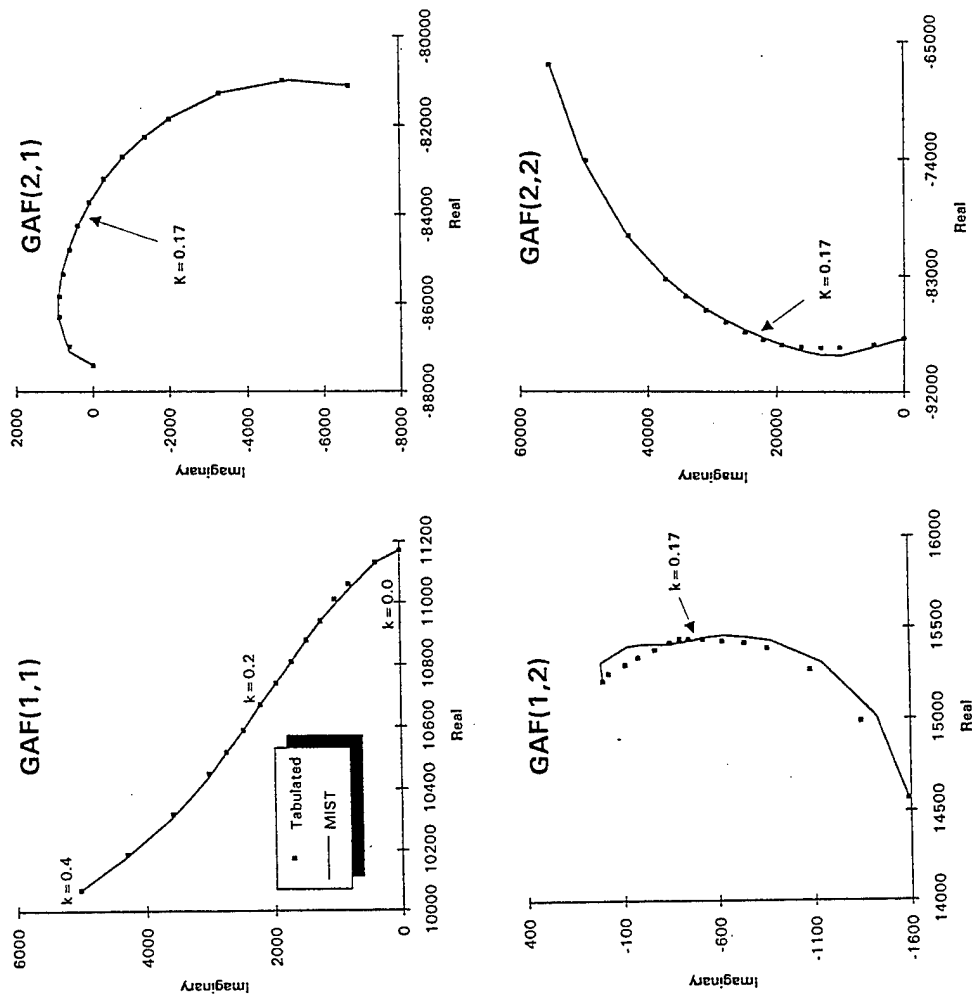


ZONA TECHNOLOGY

ZTLESTR/KOM101895

# Minimum-State (MIST) Fit of GAF 445.6 Weakened Wing, $M = 0.95$

ZTAIC Result



ZTL9STTRIKOM101893

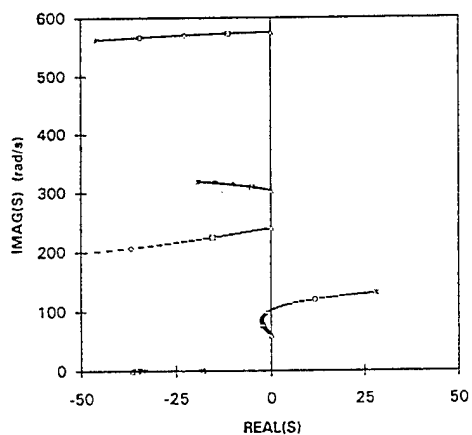


## Root-Locus Plot of 445.6 Weakened Wing at $M = 0.9$

4 Modes

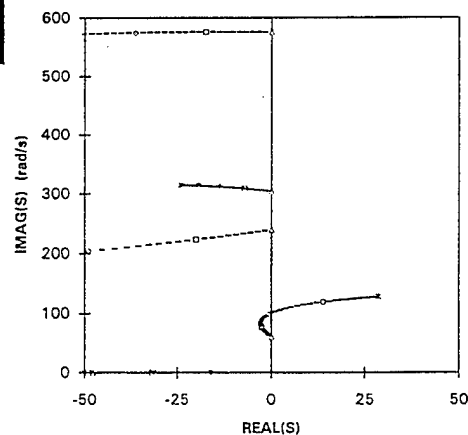
ZONA6

$q_f = 0.66$  psi,  $\omega_f = 102$  rad/s



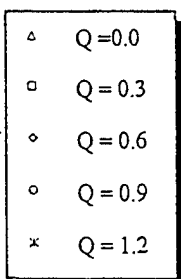
ZTAIC

$q_f = 0.63$  psi,  $\omega_f = 101$  rad/s



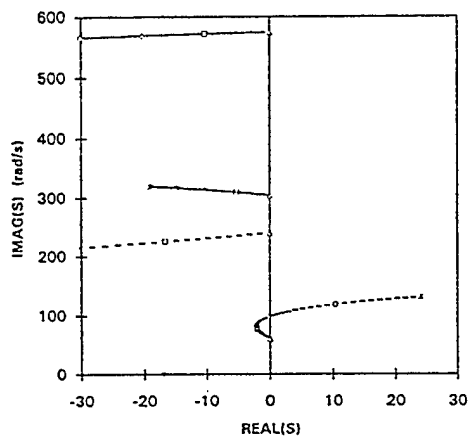
# Root-Locus Plot of 445.6 Weakened Wing at M=0.95

4 Modes



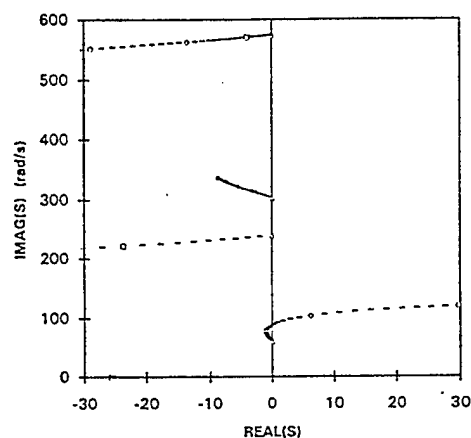
ZONA6

$q_f = 0.61 \text{ psi}$ ,  $\omega_f = 99 \text{ rad/s}$



ZTAIC

$q_f = 0.44 \text{ psi}$ ,  $\omega_f = 89 \text{ rad/s}$

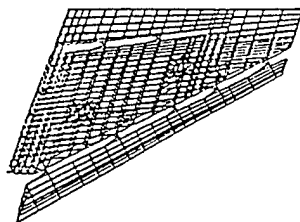


ZT/S/STTR/KOM101895

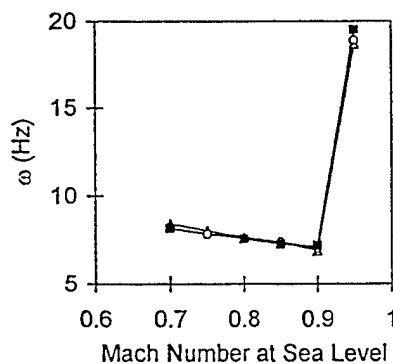
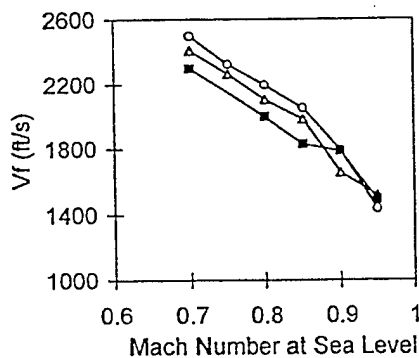
ZONA TECHNOLOGY

## MODELED F-16 WING

Flutter Speed and Frequency vs. Mach Number  
4% Parabolic Arc Airfoil Section



Structural Model

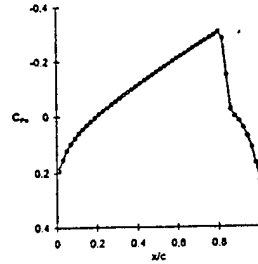


ZT/S/MSCS/M3020196

ZONA TECHNOLOGY

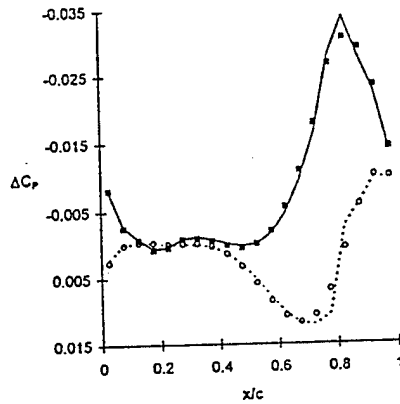
# $\Delta C_p$ of Modeled F-16 Wing

M=0.925, k=1.0, 5% Semi-Span Station

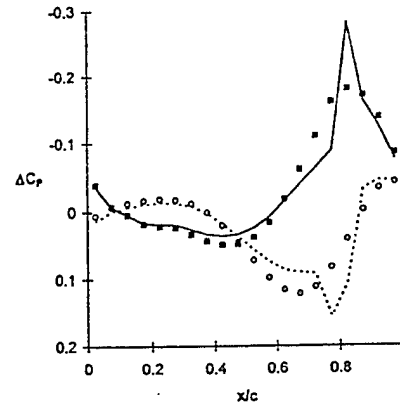


Steady  $C_p$  Computed by CAPTSD

Mode 1



Mode 2

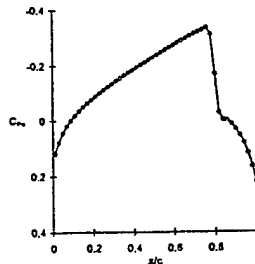


ZONA TECHNOLOGY

ZTLN-STTR/WLP-res021496

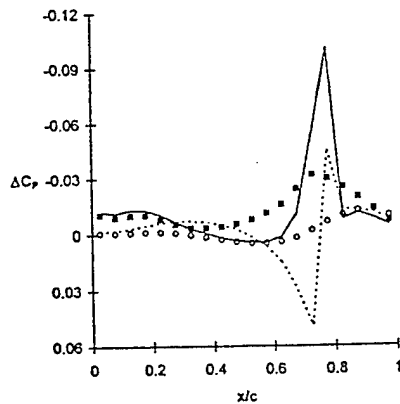
# $\Delta C_p$ of Modeled F-16 Wing

M=0.925, k=1.0, 55% Semi-Span Station

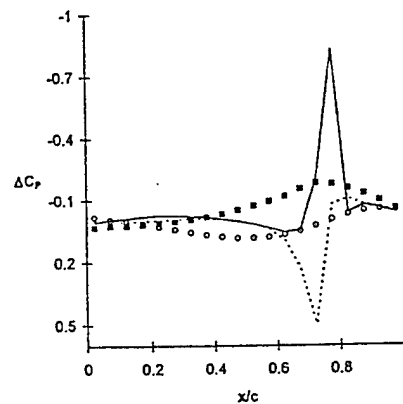


Steady  $C_p$  Computed by CAPTSD

Mode 1



Mode 2

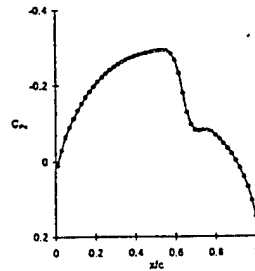


ZONA TECHNOLOGY

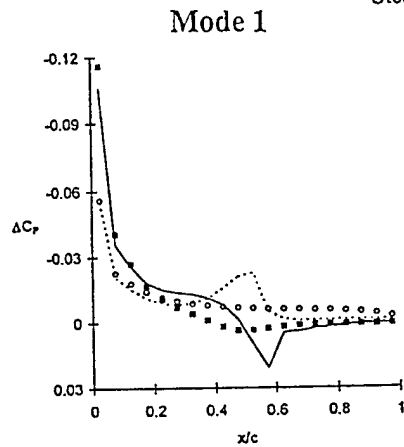
ZTLN-STTR/WLP-res021496

## $\Delta C_p$ of Modeled F-16 Wing

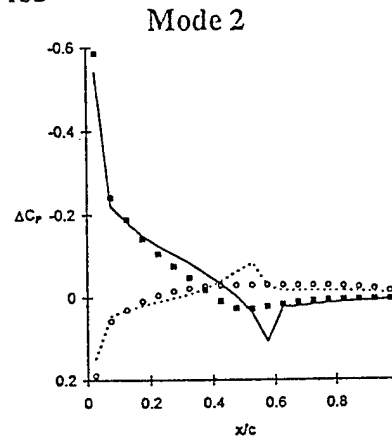
M=0.925, k=1.0, 95% Semi-Span Station



Steady  $C_p$  Computed by CAPTSD



Mode 1



Mode 2

ZONA TECHNOLOGY

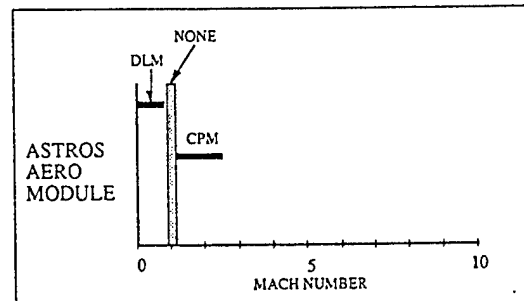
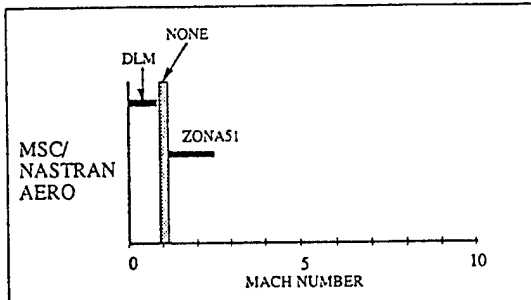
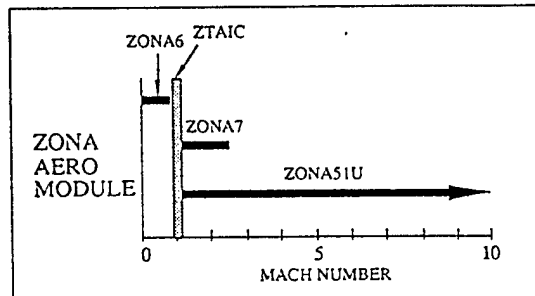
ZTL9/STTR/WLP/rev021496

## ZONA51U / ZTAIC ARE FOR ASTROS

- AIC Formulation
  - *Ideal for MDO*
- k-Domain Based Aerodynamics
  - *For All Conventional Flutter Methods*
- S-Domain Aerodynamics For ASE
  - *Through Minimum State Technique*



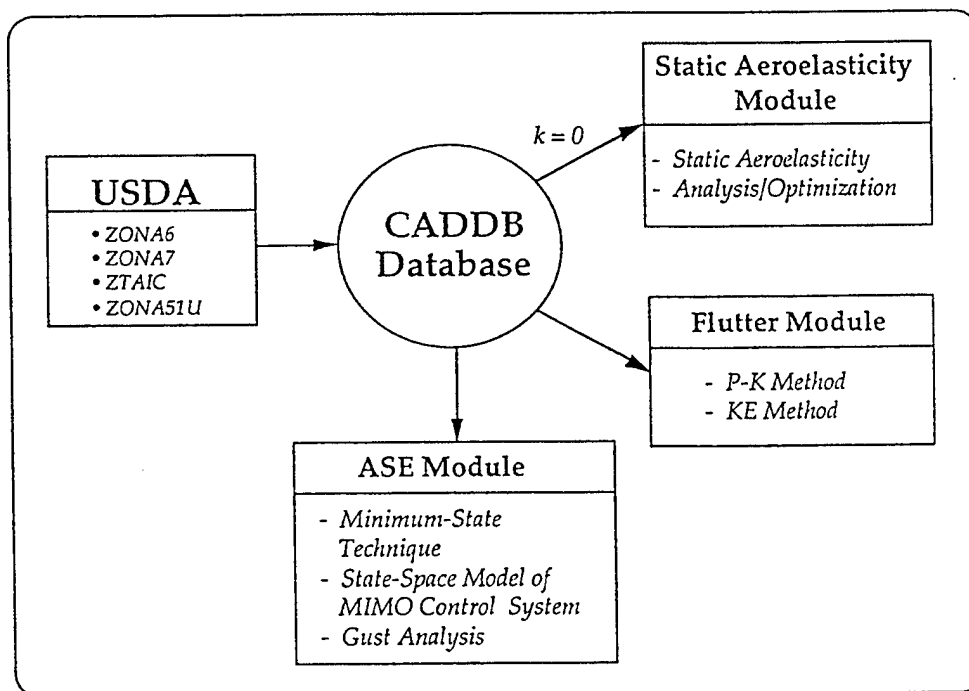
# ZONA AERODYNAMIC MODULE: *UAIC* → *USDA*



ZTL9 STTR/WLP/rev021496

ZONA TECHNOLOGY

## UNIFIED S-DOMAIN AERODYNAMICS (USDA) FOR ASTROS ENGINEERING APPLICATION MODULES

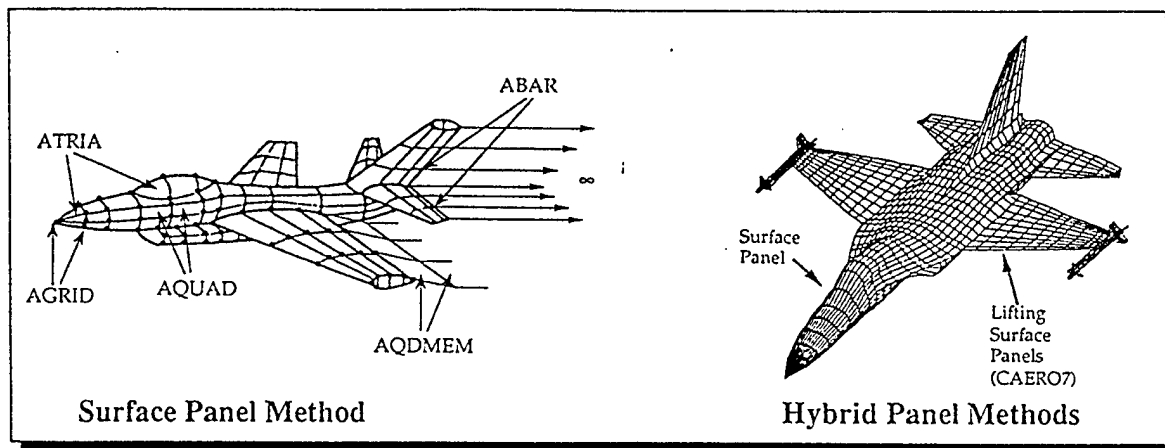


ZTL9 STTR/WLP/rev021496

ZONA TECHNOLOGY

# UNIVERSAL AERODYNAMIC GEOMETRY MODULE (AGM) I

## Goal



GOAL: to provide a universal set of input definition for aerodynamic modeling of all panel methods such as:

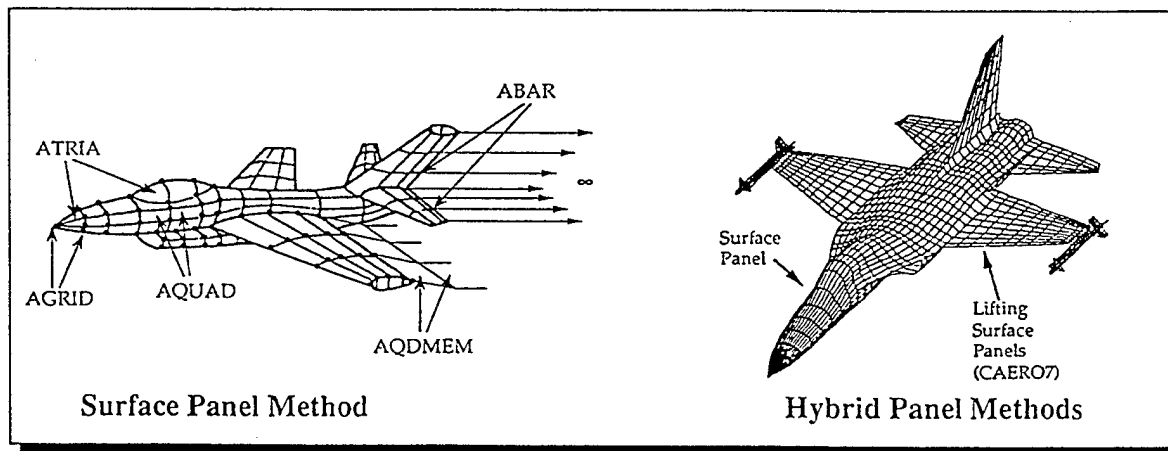
- High-Order Surface Panel Methods: *PANAIR, QUADPAN, ZONAIR, etc.*
- Lifting Surface Methods: *DLM, ZONA51, etc.*
- Hybrid Panel Methods: *ZONAIR (Thin Wing Option)*

ZTL9/STTR/WLP/rev02/1496

ZONA TECHNOLOGY

# UNIVERSAL AERODYNAMIC GEOMETRY MODULE (AGM) II

## Major Tasks



- Define New Bulk Data Entries: AGRID, ATRIA, AQUAD, AQDMEM, ABAR for surface panels and CAERO7 for lifting surface panels.
- The New Bulk Data Entries will fully represent the Geometry Data required by all panel methods such as *PANAIR, QUADPAN, ZONAIR, etc.*

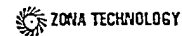
ZTL9/STTR/WLP/rev02/1496

ZONA TECHNOLOGY

# ZONA PRODUCTS

- *ZONA51*
- *ZONA51U*
- *ZONA7*
- *ZONA6*
- *ZTAIC*
- *ZONAIR*
- *ZSTORE*

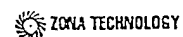
ZTL8/115012396



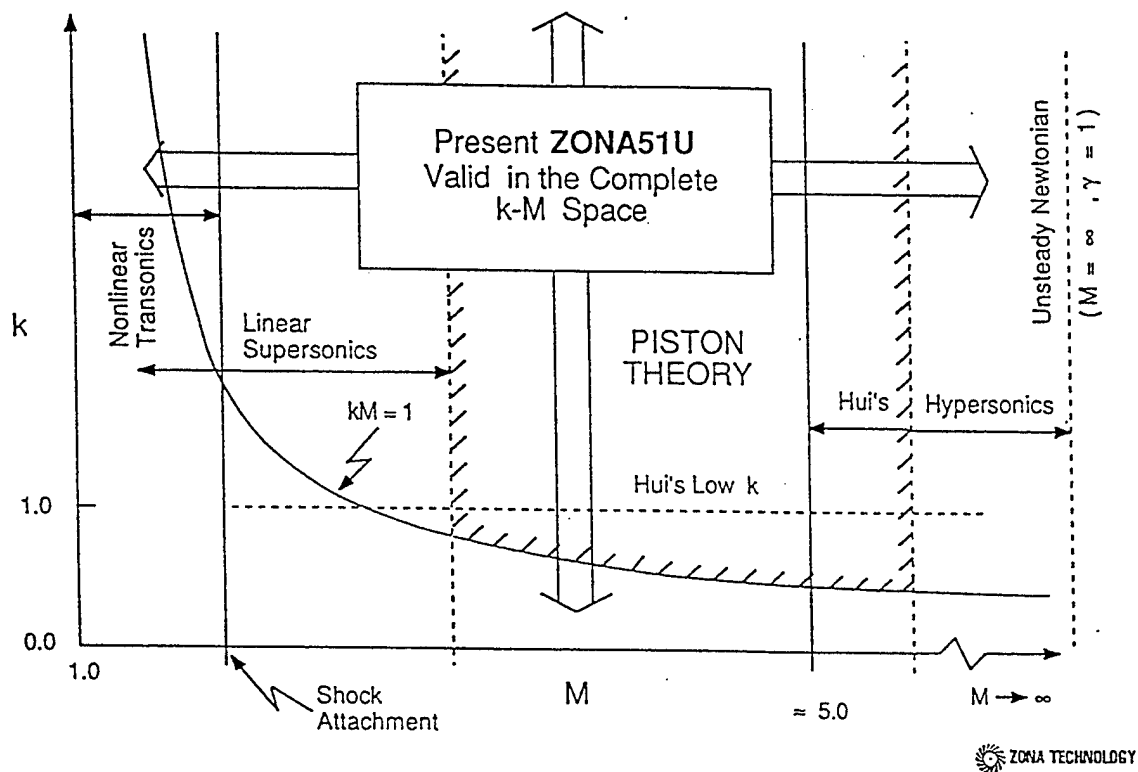
## ZONA PRODUCTS

- *ZONA51 code* generates unsteady supersonic aerodynamics for lifting surfaces.
- *ZONA51U code* generates unified supersonic/hypersonic aerodynamics for lifting surfaces.
- *ZONA7/ZONA6 codes* generate unsteady supersonic/subsonic aerodynamics for aircraft configurations with external stores.
- *ZTAIC code* generates unsteady transonic aerodynamics and transonic AIC's for wing planforms and lifting surfaces.
- *ZONAIR code* a high order panel code for computing whole aircraft aerodynamics with external stores including structural flexibility effects at subsonic and supersonic speeds.
- *ZSTORE code* generates store/aircraft aerodynamics and predicts store trajectory during the ejection and separation phases.

ZTL8/115012396

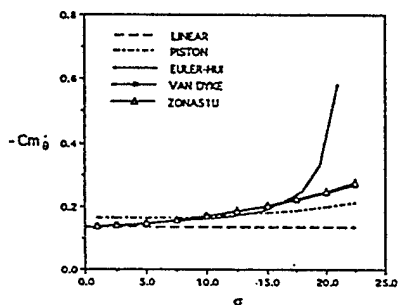


# Various Limits for Hypersonic/Supersonic Flow

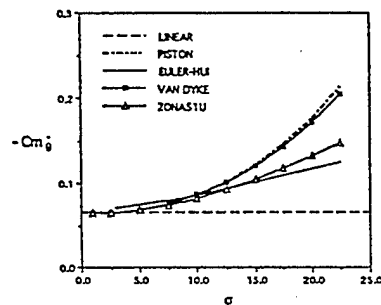


## Damping-in-Pitch Derivative vs Thickness

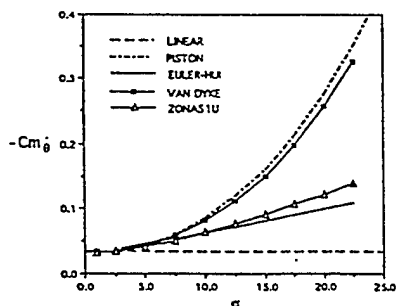
Diamond Profile ( $\tau = \tan \sigma$ )



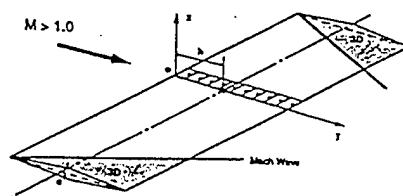
$M = 2.0$



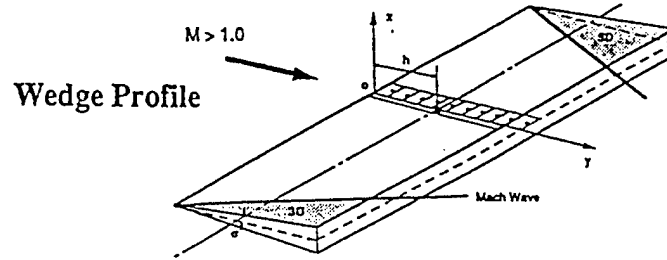
$M = 5.0$



$M = 10.0$

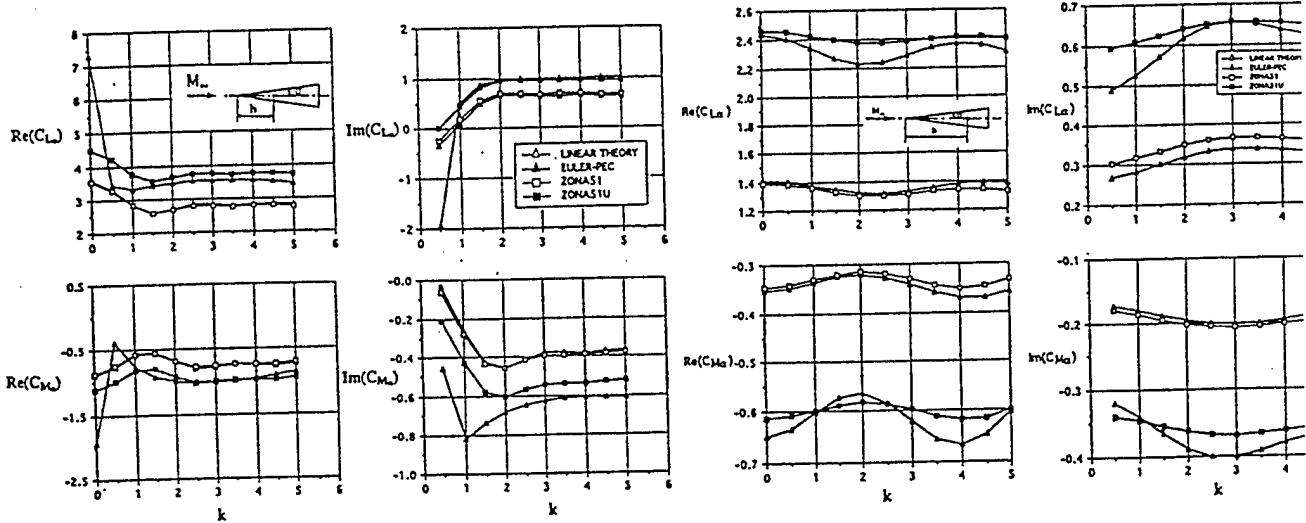


# STABILITY DERIVATIVES vs. REDUCED FREQUENCY



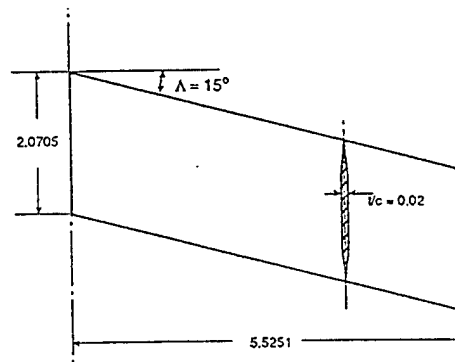
$M = 1.5, h = 0.25c, \sigma = 10^\circ$

$M = 3.0, h = 0.25c, \sigma = 10^\circ$



## Flutter Points for $15^\circ$ Swept Untapered Wing

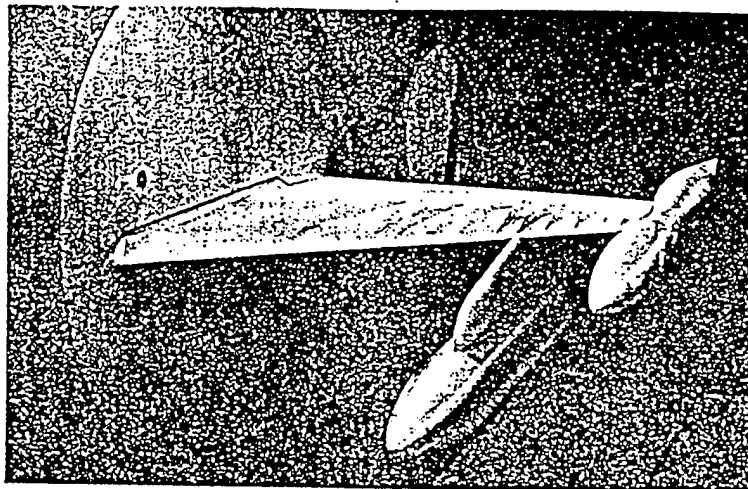
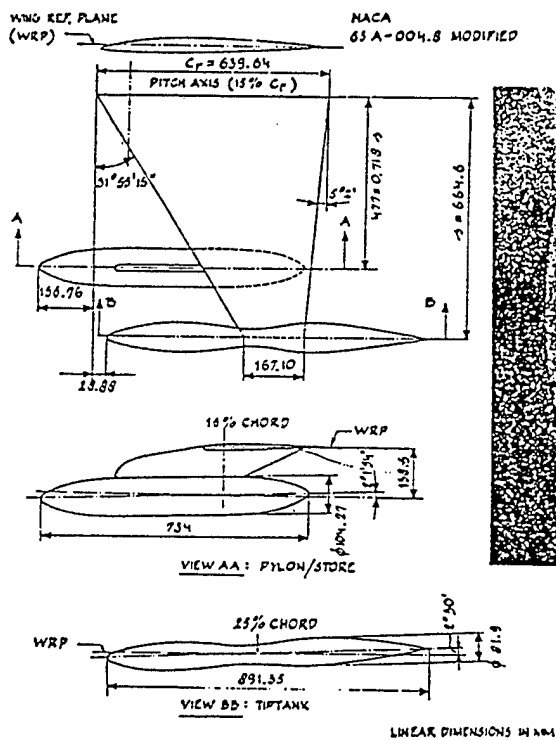
$M = 1.3 \text{ \& } 3.0$  (10 x 10 cuts)



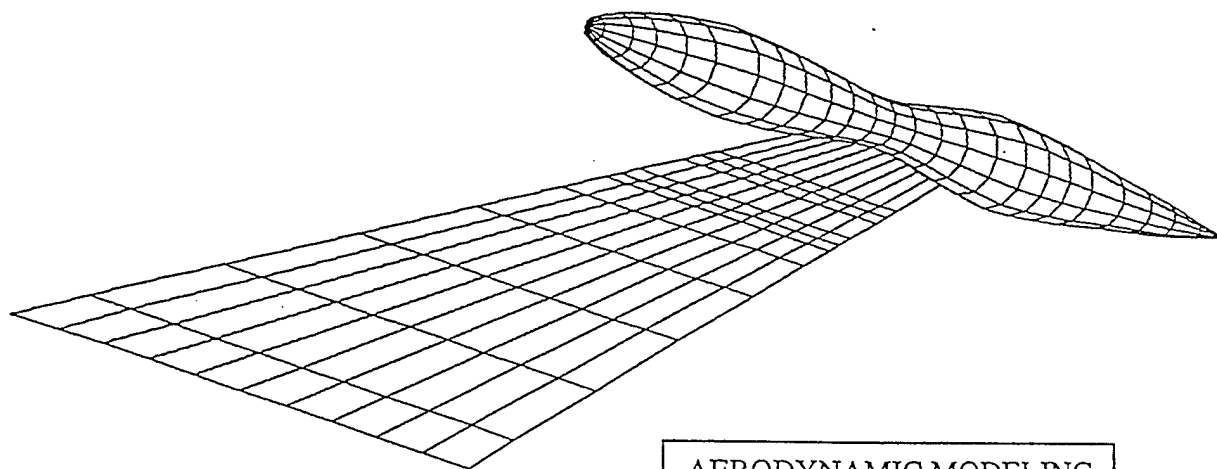
	$M = 1.3$		$M = 3.0$	
	$V_f$ (ft/s)	$f_f$ (Hz)	$V_f$ (ft/s)	$f_f$ (Hz)
Test [24]	1280	102	2030	146
Rodden [25]	1397	124	1913	149
ZONA51	1547	127	2159	148
ZONA51U	1487	124	2014	146

# NLR WIND TUNNEL MODEL

## WING + TIPTANK + PYLON + STORE



## NLR WING TIPTANK CONFIGURATION



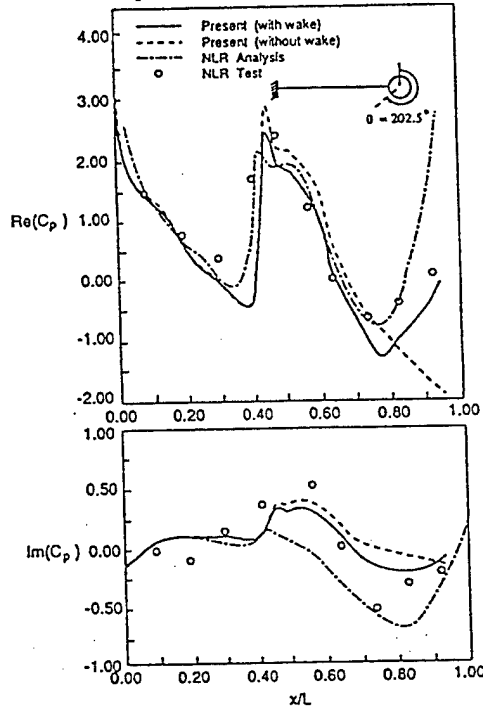
AERODYNAMIC MODELING  
WING BOXES = 90  
TANK PANELS = 264

# NLR Wing+Tiptank

$M=0.45$ ,  $k=0.305$ ,  $x_0=0.15c_R$

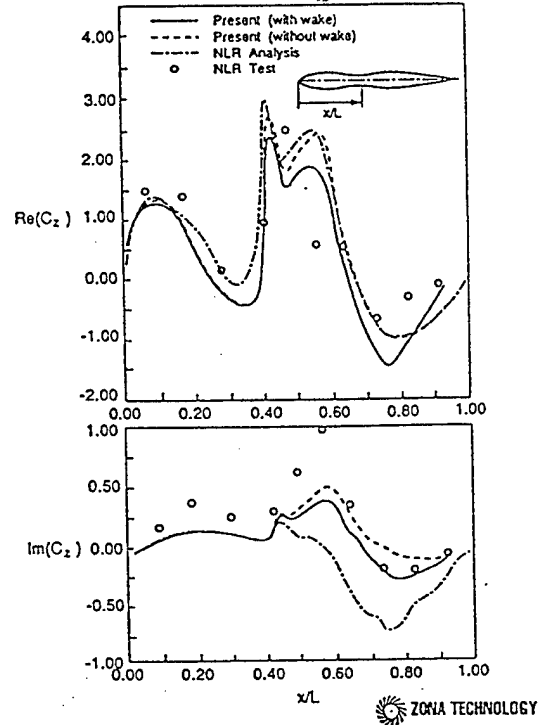
Present = ZONA6

Unsteady  $C_p$  Along Tiptank at  $\theta = 202.5^\circ$



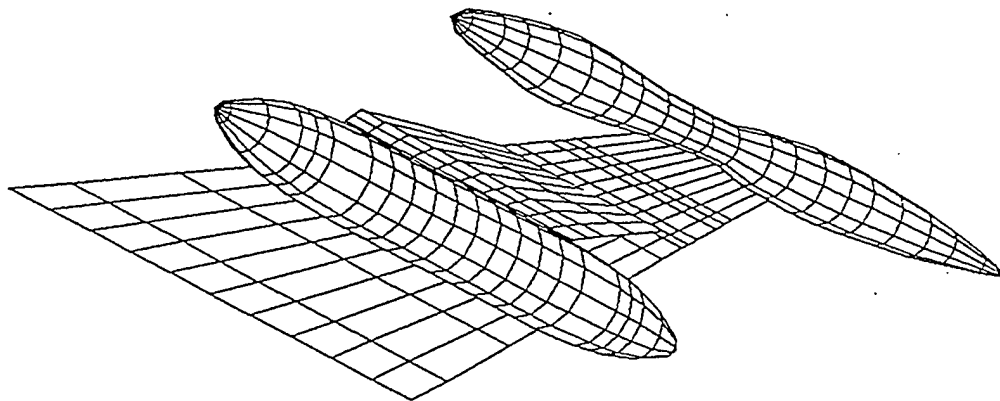
ZTL9/STTR/WLP res021496

Unsteady Normal Load ( $C_z$ ) Along Tiptank



ZONA TECHNOLOGY

## NLR WING+TIPTANK+PYLON+STORE CONFIGURATION



AERODYNAMIC MODELING  
WING BOXES = 90  
PYLON BOXES = 24  
TANK PANELS = 264  
STORE PANELS = 216

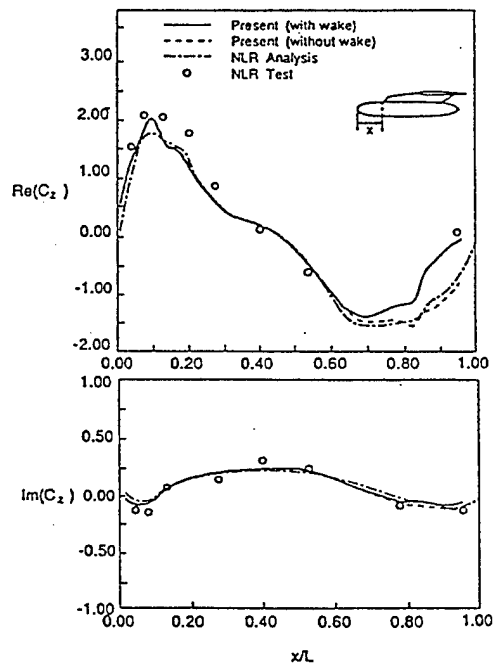
ZONA TECHNOLOGY

# NLR Wing+Tiptank+Pylon+Store

$$M=0.45, k=0.305, x_0=0.15c_R$$

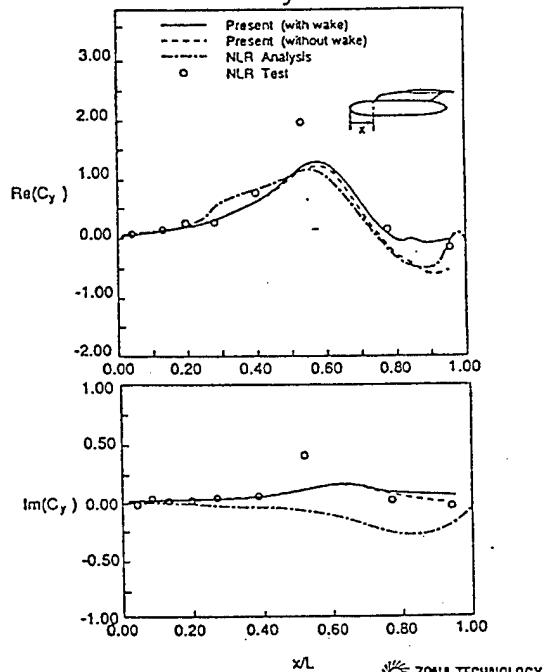
Present = ZONA6

Unsteady Normal Load ( $C_z$ ) Along Store



ZTL9STTR/WLP ref 021496

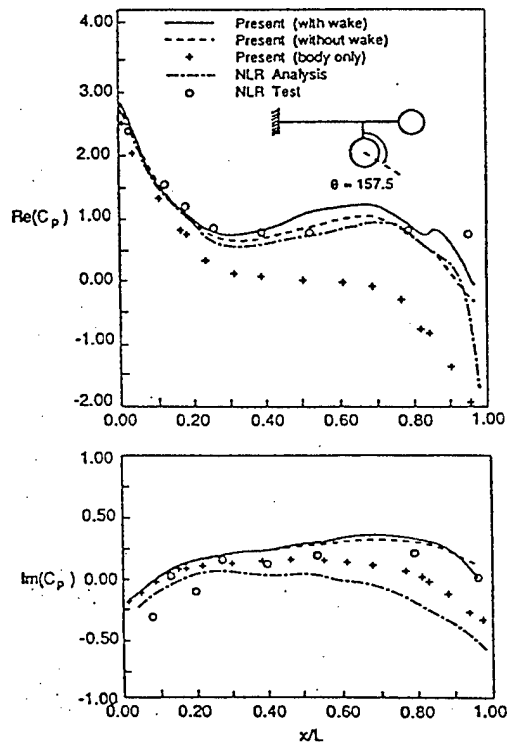
Unsteady Side Load ( $C_y$ ) Along Store



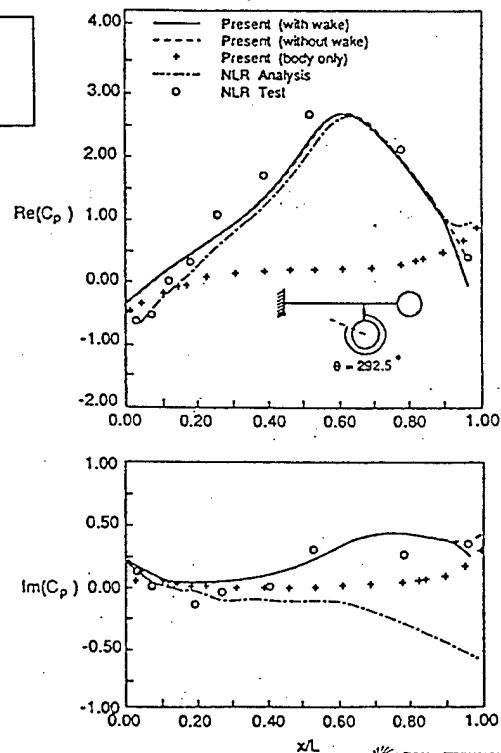
ZONA TECHNOLOGY

# NLR Wing+Tiptank+Pylon+Store

Unsteady  $C_p$  Along Store,  $M=0.45, k=0.305, x_0=0.15c_R$



Present =  
ZONA6



ZONA TECHNOLOGY

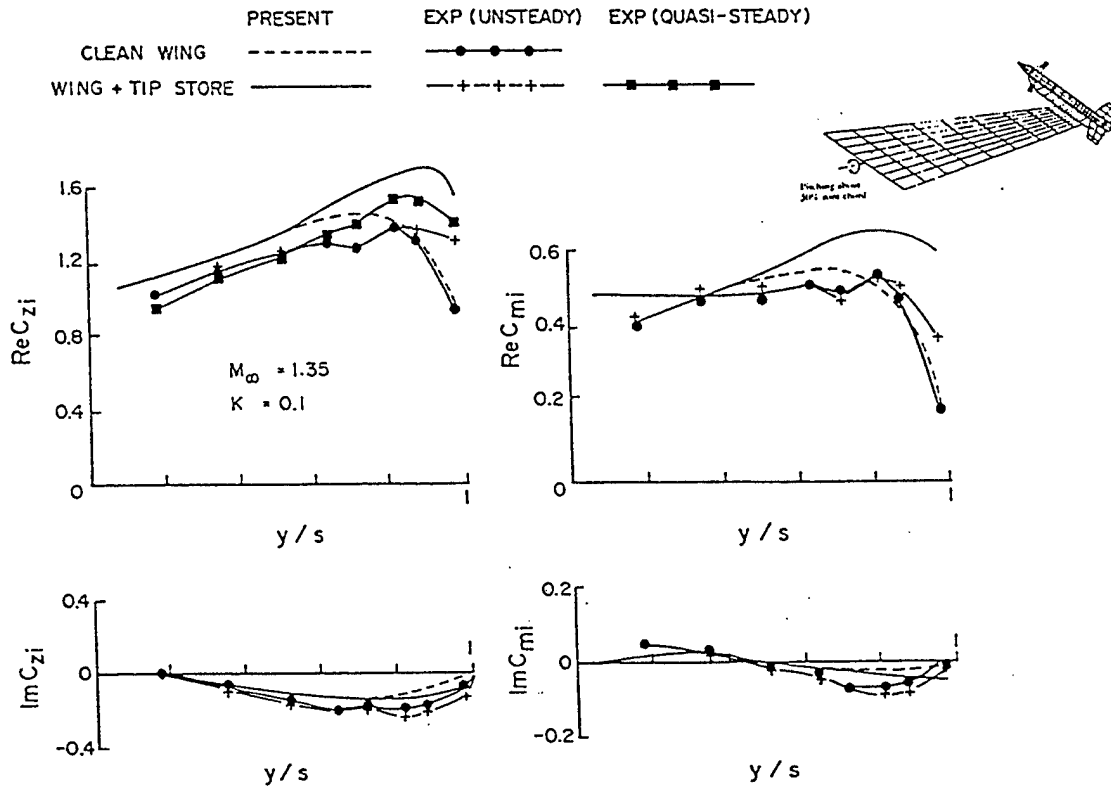
ZTL9STTR/WLP ref 021496



# NLR WING WITH TIPMISSILE V

## Spanwise forces & moments

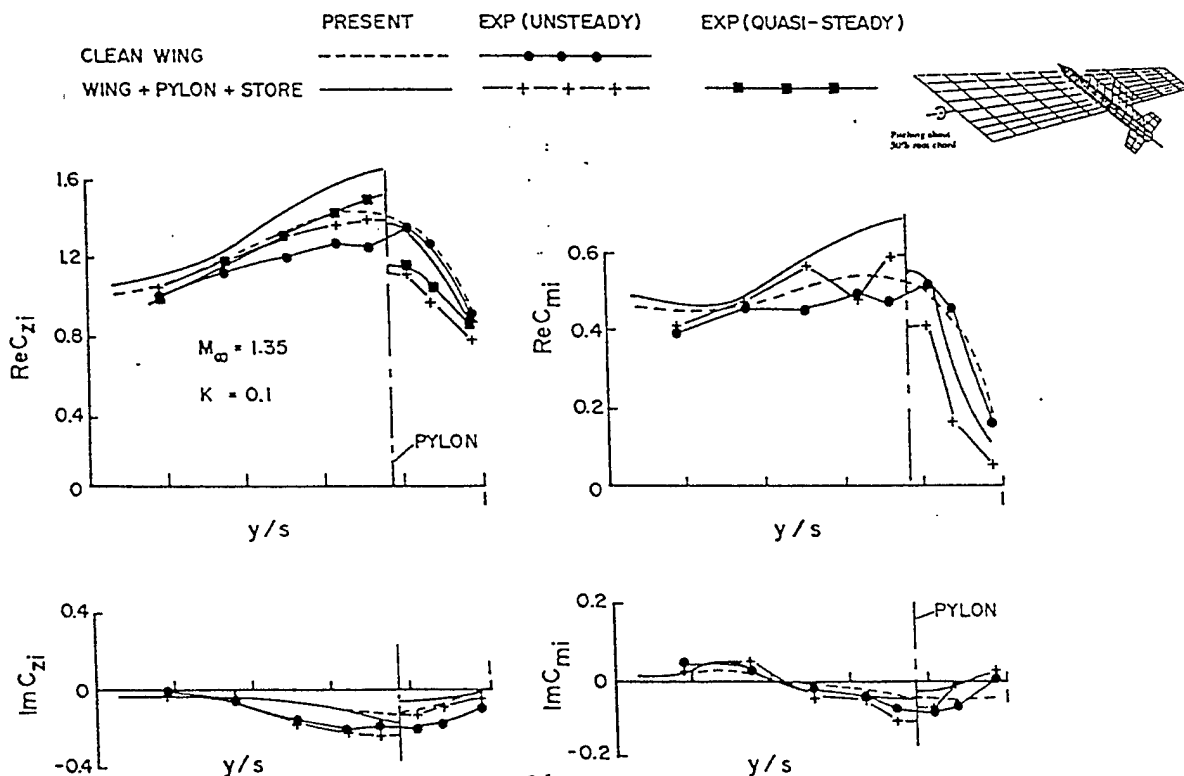
Present = ZONA7



# NLR UNDERWING STORE III

## Spanwise forces & moments

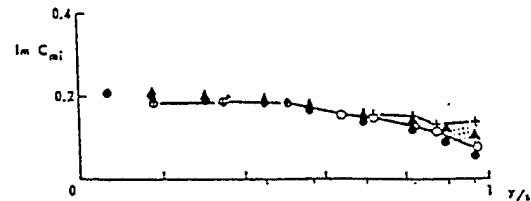
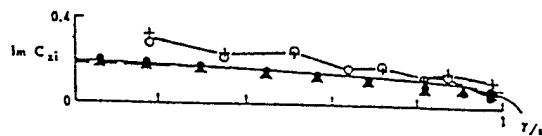
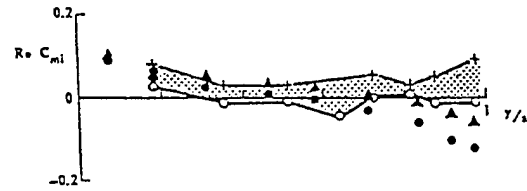
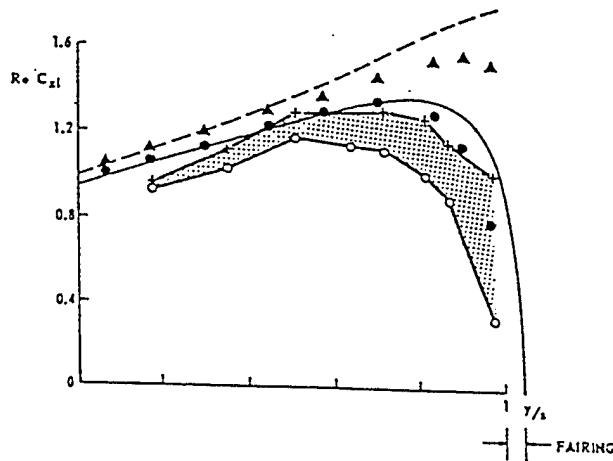
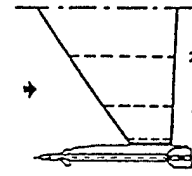
Present = ZONA7



# NLR WING WITH TIP-MISSILE

Spanwise Airload on Wing,  $M=0.6$ ,  $K=0.2$

$M_\infty = 0.6$	EXP.	THEORY	ZONAS	CONFIGURATION
$F = 20 \text{ Hz}$	$\circ$	— DL	$\bullet \bullet \bullet$	CLEAN WING
$K = 0.2$	$+$	--- NLR	$\blacktriangle \blacktriangle \blacktriangle$	WING + TIPSTORE



## Development of ASTROS/ASE Module

- Development of Software Design Blue-print: Phase I
- Submodule Development/Total Module Integration: Phase II

- OVERALL CAPABILITIES
- APPROACH
- ASE DESIGN SCENARIOS
- PROGRAM FLOW CHART OF ASE MODULE
- GROSS POTENTIALS

# OVERALL CAPABILITIES

- Inclusion of Multi-Input and Multi-Output (MIMO) Control System
- Provide Closed-Loop Robust Stability Analysis by Means of Gain Margins, Phase Margins and Singular Values
- Add Continuous Gust Response Capabilities
- Stability and Gust Response Constraints in the Structural Design Optimization
- Inclusion of User-Defined Control Parameters of a Given Control Law in the MDO Process
- Export an Efficient State-Space Representation of the ASE System to MATLAB/MATRIX X for Subsequent Analysis and Control Synthesis

*The above new features are applicable to open-loop as well as closed loop systems.*

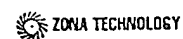
ZTL9/STTR/WLP/rev021496



## APPROACH

- Rational Approximation of Unsteady Aerodynamic Forces Provided by the ZONA Aero Module
  - Minimum State Technique
  - Roger's Approximation
- State-Space Formulation of the ASE System
- Control System is Represented by:
  - Polynomial Transfer Functions
  - State-Space Realization
- Gust Filter is Defined such that a White-Noise Input Produces an Approximation of Either Dryden's or von Karmen's PSD of Atmospheric Continuous Gusts
- Residualization of Structural States for Modal-Size-Reduction

ZTL9/STTR/WLP/rev021496

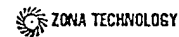


# ASE DESIGN SCENARIOS

Three *Design Scenarios* are Presented as Follows:

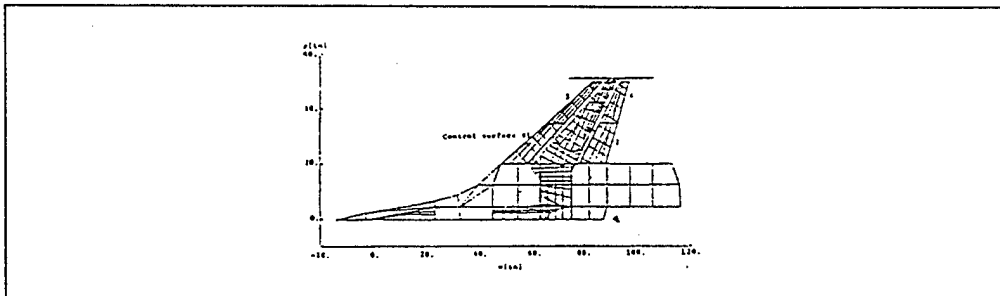
- AFW Roll Performance with Flutter Constraints
- Trade-Off Studies of Gust Load Alleviation by Passive and Active Means
- Store Flutter Suppression with Structural Uncertainties

ZTL9/STTR/WLP/rev021496



## ASE DESIGN SCENARIOS (I)

### *AFW Roll Performance with Flutter Constraints*



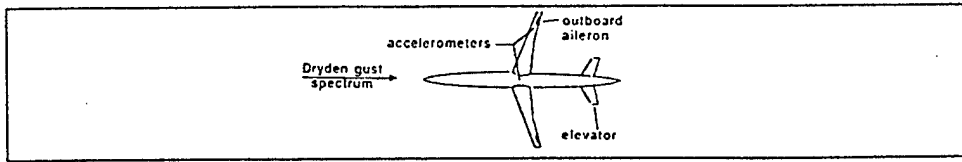
- The AFW wind tunnel model has two leading edge & two trailing edge control surfaces to meet the roll performance requirements.
- An initial control system design satisfies these roll constraints but introduces antisymmetric flutter.
- With the proposed ASTROS/ASE module, the control gains of the four control surfaces are added to the list of design variables.
- The new ASE module and the static aeroelastic module are employed to optimize the control gains and the structural design variables for satisfying the flutter and roll performance constraints with a minimal weight penalty.

ZTL9/STTR/WLP/rev021496



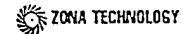
## ASE DESIGN SCENARIOS (II)

### *Trade-Off Study of Gust Load Alleviation by Passive and Active Means*



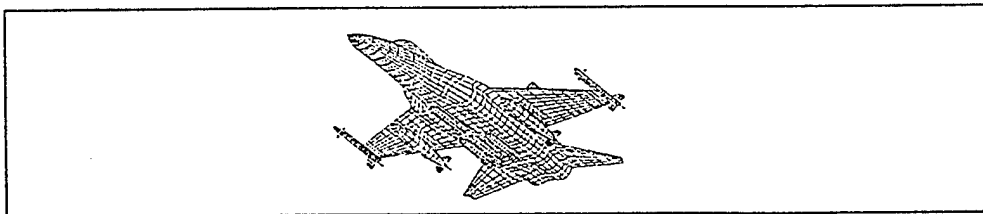
- A drone aircraft designed by ASTROS Version 11 is experiencing excessive wing root RMS bending moment in open-loop continuous gust analysis.
- With the new ASE module, the baseline structure is used as a starting point for two design studies:
  - ♦ **Passive Design** - Add gust response constraints and repeat the structural design process.
  - ♦ **Active Design**
    - Extract the plant state-space model for designing a load alleviation control system outside of ASTROS.
    - Due to the control system limitations, the control law helps but does not fully satisfy the gust-response requirements.
    - Redesign the structure in the presence of the control system with gain-margin, phase-margin and singular-value constraints added to the list of constraints.
- Supply data for trade-off studies of structural changes vs. complexity of the control system.

ZTLNSTRWLPref021496



## ASE DESIGN SCENARIOS (III)

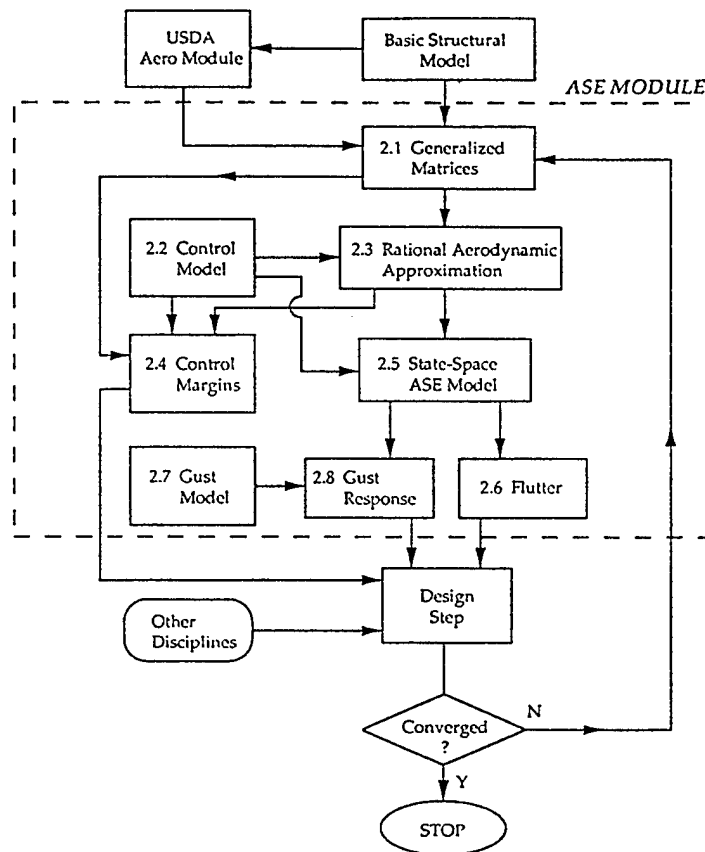
### *Store Flutter Suppression with Structural Uncertainties*



- Uncertainties of the stores/pylons structural properties require a robust control system design for store flutter suppression.
- The state-space matrices of aircraft with external stores and the derivatives of these matrices with respect to the structural properties of the stores/pylons will be generated by the new ASE modules.
- MATLAB  $\mu$ -analysis tool box will then be used to design a control system which suppresses flutter over a range of parameter uncertainties.
- The designed control law will be introduced to ASTROS for the verification with various store models at different flight conditions.

ZTLNSTRWLPref021496

# Global Flow Chart of the ASE Module



ZTL9/STTR/WLP/rev021496

ZONA TECHNOLOGY

## GROSS POTENTIALS

- Integration with *Probabilistic Design Methods*
- Introduction of *Smart-Structure Technology*
- Inclusion of Emerging *Robust Control Technique*